In presenting the dissertation as a partial fulfillment of the requirements for an advanced degree from the Georgia Institute of Technology, I agree that the Library of the Institute shall make it available for inspection and circulation in accordance with its regulations governing materials of this type. I agree that permission to copy from, or to publish from, this dissertation may be granted by the professor under whose direction it was written, or, in his absence, by the Dean of the Graduate Division when such copying or publication is solely for scholarly purposes and does not involve potential financial gain. It is understood that any copying from, or publication of, this dissertation which involves potential financial gain will not be allowed without written permission.

INSTRUMENTATION FOR THE DETERMINATION OF THE VIBRATION CHARACTERISTICS OF A SHAKING TABLE AND A SINGLE-DEGREE-OF-FREEDOM MODEL SUBJECTED TO VARIOUS EXCITATIONS

A THESIS

Presented to

The Faculty of the Graduate Division

by

Leroy Zachary Emkin

In Partial Fulfillment

of the Requirements for the Degree

Master of Science in Civil Engineering

Georgia Institute of Technology

September, 1966

INSTRUMENTATION FOR THE DETERMINATION OF THE VIBRATION CHARACTERISTICS OF A SHAKING TABLE AND A SINGLE-DEGREE-OF-FREEDOM MODEL SUBJECTED TO VARIOUS EXCITATIONS

Approved:

Chairman

Date approved by Chairman: 30 MAY 1967

ACKNOWLEDGMENTS

The writer wishes to express his grateful appreciation to Professor J. R. Fincher for his guidance, assistance, and encouragement in the preparation of this dissertation.

Thanks are due to Dr. P. H. Sanders and Professor R. M. Dinnat, members of the reading committee, whose courteous and constructive criticisms have been so helpful in the final phase of preparation of this dissertation.

To Mr. C. M. Pavey of the Civil Engineering Department machine shop go thanks for his invaluable assistance in fabricating the test equipment.

TABLE OF CONTENTS

Page

ACKNOWLEDGMENTS ii

LIST OF TABLES v

LIST OF ILLUSTRATIONS vi

SUMMARY viii

LIST OF SYMBOLS ix

Chapter

I. INTRODUCTION 1

II. THE SHAKING TABLE 3

General Description of Shaking Table System
Shaking Table and Applied Load Measuring Systems
Dynamic Properties of Shaking Table

III. THE MODEL 32

Design of the Model
Response Measurements of Model
Dynamic Properties of Model

IV. RESPONSE OF SHAKING TABLE TO BREAKING WIRES 50

Determination of the Type of Applied Load to the Shaking Table
Effect of Breaking Various Numbers of Wires Connected to the Shaking Table
Wire Testing

V. INSTRUMENTATION CHECK-OUT 67

VI. CONCLUSIONS 78

VII. RECOMMENDATIONS 79

APPENDIX

A. DESIGN OF TABLE LEAF-SPRINGS 82

APPENDIX Page

B. BALANCING PROCEDURE FOR THE SANBORN STRAIN GAGE AMPLIFIER 86

C. CALIBRATION DATA AND CALCULATIONS FOR THE PENDULUM'S DEFLECTION MEASURING DEVICE 87

D. DATA AND CALCULATIONS TO DETERMINE SHAKING TABLE SPRING CONSTANT 92

E. DATA AND CALCULATIONS TO DETERMINE THE NATURAL FREQUENCY, DAMPING RATIO, CRITICAL DAMPING, DAMPING CONSTANT, EQUIVALENT MASS, AND WEIGHT OF SHAKING TABLE 97

F. BALANCING PROCEDURE FOR THE SANBORN TRANSDUCER AMPLIFIER 106

G. BALANCING PROCEDURE FOR THE SANBORN DC GENERAL PURPOSE AMPLIFIER 108

H. DATA AND CALCULATIONS TO DETERMINE MODEL SPRING CONSTANT 109

J. DATA AND CALCULATIONS TO DETERMINE THE NATURAL FREQUENCY, DAMPING RATIO, CRITICAL DAMPING, DAMPING CONSTANT, EQUIVALENT MASS, AND WEIGHT OF MODEL 115

K. DATA SHOWING THE EFFECT OF BREAKING WIRES CONNECTED TO THE SHAKING TABLE 127

L. COMPARISON OF MEASURED AND CALCULATED PEAK VALUES OF X_t AND D_r 130

M. COMPARISON OF MEASURED AND CALCULATED PEAK VALUES OF $\ddot{X}_m$ 132

N. LOAD-STRAIN CURVE OF THE WIRE 134

LITERATURE CITED 137

LIST OF TABLES

Table | Page

1. Data for Determination of Calibration Constant for Pendulum Rotations 88
2. Data for Table Spring Constant Determination 93
3. Summary of Measured Dynamic Properties of Shaking Table 104
4. Data for Model Spring Constant Determination 110
5. Summary of Measured Dynamic Properties of Model 125
6. Results of Wire Testing 128
7. Comparison of Measured and Calculated Peak Values of X_t and D_r for Five, Seven and Ten Wires Tests 131
8. Comparison of Measured and Calculated Peak Values of $\ddot{X}_m$ for One, Three and Five Wire Tests 133
9. Data for the Determination of the Load-Strain Curve of the Wire 135

LIST OF ILLUSTRATIONS

Figure Page

1. Shaking Table and Pendulum 4
2. Connection of Wires to Shaking Table 4
3. Wheatstone Bridge Circuit 7
4. Arrangement of Wheatstone Bridge Circuit on Shaking Table 9
5. Deflected Shape of Table Leaf-Springs 11
6. Wheatstone Bridge Connection to the Sanborn Strain Gage Amplifier 13
7. Calibration of Deflection Measuring System for Shaking Table 15
8. Deflection Measuring Device for Pendulum 18
9. Calibration of Deflection Measuring Device for Pendulum 20
10. Device to Measure Time of Breaking Wires 23
11. Equivalent Single-Degree-of-Freedom Table System 24
12. Experimental Determination of the Table Spring Constant 26
13. Equivalent Model and Actual Model Leaf-Spring 34
14. Details of Model 37
15. Model in Place on Shaking Table 38
16. Accelerometer Connection Circuit 39
17. Wheatstone Bridge Circuit Mounted on Model 41
18. Wheatstone Bridge Connection to the Sanborn Preamplifier 43

Figure Page

19. Experimental Determination of the Model Spring Constant 47

20. Typical Dynamic Load and Single-Degree-of-Freedom System 51

21. Configuration of Wires at Time of Breaking 56

22. Variation of Maximum Table Displacement with Number of Wires Broken 62

23. Variation of Initial Table Velocity with Number of Wires Broken 63

24. Variation of Time of Breaking Wires with Number of Wires Broken 64

25. Variation of Loss of Potential Energy of the Pendulum with Number of Wires Broken 65

26. Equivalent Two-Degree-of-Freedom System of Model and Table 68

27. Comparison of Calculated and Measured Table Deflection for a Seven-Wire Test 73

28. Comparison of Calculated and Measured Values of D_r for a Seven-Wire Test 74

29. Comparison of Calculated and Measured Model Accelerations for a Three-Wire Test 76

30. Cross-Section of the Shaking Table 83

31. Statistical Variation of C_p 90

32. Statistical Variation of K 95

33. Statistical Variation of k 113

34. Load-Strain Curve of the Wire 136

SUMMARY

A study was undertaken to develop a method of testing to be used in the study of the response of model structures subjected to base excitations. To accomplish this, a shaking table was constructed such that model structures could be mounted on it. The table was excited by breaking a series of wires connected to it. Insturmentation was developed to measure the response of the table and a single-degree-of-freedom model mounted on the table. The measured response was compared to the calculated theoretical response to determine if the measuring systems were operating in a predictable manner.

Conclusions drawn from the data indicate:

(1) The applied load to the table may be considered a pure impulsive load.

(2) The deflection measuring systems are behaving in a predictable manner.

(3) There are limitations on the use of the shaking table as a source of base excitation.

LIST OF SYMBOLS

A = attenuation of the Sanborn Strain Gage Amplifier

A_{DC} = Sanborn DC General Purpose Amplifier

a = horizontal distance from transit to plane of pendulum

a_1 = distance from free end of model leaf-spring to strain gage R_1

a_2 = distance from free end of model leaf-spring to strain gage R_2

a_3 = distance from free end of model leaf-spring to any point on the leaf-spring

a_b = Helipot potentiometer

B = attenuation of the Sanborn preamplifier

b_m = width of the model leaf-spring

b_t = width of the table leaf-spring

C_s = calibration constant of the dynamometer

C_a = calibration constant of the accelerometer

C_m = damping constant of the model

C_{mcr} = critical damping constant of the model

C_p = calibration constant of the pendulum's measuring system

$\overline{C}_p$ = arithmetic mean of the measured C_p's

C_t = damping constant of the shaking table

D_r = relative displacement between the mass at the free end of the model leaf-spring and the shaking table

d = stylus deflection

d_r = relative displacement between the ends of the shaking table leaf-spring

E_a = modulus of elasticity of aluminum

ΔE = voltage change across the Helipot potentiometer

E_h = Hewlett Packard power supply

E_o = votage change measured by the Sanborn recording galvanometer

E_s = modulus of elasticity of steel

E_v = 12 volt battery

E_w = modulus of elasticity of plywood

$e(a_3)$ = strain in the model leaf-spring at any distance, a_3, from the free end

e_1, e_2, e_3, e_4 = applied strains in strain gages R_1, R_2, R_3, and R_4 respectively

e_t = maximum induced strain in the shaking table leaf-springs

F = strain gage factor

f = maximum induced stress in the shaking table leaf-spring

$f(a_3)$ = stress in model leaf-spring at any distance, a_3, from the free end

f_m = natural frequency of the model

f_t = natural frequency of the shaking table

f_y = yield stress of aluminum

G = horizontal angle

g = acceleration due to gravity

H = area under the load-time curve

h_m = thickness of the model leaf-spring

h_t = thickness of the shaking table leaf-springs

I = current

I_m = moment of inertia of the model leaf-spring

I_t = moment of inertia of the shaking table leaf-springs

I_w = moment of inertia of the shaking table

J_b = maximum potential energy of the pendulum after breaking wires

ΔJ = loss of potential energy of the pendulum

J_t = maximum potential energy of the pendulum

K = shaking table spring constant

$\overline{K}$ = arithmetic mean of the measured K's

k = model spring constant

$\overline{k}$ = arithmetic mean of the measured k's

L_m = length of the model leaf-spring

L_p = length of pendulum

L_t = length of the shaking table leaf-springs

L_w = length of wire between supports

M = maximum moment of table leaf-spring

M_m = equivalent mass of the model

M_t = equivalent mass of the shaking table

N = number of wires to be broken

P = lateral load on shaking table

$P(t)$ = typical dynamic load

Q = any applied known force

q_m = natural frequency of model

q_t = natural frequency of shaking table

$R_1, R_2,$
$R_3, R_4,$ = SR-4 strain gages in the Wheatstone Bridge circuit

R_L = resistance of the Sanborn recording galvanometer

R_o = resistance of the oscilliscope

R_t = resistor in the circuit to measure the time of breaking the wires

$R(X)$ = resistance of spring as a function of displacement

r = distance from axis of pendulum to point (la) on pendulum

r_w = horizontal extension of wire

S = basic sensitivity

S_d = standard deviation

SL = slider of Helipot potentiometer

SW = switch

T = duration of applied load to the shaking table

t = time

t_m = time of maximum table deflection

U = applied known deflection

V = applied voltage to Wheatstone Bridge circuit

V_o = initial velocity of shaking table

W = weight of mass at free end of the model leaf-spring

W_m = equivalent weight of model

W_p = weight of pendulum

W_{PL} = weight of plate at end of pendulum

W_r = work done ignoring the contribution of internal resistance

W_t = equivalent weight of shaking table

$W(t)$ = external work done at any time t

X_m = deflection of the model

X_o = initial deflection of shaking table

X_t = horizontal deflection of shaking table

$\dot{X}$ = velocity of shaking table at any time t

$\ddot{X}_t$ = acceleration of shaking table at any time t

X_{tm} = first maximum deflection of shaking table

Y = vertical distance from point (la) to point (lb) on the pendulum

Z = horizontal distance from point (la) to point (lb) on the pendulum

Z_m = damping ratio of the model

Z_t = damping ratio of the shaking table

ϕ = phase angle

θ = angular displacement of pendulum

θ_b = angle through which the pendulum rises, measured from the vertical, after breaking wires

θ_t = angle through which the pendulum rises, measured from the vertical, without braking any wires

$\Delta\theta$ = $\theta_t - \theta_b$

CHAPTER I

INTRODUCTION

The response of Civil Engineering type structures to dynamic loads is an extremely complex problem. At present, theoretical calculations can be carried out only after gross simplifications and approximations have been made. The more complex the structure being considered, the more questionable the theoretical calculations become. As a result, methods of experimental analysis are becoming very important. Full-scale testing would be the most desirable. However, cost makes this, for the most part, impossible. Therefore, model testing is the most practical.

It is the purpose of this thesis to develop a method of testing to be used in the study of the response of model structures subjected to base excitations. It is assumed that the reader is familiar with the terminology used in elementary engineering vibrations.

The objectives are twofold: first, to determine various dynamic loadings that can be derived from a shaking table to be applied to the model structures mounted on the table; second, to develop the instrumentation necessary to record the vibration characteristics of the shaking table and of the model structures.

The method of attack was to construct a shaking table to be connected to the floor by means of thin steel leaves. These leaves acted as the spring restoring force of the table. Loading was accomplished by suddenly breaking steel wires connected to the table. By varying the number of wires various type time-displacement functions were determined. These time-displacement functions were then used to excite a single-degree-of-freedom model structure which was instrumented to determine its response. The measured response was compared to the calculated response.

CHAPTER II

THE SHAKING TABLE

General Description of Shaking Table System

A shaking table was used as a source of base excitations for the model structures to be mounted on it. For convenience in construction, use, and ease of modification, the table was constructed of plywood. Three sheets of 3/4 in. (five-ply) plywood were glued and nailed together to form a stiff table 8 ft. long by 4 ft. wide by $2\frac{1}{4}$ in. thick. Four rectangular steel leaves, henceforth referred to as leaf springs, each 10 in. high by 3 in. wide and 1/8 in. thick were used as the spring restoring force of the table. Their design, based on a maximum horizontal table deflection of $\frac{1}{2}$ in., can be found in Appendix A. A photograph of the shaking table can be found in Fig. 1.

The response of the shaking table was caused by breaking a series of steel wires connected to it. The ends of the wires were clamped around steel pipes rigidly attached to one end of the table. A photograph of this attachment can be found in Fig. 2.

The system used to break the wires had to provide sufficient energy to break a large number of wires in a time short enough that the resulting loading to the table could be considered as an impulse load. A system that develops both high kinetic energy and high velocity could satisfy these conditions. A pendulum was used to develop the necessary energy and velocity. An 8I 18.4 beam, 85.7 in. long, was constructed so that one end was attached to an axle which was supported at the ceiling.

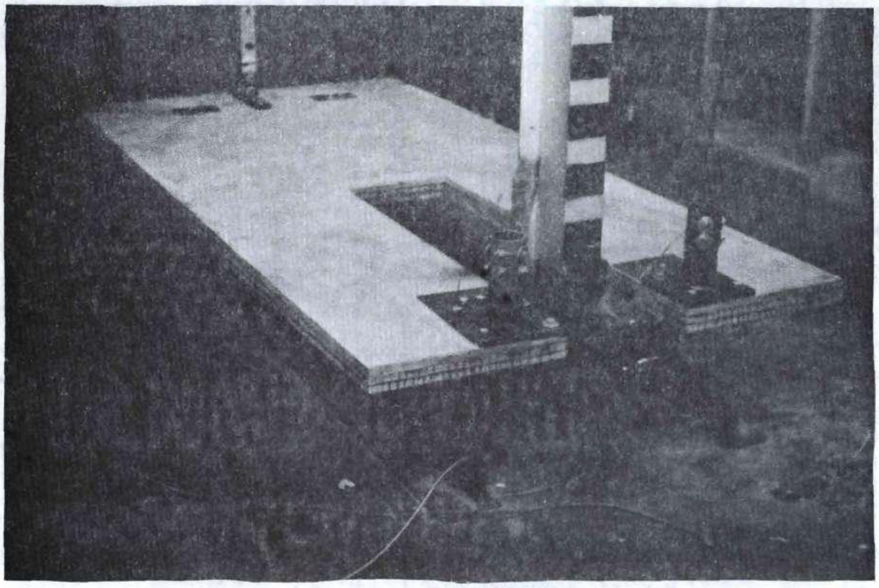

Figure 1. Shaking Table and Pendulum

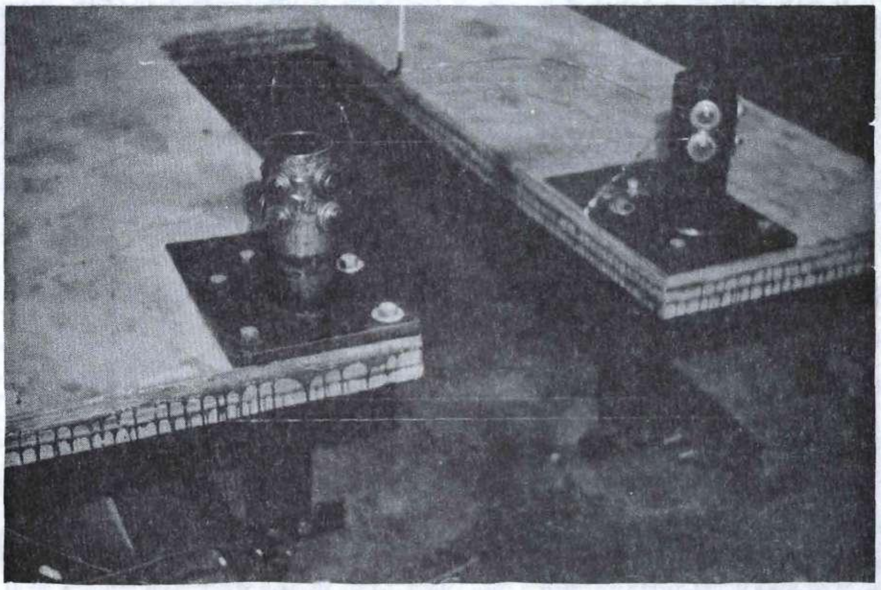

Figure 2. Connection of Wires to Shaking Table

The I-beam, henceforth to be referred to as the pendulum, was raised to a position of high potential energy above the level of the wires. Upon release, the pendulum swung down, converting its potential energy into kinetic energy. The system was arranged so that the pendulum struck the wires at the point of maximum kinetic energy, i.e. the vertical position of the pendulum.

Shaking Table and Applied Load Measuring Systems

To measure the motion of the shaking table, a series of strain gages were attached to the leaf-springs and electrically connected to one channel of a dual channel Sanborn model 60, recording galvanometer. Upon deflection of the table, the leaf-springs and correspondingly the strain gages were strained thereby causing the stylus of the Sanborn recorder to deflect and plot the time-deflection record of the table's motion.

A Helipot potentiometer was used to measure the angular motion of the pendulum. The armature of the potentiometer was attached to a rigid rod connected to the pendulum's axle by a stiff plastic tube. The tube fit tightly over both the armature and rigid rod. The potentiometer was electrically connected to the second channel of the Sanborn recorder. By measuring the final position of the pendulum both before and after breaking the wires, the amount of potential energy of the pendulum used to break the wires and move the table could be determined.

In order to assure that the load applied to the table was an impulse load, the time of the applied load had to be measured, i.e. the time of breaking the wires. To do this, a simple electrical circuit consisting of a battery and a resistor was constructed. The pendulum and wires served the function of a switch. When the pendulum contacted the wires, a current began to flow through the resistor. A Tektronix Type 531A oscilloscope was used to measure the voltage drop across the resistor. This voltage drop existed as long as the pendulum was in contact with the wires. When the wires broke, the current stopped flowing. The resulting trace on the oscilloscope screen appeared as a rectangular wave pulse. The time the pulse existed, and correspondingly the time of breaking the wires, could be measured directly from the oscilloscope screen.

A more detailed description of the shaking table's and pendulum's measuring devices and their calibration follows.

Response Measurements of Shaking Table

Discussion. The response of the shaking table induced by shock loading was measured by a full Wheatstone bridge circuit, i.e. four active SR-4 strain gages. This system is capable of measuring the deflection-time history of the shaking table. A schematic diagram of the circuit is shown in Fig. 3.

R_1, R_2, R_3, and R_4 are the SR-4 strain gages each equal to 120 ohms $\pm$ 0.2 ohms. The strain gage factor F, which is a property of the gages, is 2.06. R_L represents the resistance of the measuring device, in this case, the resistance of the Sanborn Strain Gage Amplifier and recording galvanometer. Compared to the resistance of the gages, R_L is large enough so that it may be considered as infinite. V represents the applied voltage.

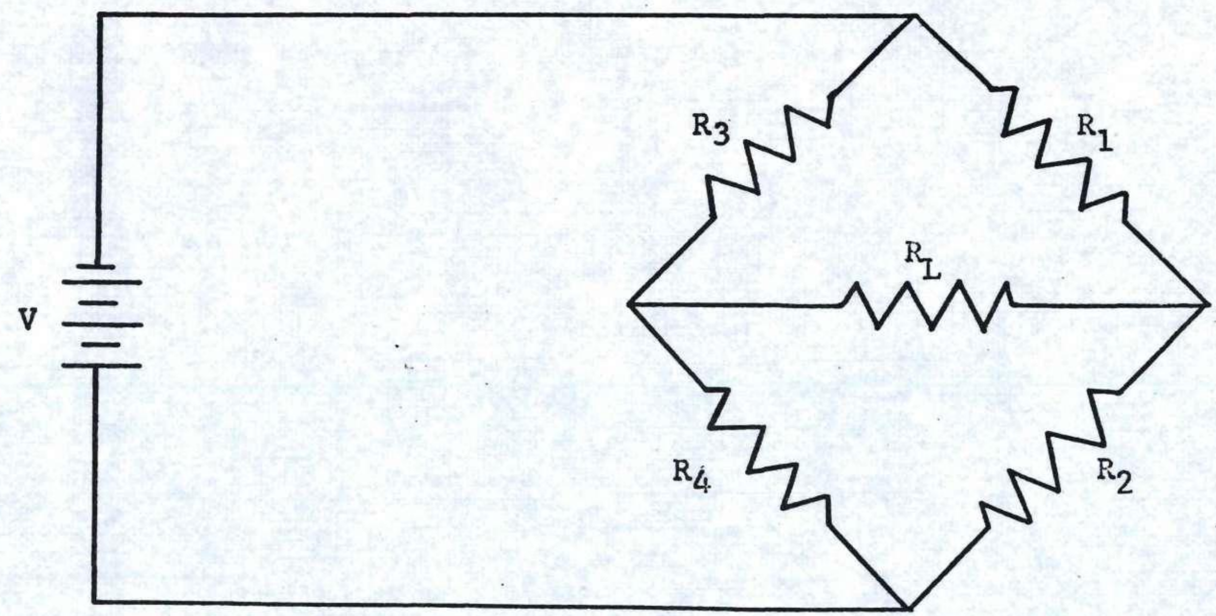

Figure 3. Wheatstone Bridge Circuit

The analysis of the full Wheatstone bridge circuit is well known (1). The result is an equation showing the relationship between the applied bridge strain and the voltage change across R_L such that

$$E_o = VF\left(\frac{e_1 - e_2 - e_3 + e_4}{4}\right) \tag{1}$$

where,

E_o = voltage change across R_L

e_1 = strain in gage R_1

e_2 = strain in gage R_2

e_3 = strain in gage R_3

e_4 = strain in gage R_4

For the purpose of measuring the deflection-time history of the table, Eq. 1 was only used qualitatively to determine the best arrangement of the SR-4 gages that would produce maximum read-out or maximum voltage change E_o. It is obvious that maximum E_o will occur when e_1 and e_4 are of the same type strain, while e_2 and e_3 are of the same type strain but of opposite sign than e_1 and e_4. It should be noted that the full Wheatstone bridge is temperature compensating. Provided all the gages undergo the same temperature change, they will undergo the same type and amount of strain, thereby resulting in a zero change in voltage as shown by Eq. 1.

The Wheatstone bridge was constructed so that the SR-4 strain gages would measure the strain induced in the leaf-springs by a deflection of the shaking table. In order to produce maximum read-out E_o, R_1, and R_4 had to simultaneously undergo a condition of strain, say tension, while R_2 and R_3 simultaneously undergo the strain condition

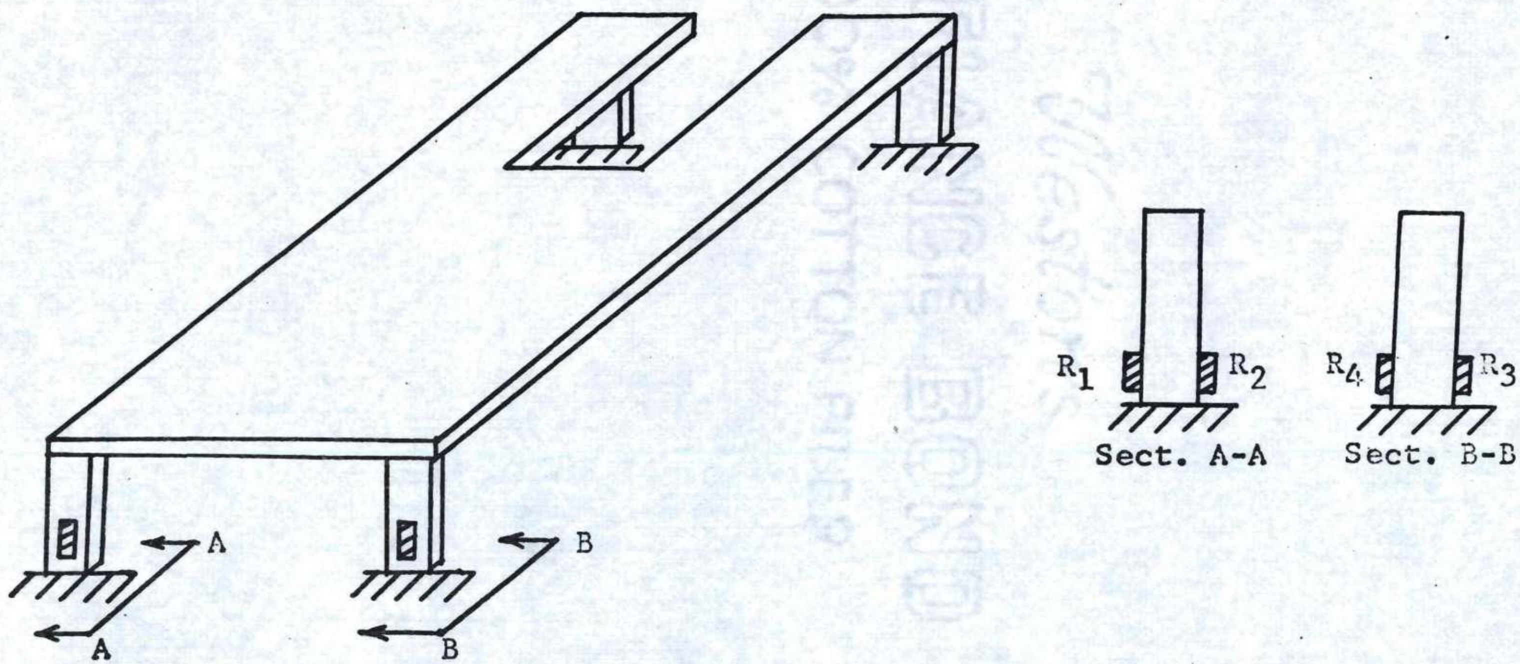

Figure 4. Arrangement of Wheatstone Bridge Circuit on Shaking Table

of compression, or vice versa. A schematic diagram showing the arrangement that accomplished this is shown in Fig. 4.

Now, assuming a deflected shape such that

$$e_1 = e_4 = +e, \text{ tension}$$

and $$e_2 = e_3 = -e, \text{ compression}$$

Eq. 1 results in

$$E_o = VFe \qquad (2)$$

The only problem that may arise is that the strain level, e, may not cause a voltage change, E_o, large enough to be measured. The sensitivity of the system, therefore, was checked at a minimum desirable table deflection of 0.01 in. as follows: Assuming complete fixity at both ends of the leaf-springs and neglecting the small effects of axial load, the maximum moment, M, as shown in Fig. 5, for a given d_r is

$$M = \frac{6E_s I_t d_r}{L^2} \qquad (3)$$

The corresponding maximum induced strain e_t is

$$e_t = \frac{f}{E_s} = \frac{\frac{MC}{I_t}}{E_s} = \frac{\frac{6E_s I_t d_r}{L_t^2} \cdot \frac{h_t}{2}}{E_s \, I_t}$$

and for d_r = 0.01 in. becomes

$$e_t = \frac{6d_r h_t}{2L_t^2} = \frac{6\,(.01)\,(1/8)}{2\,(10)^2} = 37.5 \times 10^{-6}\ \frac{\text{in.}}{\text{in.}}$$

So,

$$e = 37.5\ \frac{\text{micro-inches}}{\text{inch}}$$

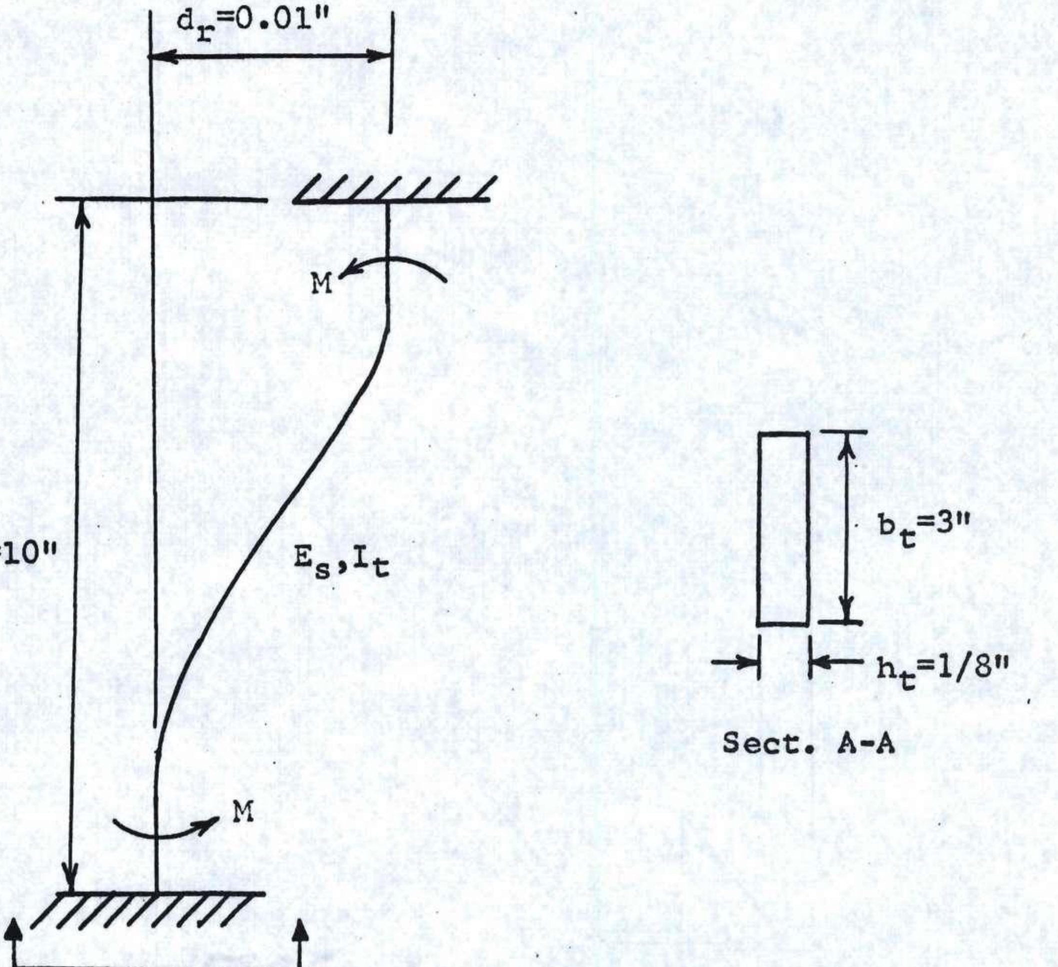

Figure 5. Deflected Shape of Table Leaf Springs

and

$$E_o = VFe = VF\,(.0000375) \tag{4}$$

Eq. 4 could be used to determine the necessary voltage, V, to produce a measurable voltage change, E_o. However, the Sanborn Strain Gage Amplifier supplies the necessary voltage such that 10 $\frac{\text{micro-inches}}{\text{inch}}$ strain causes a one-centimeter stylus deflection. As a result, the sensitivity of the system was sufficient to cause adequate stylus deflection to measure the minimum desirable table deflection.

A schematic diagram of the bridge hook-up with the amplifier is shown in Fig. 6. The TRANS socket is located on the amplifier.

Calibration. The calibration of the Wheatstone bridge and the Sanborn Strain Gage Amplifier was necessary to establish the correspondence between horizontal table deflection and stylus deflection.

The principle was to apply a known horizontal deflection to the table, U, and then adjust the amplifier to produce a desired stylus deflection, d, at a particular attenuation, A. The basic sensitivity, S, or the amount of table deflection per unit stylus deflection at an attenuation of 1 (position X1) was then calculated as

$$S = \left(\frac{U}{d}\right)\left(\frac{1}{A}\right) \frac{\text{inches}}{\text{block}} \tag{5}$$

Correspondingly, once the basic sensitivity had been established, the following formula was used to determine the deflection of the shaking table.

$$X_t = SdA \tag{6}$$

where,

X_t = horizontal deflection of table, inches,

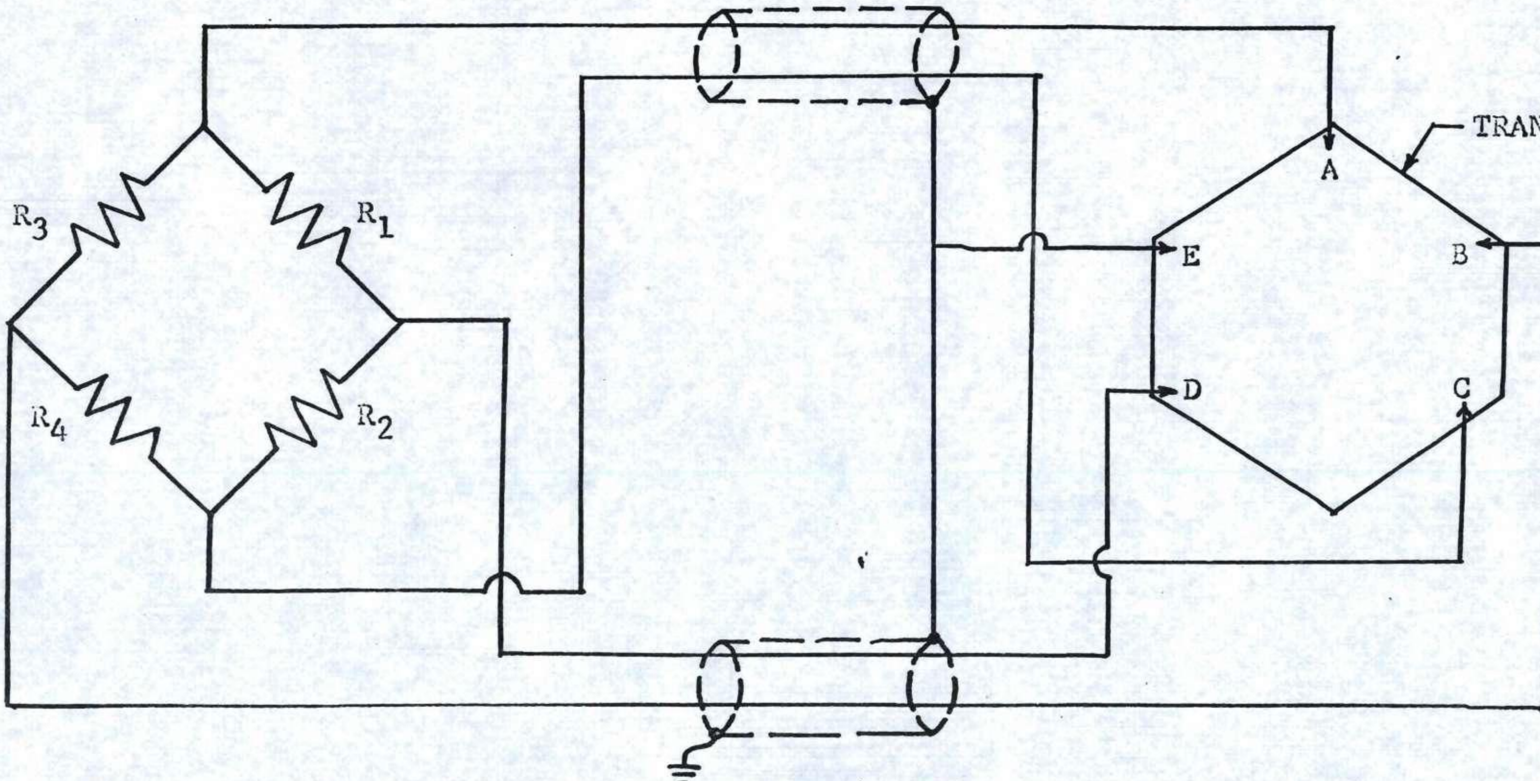

Figure 6. Wheatstone Bridge Connection to the Sanborn Strain Gage Amplifier

S = Basic sensitivity, inches/block,

d = stylus deflection, blocks

A = attenuation.

The steps followed to determine the procedure for calibration of the stylus were as follows:

1. The strain gage amplifier was first adjusted in accordance with Appendix B.
2. The ZERO control was adjusted to set the stylus at mid-scale of the read-out paper.
3. Since a maximum table deflection of approximately $\frac{1}{2}$ inch would be attained, the table was deflected U = 0.50 inches by advancing a nut along the threaded rod as shown in Fig. 7.
4. The ATTENUATOR and GAIN controls were then adjusted so that the stylus recorded at its maximum deflection on the recording paper, d = 25 blocks. It was found that an attenuation of A = 100 and no adjustment of the GAIN control accomplished this.
5. The basic sensitivity, therefore, was

$$S = \frac{(U)}{d}\ \frac{(1)}{A} = \frac{(0.50)}{25}\ \frac{(1)}{100}\ \frac{\text{inches}}{\text{block}}$$

The results of the preceding steps constituted a procedure that was used to calibrate the system before each test. It was as follows:

a. The strain gage amplifier was adjusted in accordance with Appendix B.

b. A base line was established with the ZERO control.

Therefore, the resulting basic sensitivity was

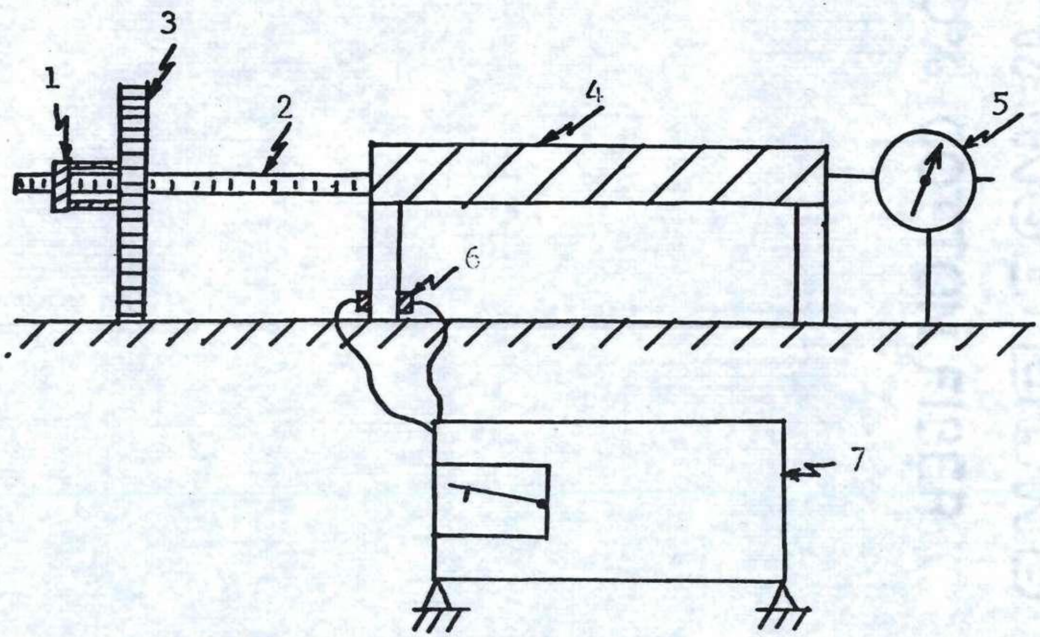

(1) nut

(2) threaded rod

(3) wall anchoring threaded rod

(4) shaking table

(5) dial gage

(6) SR-4 strain gages

(7) Sanborn Strain Gage Amplifier and recorder

Figure 7. Calibration of Deflection Measuring System for Shaking Table

$$S = 0.0002 \frac{\text{inches}}{\text{blocks}}$$

and correspondingly, the resulting table deflection was calculated as

$$X_t = (0.0002) \ d \ A \tag{7}$$

where,

X_t = table deflection, inches

d = stylus deflection, blocks

A = attenuation of strain gage amplifier.

Deflection Measurements of Pendulum

Discussion. The pendulum will not only be used as a source of applied load, but it will also be used to measure the total energy causing the table's motion.

To measure the total energy causing table motion, the pendulum was first released and allowed to swing to a position of maximum potential energy, say position θ_t, as determined by a read-out device. Wires were then attached to the table, after which the pendulum was again released, breaking the wires and rising to a new position of maximum potential energy, say position θ_b.

The angular difference, $\Delta\theta=\theta_t-\theta_b$, is a direct measure of the conversion of rotational energy of the pendulum into the energy causing table motion provided the following assumptions are made:

1. Energy losses due to friction in the bearings of the pendulum's axis and air resistance can be neglected since they occur whether or not wires are broken and are the same in each test.
2. Energy losses associated with induced vibrations in the pendulum, heat produced by breaking the wires, and deformations

of the pendulum upon breaking the wires are very small and can be neglected.

3. Other energy losses such as slippage of the wires at their supports, shock waves traveling through the table, table deformations, and strain energy in the leaf-springs during the application of the load are small enough so that they also can be neglected.

Therefore, the loss in potential energy of the pendulum as measured by $\Delta\theta$ is due to the breaking of the wires which is directly converted into the initial velocity of the table.

A system comprised of a Helipot potentiometer, which was connected to the axis of the rotating pendulum as previously described, and a Sanborn DC General Purpose Amplifier and recording galvanometer, which records the voltage changes ΔE, across the potentiometer, was used to measure θ_t and θ_b. A schematic diagram of the system can be found in Fig. 8. The initial position of the slider, SL, the value of the power supply voltage, E_s, and the attenuation of the DC amplifier were determined by trial and error to produce the maximum sensitivity of the system.

The results were that the slider, SL, needed to be near one end of the slide; the best power supply voltage, E_h, was six volts; and the DC amplifier attenuation was X2 with the SENSITIVITY control at full right.

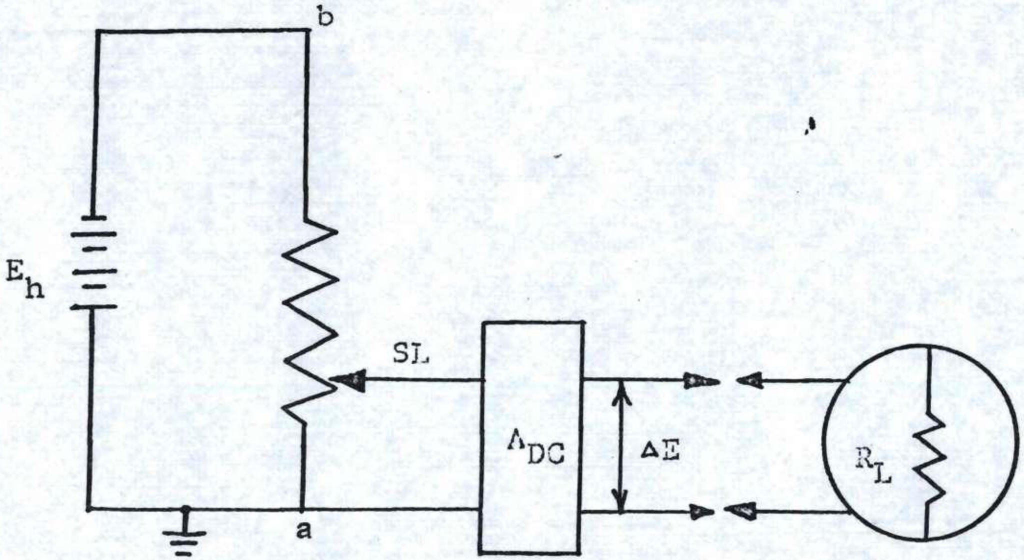

ab - Helipot Potentiometer, 10 turns, 1000 ohms

E_h - Hewlett Packard, Model 712B, power supply

A_{DC} - Sanborn DC General Purpose Amplifier

R_L - Sanborn Recording Galvanometer

Figure 8. Deflection Measuring Device for Pendulum

Calibration. The calibration of the pendulum's measuring system was accomplished by rotating the pendulum through a known angle, as measured by a transit, and noting the corresponding stylus deflection. Referring to Fig. 9, plane I is the plane of the rotating pendulum.

The transit was arbitrarily set up on a line perpendicular to plane I and passing through an arbitrary point (1a) which lies on the ℄ of the freely hanging pendulum. Distances a and r are measured. The pendulum was then rotated to various positions, say point (1b), at which the horizontal angle G was determined by sitting the transit on point (1b) and reading G directly from the transit. The horizontal displacement, Z, of point (1a) going from (1a) to (1b) is

$$Z = a \operatorname{Tan}(G) \tag{8}$$

The angular displacement, θ, corresponding to a horizontal displacement, Z, is

$$\operatorname{Sin} \theta = \frac{Z}{r} = \frac{a \operatorname{Tan}(G)}{r}$$

$$\theta = \operatorname{Sin}^{-1} \left(\frac{a \operatorname{Tan}(G)}{r}\right) \tag{9}$$

The angular displacement of the pendulum, θ, causes the armature of the potentiometer to rotate an equal angle θ, thereby resulting in a change in voltage in the potentiometer. The voltage change causes a stylus deflection of the Sanborn recording galvanometer of d blocks on the recording paper.

After a sufficient number of measurements of corresponding θ's and d's, a distribution of "C_p" vs. "Number of Occurrences" was plotted where C_p represents the calibration constant of the pendulum measuring

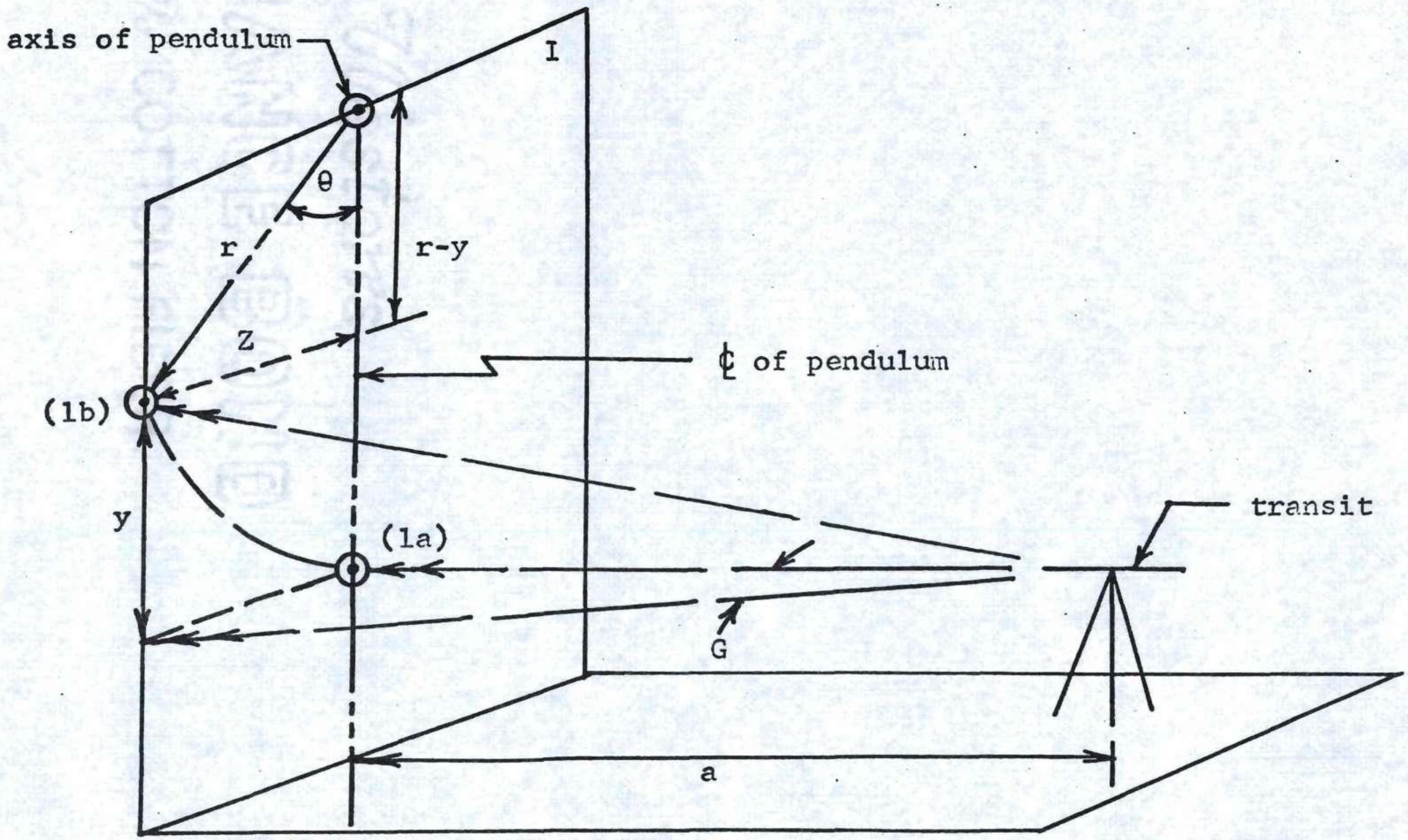

Figure 9. Calibration of Deflection Measuring Device for Pendulum

system, or

$$C_p = \frac{\theta}{N}, \frac{\text{degrees}}{\text{block}} \tag{10}$$

The results of the measurements are summarized in Appendix C.

The value of C_p was determined by assuming a normal distribution of the measured values and calculating the arithmetic mean, $\bar{C}_p$, and standard deviation, S_d. The result was that

$$\bar{C}_p = 4.1°/\text{block},$$

$$S_d = 0.144°.$$

Therefore, with a 95 per cent probability

$$C_p = M \pm 2S_d$$

or,

$$C_p = 4.1°/\text{block} \pm 0.3° \tag{11}$$

Time Measurements of Applied Load to Shaking Table

Discussion. The time of the applied load to the table, i.e. the time of breaking the wires, had to be found so that it could be determined whether or not the load could be considered as an impulse. To accomplish this, a simple electrical circuit consisting of a battery, E_v, and a resistor, R_t, was constructed. The pendulum and wires served the function of a switch, SW. When the pendulum contacted the wires, a current began to flow through the resistor. A Tektronix Type 531A oscilloscope, R_o, was used to measure the voltage drop across the resistor. The oscilloscope was adjusted so that the closing of the switch, SW, triggered the resulting trace while allowing only a single sweep. The voltage drop existed as long as the pendulum was in contact with the wires. When the wires broke, the current, I, stopped flowing. The resulting trace on the oscilloscope screen appeared as a rectangular wave pulse. The time the pulse existed, and correspondingly the time of breaking the wires, could be measured directly from the oscilloscope screen. A schematic diagram of the circuit can be found in Fig. 10.

Calibration. The oscilloscope was capable of directly measuring the elapsed time of an electrical signal from 0.1×10^{-6} sec. to 5.0 sec. The calibration of the oscilloscope was accepted as being correct.

Dynamic Properties of Shaking Table

Determination of Table Spring Constant

The shaking table was represented dynamically by an equivalent single-degree-of-freedom system as shown in Fig. 11. This was a reasonable approximation, especially since the entire mass of the system was essentially concentrated at the level of the table and also since the stiffness of the table has been shown to be large enough so that it could be considered as infinited when compared to the stiffness of the leaf-springs.

The first important parameter determined was the spring constant, K, or the amount of force required to produce a deflection, t, of the mass, M_t. The procedure followed to measure K was to apply a known force, Q, to the table, measure the resulting table deflection, X_t, and calculate the spring constant as

$$K = \frac{Q}{X_t} \ \frac{\text{lb.}}{\text{in.}} \qquad (12)$$

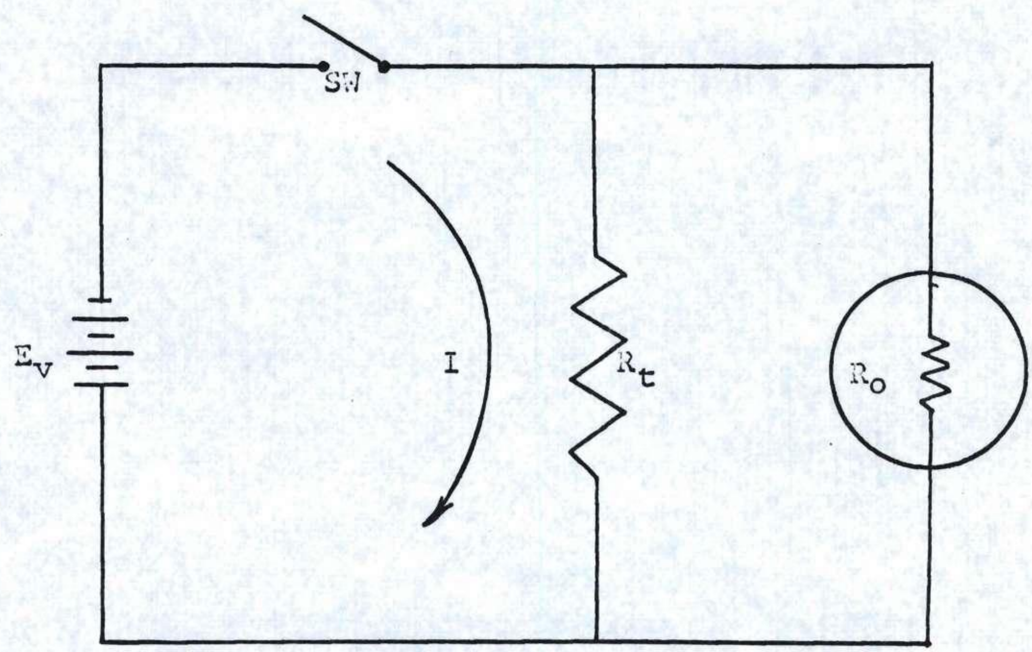

Figure 10. Device to Measure Time of Breaking Wires

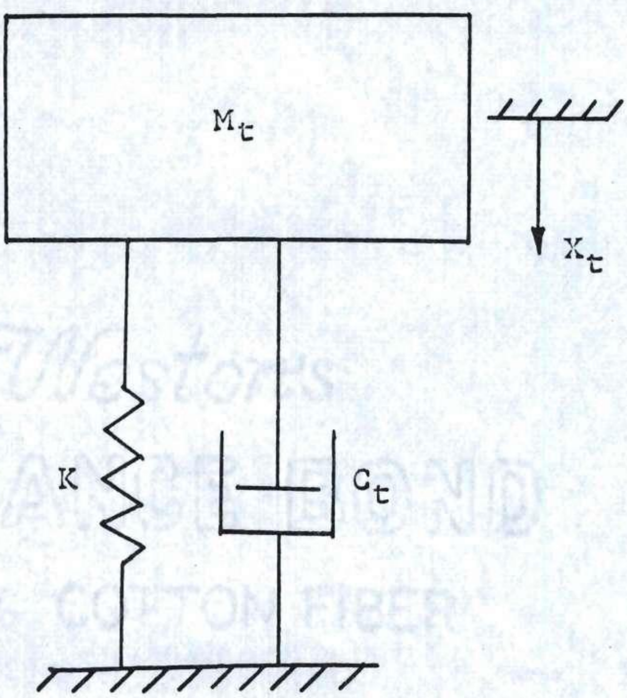

M_t - equivalent mass of table

K - spring constant

C_t - damping constant

X_t - deflection of M_t from its equilibrium position

Figure 11. Equivalent Single-Degree-of-Freedom Table System

A schematic diagram of the arrangement used to measure K is shown in Fig. 12. The horizontal force, Q, was applied by advancing a nut along a threaded rod, one end of which was anchored at a wall and the other end attached to the table. The force in the rod was measured by a dynamometer. The dynamometer, built and calibrated by Professor R. M. Dinnat, was used to measure the force in the rod. It consisted of a Wheatstone Bridge circuit attached to an aluminum bar and calibrated to operate with a Baldwin-Lima-Hamilton Type N strain indicator. The calibration constant, C_s, was

$$C_s = 0.956 \frac{\text{micro-inches/inch}}{\text{lb.}} \quad @ \quad F = 2.0$$

The deflection, X_t, of the table was measured by a Starrett dial gage with a least count of 0.001 inches.

After a sufficient number of measurements of corresponding Q's and X_t's, a statistical distribution of "K" vs. "Number of Occurrences" was plotted. The data, graph, and calculations are included in Appendix D. The spring constant was determined by assuming a normal distribution of data, calculating the arithmetic mean $\bar{K}$, and calculating the standard deviation, S_d. The results were that

$$\bar{K} = 796.7 \ \frac{\text{lb.}}{\text{in.}}$$

$$S_d = 9.2 \ \frac{\text{lb.}}{\text{in.}}$$

With a 95 per cent probability

$$K = \bar{K}_t \pm 2S$$

Therefore,

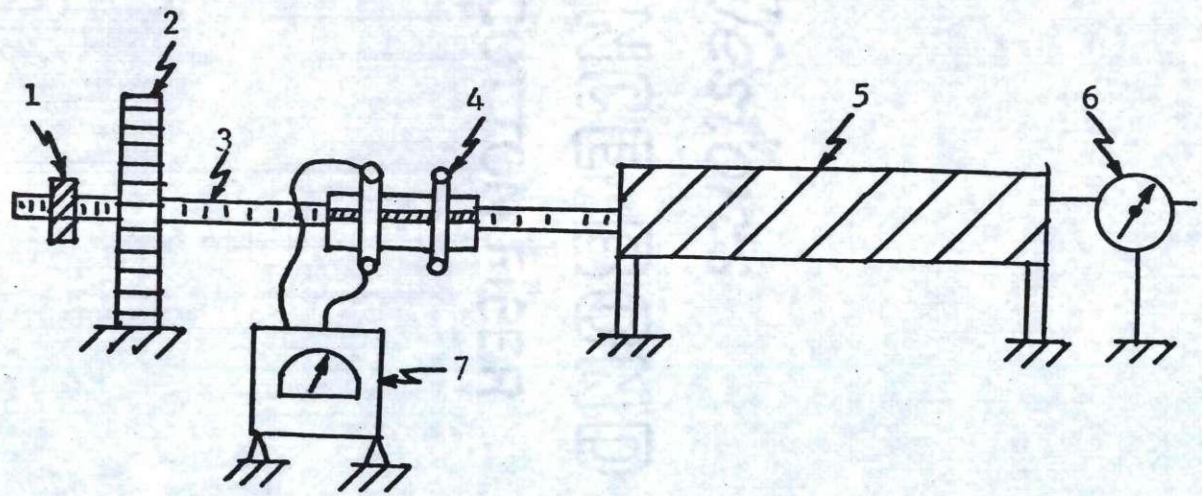

(1) nut
(2) wall
(3) threaded rod
(4) dynamometer
(5) shaking table
(6) dial gage
(7) strain indicator

Figure 12. Experimental Determination of the Table Spring Constant

$$K = 796.7 \ \frac{\text{lb.}}{\text{in.}} \pm 18.4 \ \frac{\text{lb.}}{\text{in.}} \tag{14}$$

<u>Determination of the Equivalent Mass, Natural Frequency, Weight, Damping Ratio, Critical Damping, and Damping Constant of the Shaking Table</u>

Other important parameters determined for the shaking table were the equivalent mass, M_t, natural frequency, q_t or f_t, weight, W_t, damping ratio or per cent of critical damping, Z_t, critical damping, C_{tcr}, and damping constant, C_t.

Since K is a linear function of table displacement, X_t, and assuming the damping constant to be a linear function of table velocity, $\dot{X}_t$, the equation of motion of the equivalent system as drawn in Fig. 11 due to some initial conditions of velocity, V_o, and displacement, X_o, is

$$M_t \ddot{X}_t = -K X_t - C_t \dot{X}_t \tag{15}$$

Rearranging and dividing by M_t results in

$$\ddot{X}_t + \frac{C_t}{M_t}\dot{X}_t + \frac{KX_t}{M_t} = 0 \tag{16}$$

The solution of Eq. 16 is well known (2) and is

$$X_t = \sqrt{\left[\frac{V_o + Z_t q_t X_o}{q_t\sqrt{1-Z_t^{\,2}}}\right]^2 + X_o^{\,2}} \quad e^{-Z_t q_t t} \quad \mathrm{Sin}\left(\sqrt{1-Z_t^{\,2}} \quad q_t t + \phi\right) \tag{17}$$

where,

X_t = displacement of any time t of table.

$$q_t = \sqrt{\frac{K}{M_t}}$$

$$\theta = \mathrm{Tan}^{-1}\left(\frac{X_o q_t \sqrt{1-Z_t^2}}{V_o + Z_t q_t X_o}\right)$$

$$C_{tcr} = 2M_t\ q_t$$

$$Z_t = \frac{C_t}{C_{crt}} = \frac{C_t}{2M_{tqt}}$$

The frequency of oscillation, f_t, of Eq. 17 s a function of both q_t and Z_t such that

$$2\,\pi f_t = \sqrt{1-Z_t^2}\ q_t$$

or,

$$f_t = \frac{\sqrt{1-Z_t^2}\ q_t}{2\pi} = \text{damped natural frequency, } \frac{\text{cycles}}{\text{sec.}} \tag{18}$$

The damped natural frequency can be measured directly by the Sanborn recorder for a free vibration of the table. Before M_t can be determined, however, the damping ratio Z_t must be found.

Eq. 17 is an exponentially decaying function such that

$$X_{n+1} = X_n\ e^{-Z_t} \tag{19}$$

where X_{n+1} and X_n represent two adjacent peak amplitudes of Eq. 17. X_{n+1} and X_n could have been measured by the Sanborn recorder and Z_t calculated by Eq. 19. However, due to small inaccuracies in the measuring system itself, a longer time was allowed between measurements of amplitudes for better results.

Expanding Eq. 19 results in a pattern that was used to determine the general formula for the relationship between two non-adjacent amplitudes as follows:

$$X_{n+1} = X_n e^{-Z_t},$$

$$X_2 = X_1 e\text{-}Z_t,$$

$$X_3 = X_2 e^{-Z_t} = X_1 (e^{-Z_t})^2,$$

$$X_4 = X_3 e^{-Z_t} = X_1 (e^{-Z_t})^3,$$

$$\vdots$$

$$X_i = X_1 (e^{i-1})^{-Z_t}, \quad @\ i^{\underline{th}} \text{ peak amplitude} \tag{20}$$

Solving Eq. 20 for Z_t,

$$\text{Ln} \frac{X_1}{X_i} = (i-1) Z_t$$

$$Z_t = \frac{1}{i-1} \text{ Ln } \left(\frac{X_1}{X_i}\right) \tag{21}$$

where,

Z_t = damping ratio,

X_1 = amplitude of arbitrarily chosen 1^{st} cycle,

X_i = amplitude of i^{th} cycle.

Once the damped natural frequency, f_t, and damping ratio, Z_t, had been determined, the equivalent mass, M_t, and weight, W_t, were calculated as follows:

$$2\pi f_t = \sqrt{1-Z_t^2}\ q_t$$

but,

$$q_t = \sqrt{\frac{K}{M_t}}$$

so,

$$2\,\pi f_t = \sqrt{1-Z_t^{\,2}}\;\sqrt{\frac{K}{M_t}} \;.$$

and,

$$M_t = \frac{(1-Z_t^{\,2})\;K}{(2\,\pi f_t)^2} \tag{22}$$

also,

$$W_t = \frac{M_t}{g} \tag{23}$$

where g = acceleration due to gravity.

The procedure used to determine these parameters was to apply an arbitrary set of initial conditions, velocity and displacement, to the table and record the resulting free vibration with the Sanborn recorder. The damped natural frequency, f_t, was determined directly from the recording by counting the number of cycles per second. From the same recording amplitude, X_1 and X_i were chosen and Eq. 21 applied to calculate the damping ratio, Z_t. Since the spring constant, K, had previously been determined, the equivalent mass, M_t, and weight, W_t, were then calculated by Eqs. 22 and 23.

The data and calculations are tabulated in Appendix E. Five tests were run and the arithmetic mean of each of the parameters calculated are as follows:

$$f_t = 5.45 \ \frac{\text{cycles}}{\text{sec.}}$$

$$q_t = 34.32 \ \frac{\text{radians}}{\text{sec.}}$$

$$M_t = 0.676 \ \frac{\text{lb.-sec.}^2}{\text{in.}}$$

$$W_t = 261.2 \ \text{lb.}$$

$$Z_t = 6.7 \text{ per cent}$$

$$C_{tcr} = 46.4 \ \frac{\text{lb.-sec.}}{\text{in.}}$$

$$C_t = 3.1 \ \frac{\text{lb.-sec.}}{\text{in.}}$$

CHAPTER III

THE MODEL

Design of the Model

A single-degree-of-freedom model structure was designed so that instrumentation could be developed to measure the model's response. It was desired that the shaking table act as the source of base excitation for the model and not to have the model appreciably effect the motion of the shaking table. The model was designed so that its natural frequency closely matched the natural frequency of the shaking table, thereby resulting in a model response approaching resonance.

The design of the model was based on a simple cantilever aluminum leaf-spring with a relatively heavy mass at the free end. Referring to Fig. 13, the length, L_m, width, b_m, and thickness, h_m, of the leaf-spring and the weight, W_m, of the equivalent mass had to be determined so that the natural frequency of the model would be

$$q_m = 34.32 \, \frac{\text{radians}}{\text{sec.}} \tag{24}$$

The equivalent mass of the model is represented by M_m. The stiffness of the leaf-spring is represented by k. The deflection of the mass is represented by X_m.

The stiffness, k, of the leaf-spring is defined as the ratio of the load Q, required to produce a deflection U, to the deflection U, or,

$$k = \frac{Q}{U} \tag{25}$$

The deflection, U, of the end of a simple cantilever of length L_m, due to a load Q, applied at the end, is well known (3) and is

$$U = \frac{QL_m^3}{3E_aI_m} \tag{26}$$

where,

E_a = modulus of elasticity of aluminum,

I_m = moment of inertia of the leaf-spring.

Substituting Eq. 26 into Eq. 25 results in

$$k = \frac{3E_aI_m}{L_m^3} \tag{27}$$

The model's natural frequency, q_m, is defined as

$$q_m = \sqrt{\frac{k}{M_m}} = \sqrt{\frac{k\,g}{W_m}} \tag{28}$$

where,

$$g = 386 \frac{\text{in.}}{\text{sec.}^2} = \text{acceleration due to gravity}$$

Substituting Eqs. 24 and 27 into Eq. 28 and solving for the required moment of inertia results in

$$I_m = (34.32)^2 \frac{W_mL_m^3}{3E_ag} \tag{29}$$

For the rectangular leaf-springs as shown in Fig. 13

$$E_a = 10\text{x}10^6 \text{ psi.}$$

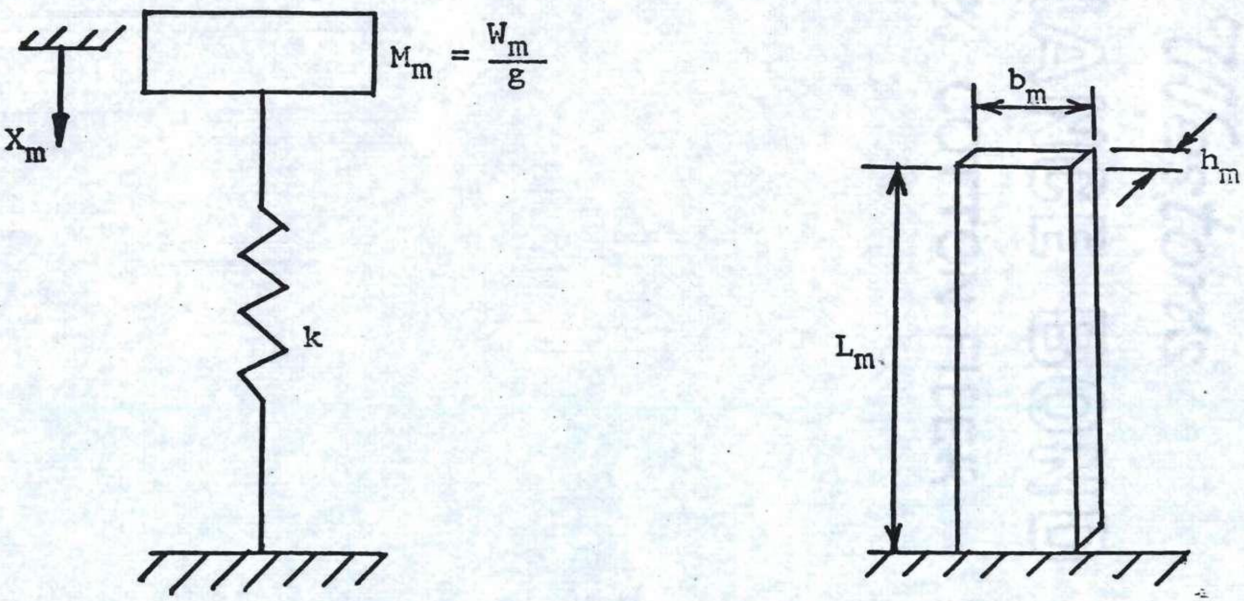

Figure 13. Equivalent Model and Actual Model Leaf-Spring

$$I_m = \frac{b_m h_m^3}{12},$$

and when substituted into Eq. 29 results in a required width, b_m, of

$$b_m = 12.2x10^{-7} \left(\frac{L_m}{h_m}\right) W_m \tag{30}$$

From a materials availability standpoint, it was convenient to choose a value for the thickness, width, and length of the leaf-spring such that

$$h_m = 1/8 \text{ inch},$$

$$b_m = 2 \text{ inches},$$

$$L_m = 12 \text{ inches}.$$

The resulting equivalent weight is

$$W_m = 1.85 \text{ lb.} \tag{31}$$

The equivalent weight of the model is composed of two parts. One part is the weight, W, of the mass at the free end of the leaf-spring. The other part is the per cent of the leaf-spring's weight that can be assumed to act at the position of the mass in contributing to the natural frequency of the model. The contribution of the leaf-spring's weight was taken as 24.27 per cent (4). Therefore, since the unit weight of aluminum is 0.095 $\frac{\text{lb.}}{\text{in.}^3}$,

$$W_m = W + (0.2427)\,(b_m h_m L_m)\,(0.095) \tag{32}$$

The width, thickness, and length of the leaf-spring have already been chosen. Substituting these values and Eq. 31 into Eq. 32 and solving for W, the weight of the mass at the free end of the leaf-spring results in

$$W = 1.78 \text{ lb.} \tag{33}$$

A detailed sketch of the model and its connection to the shaking table can be found in Fig. 14. A photograph of the model in place is shown in Fig. 15. The mass at the end of the leaf-spring was made of two blocks of lead which were ground down so that the total weight of the lead and the bolts connecting the lead to the leaf-spring was 1.78 lb.

It was obvious that the real model would not act exactly as the ideal model was designed since the mass was considered as a point mass and the base of the leaf-spring was considered to be completely fixed. However, once the model was instrumented, the equivalent mass, M_m, and spring constant, k, could be determined experimentally.

Response Measurements of Model

Description

The response of the model was measured by two independent system.

One system consisted of a CEC Type 4-275-0002 Piezo-electric Accelerometer, mounted on the model, and a CEC Type 1-304-0001 Source Follower, electrically connected to a Tektronix Type 503 Oscilloscope. This system was capable of measuring directly the acceleration-time history of the model. This record was traced on the oscilloscope screen and photographed by a Polaroid camera. The resulting plot was retraced on a set of coordinate axes with the proper scale. It was then compared to the acceleration-time history derived from a theoretical analysis of the two mass system of model and table as will be described in Chapter V. A sketch of the connection circuit is shown in Fig. 16.

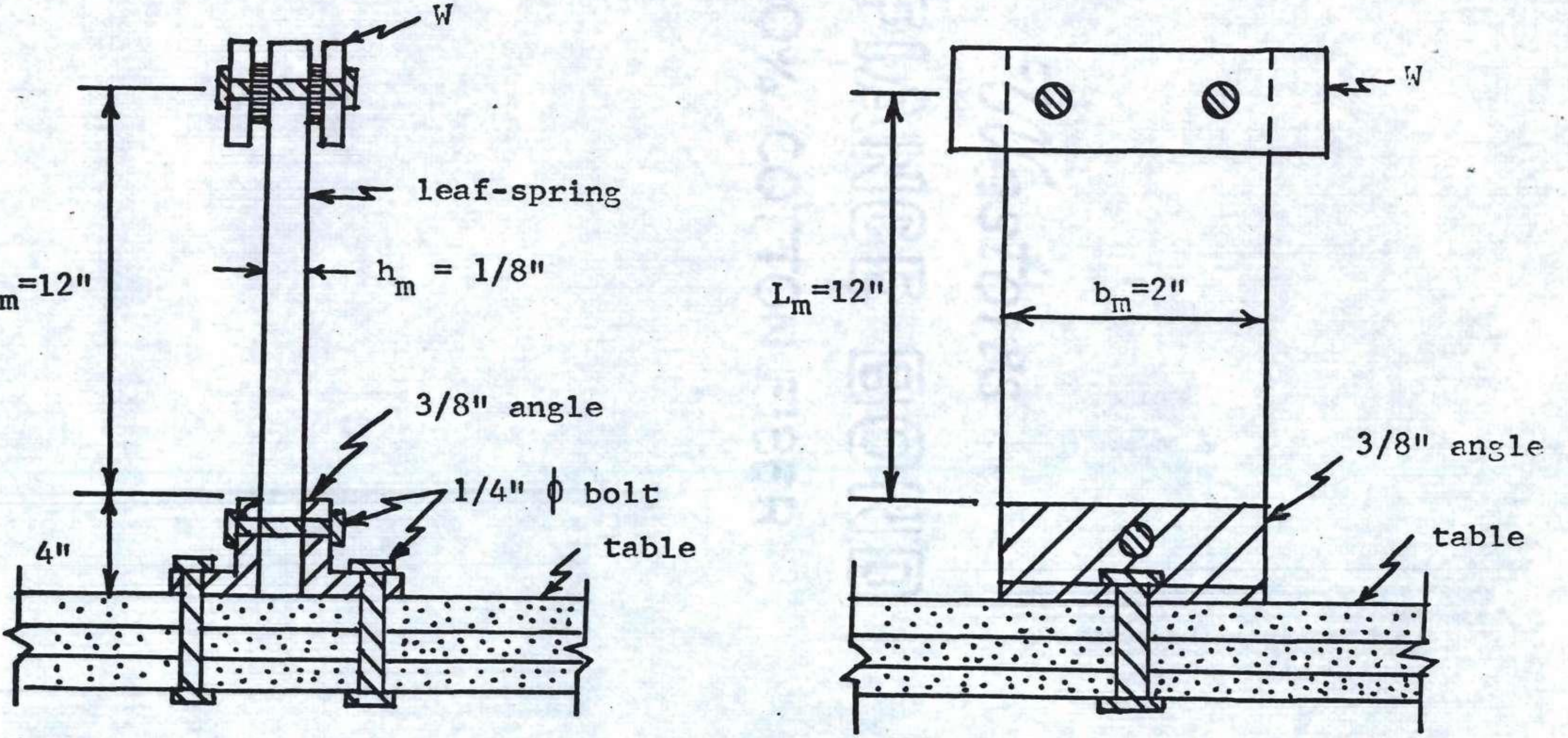

Figure 14. Details of Model

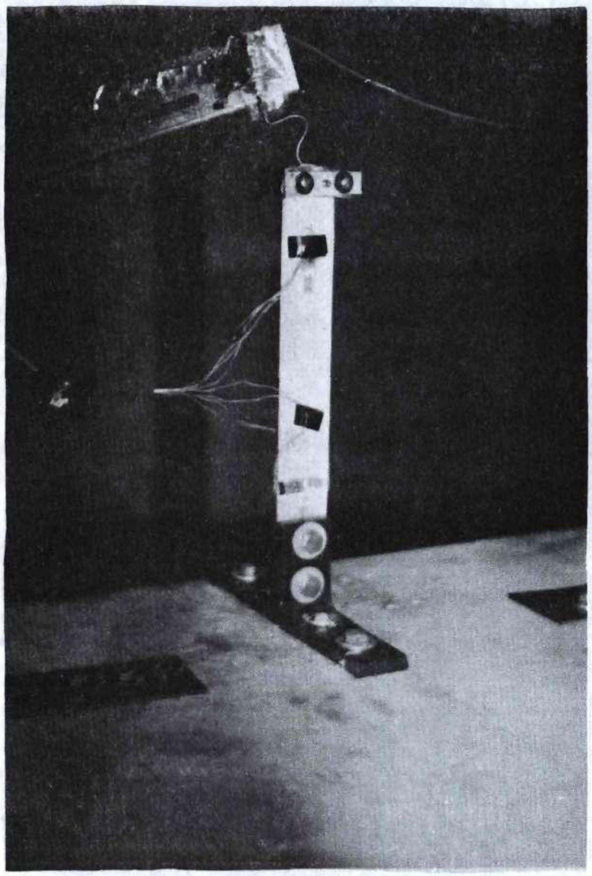

Figure 15. Model in Place on Shaking Table

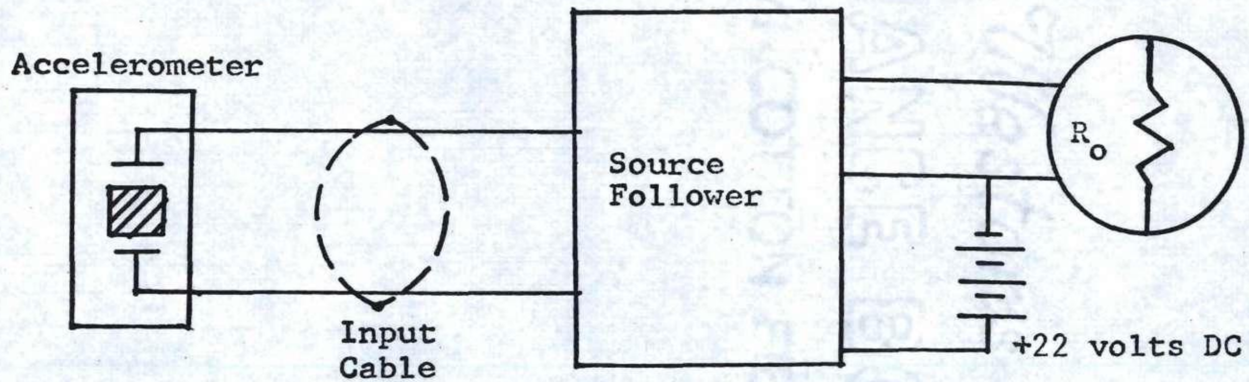

Figure 16. Accelerometer Connection Circuit

The second system of model measurement consisted of a full Wheatstone bridge circuit mounted on the leaf-spring of the model. It is important to note that this system measures the relative displacement between the shaking table and the mass at the free end of the leaf-spring. A schematic diagram of the circuit is shown in Fig. 3. The bridge circuit theory has been covered in Chapter I. The gages were mounted such that R_1 and R_2 were on the same side of the leaf-spring, while R_3 and R_4 were on the opposite side from R_1 and R_2. A schematic diagram of this arrangement is shown in Fig. 17.

The location, a_1, of R_1 and R_3 and the location, a_2, of R_2 and R_4 was selected so that the expected large displacements of the model did not cause strains greater than $1000\text{x}10^{-6}$ $\frac{\text{inches}}{\text{inch}}$ in the strain gages. These locations were based on the yield stress, f_y, of the aluminum leaf-spring being at maximum stress level where

$$f_y = 35{,}000 \text{ psi.}$$

The length, L_m, of the leaf-spring is 12 inches. The distance from the free end of the leaf-spring will be designated by A_3. The modulus of elesticity of aluminum, E_a, is $10\text{x}10^6$ psi. Since the maximum stress at any section, $f(a_3)$, is a linear function of the distance from the free end such that

$$f(a_3) = \frac{f_y}{L_m} a_3 \qquad (34)$$

then the strain at any section, $e(a_3)$, is

$$e(a_3) = \frac{1}{E_a} \frac{f_y}{L_m} a_3 \qquad (35)$$

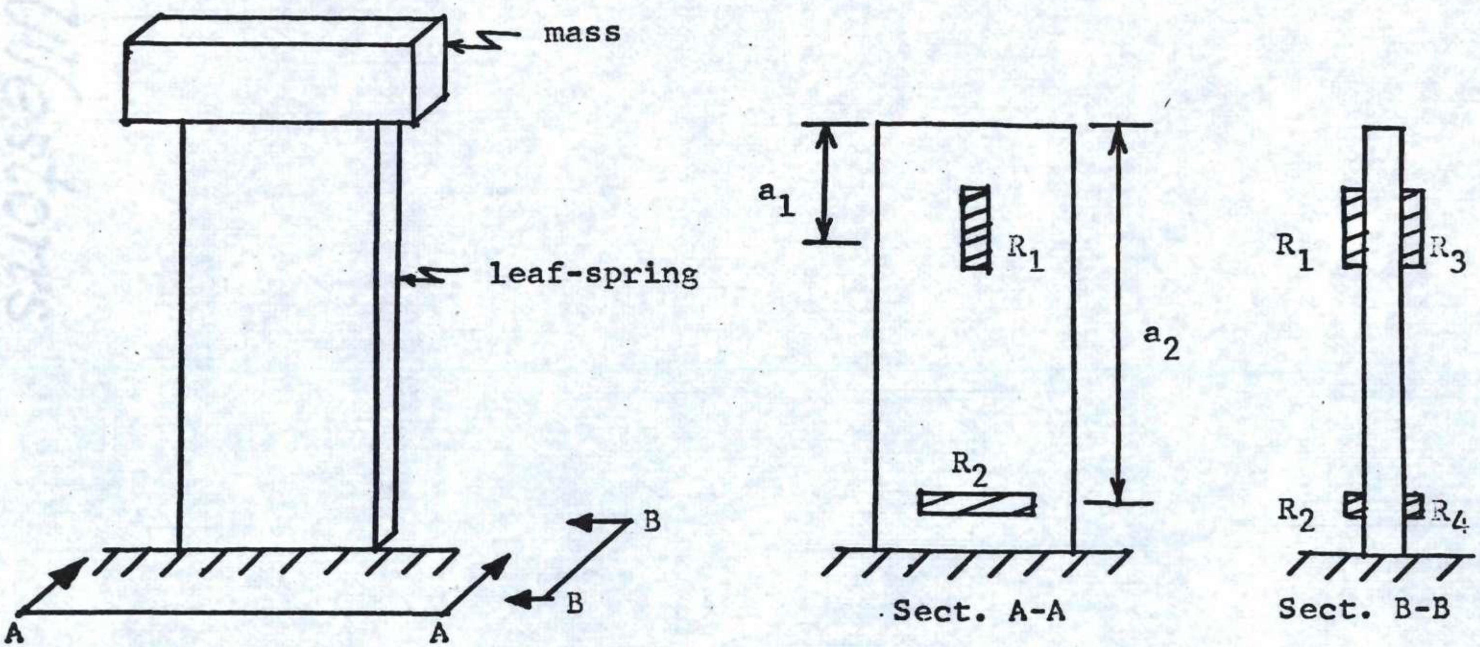

Figure 17. Wheatstone Bridge Circuit Mounted on Model

It is desired that the strain in gages R_1, R_2, R_3, and R_4 be limited to 1000×10^{-6} $\frac{\text{inches}}{\text{inch}}$. So, considering R_1 and R_3,

$$e(a_1) = \frac{1}{E_a} \quad \frac{f_y}{L} \; a_1 \quad 1000 \times 10^{-6}$$

or,

$$a_1 \le 3.43 \text{ inches.}$$

Gages R_2 and R_4 measure Poisson's effect where Poisson's ratio was taken to be 0.2. So,

$$e(a_2) = \frac{1}{E_a} \quad \frac{f_y}{L_m} \; a_2 \le \frac{1000 \times 10^{-6}}{0.2}$$

or,

$$a_2 \le 17.15 \text{ inches.}$$

The locations selected are as follows:

$$a_1 = 3.4 \text{ inches} \tag{36}$$

$$a_2 = 10.5 \text{ inches} \tag{37}$$

A second strain gage amplifier was not available. Therefore, a Sanborn Model 311A Transducer Amplifier, henceforth referred to as the preamplifier, was used to convert the Sanborn DC amplifier into a strain gage amplifier. A schematic diagram of the bridge connection to the preamplifier is shown in Fig. 18 The socket is found at the rear of the preamplifier.

<u>Calibration</u>. The calibration of the accelerometer was not carried out since special equipment would have been needed and was not available at the time. However, since the accelerometer was new and

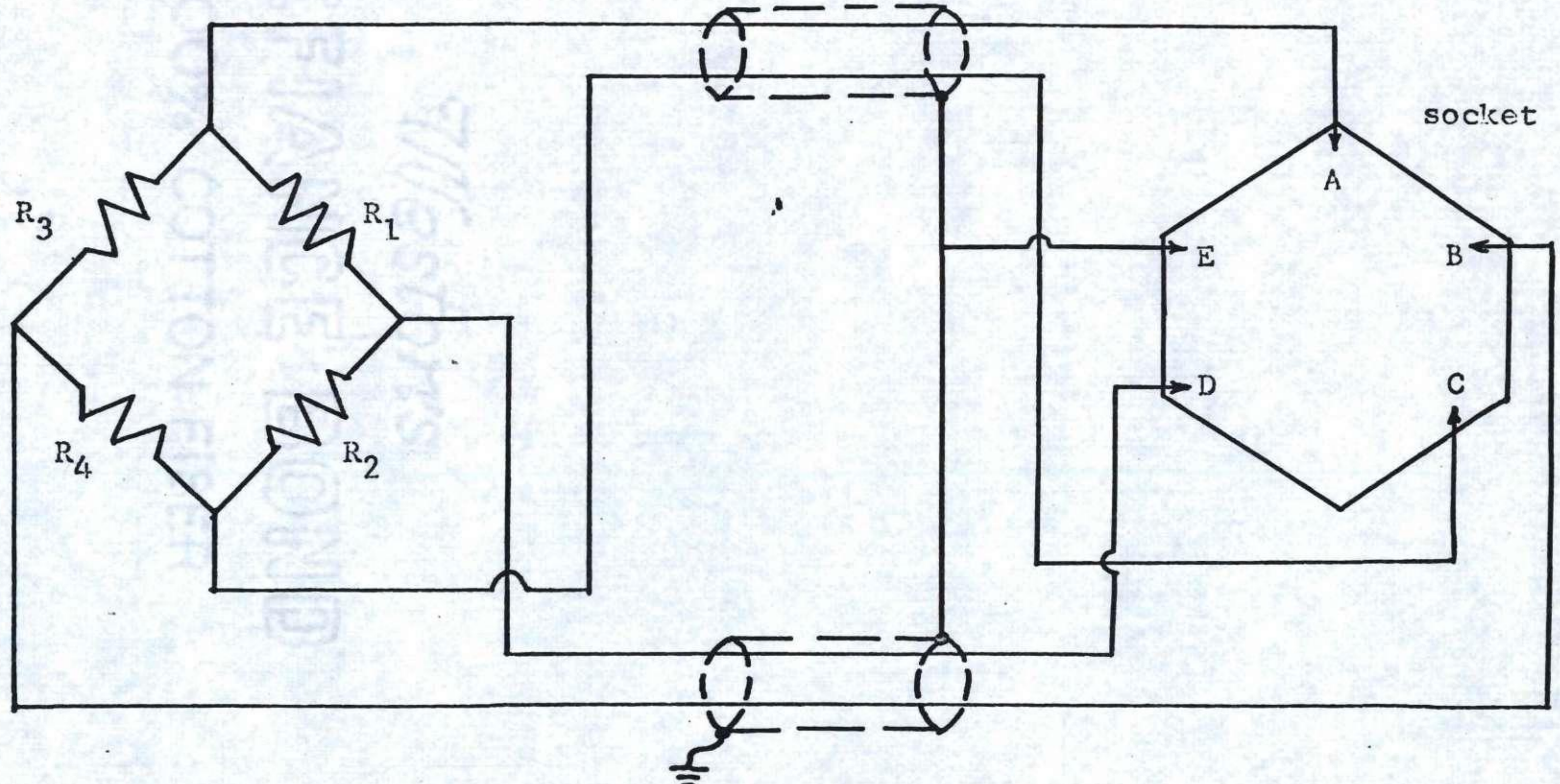

Figure 18. Wheatstone Bridge Connection to the Sanborn Preamplifier

had not been used previously, the manufacturer's calibration constant, C_a, was accepted as being correct. It was

$$C_a = 6.3 \times 10^{-3} \text{ volts/g.}$$

The calibration of the Wheatstone bridge circuit attached to the model's leaf-spring was necessary to determine the correspondence between stylus deflection of the DC amplifier and the relative displacement, D_r, between the mass and table.

The procedure followed was essentially trial and error. With the base of the model fixed against movement and no strain in the bridge, the preamplifier was balanced in accordance with Appendix F, and the DC amplifier was balanced in accordance with Appendix G.

The attenuator of the DC amplifier was then stepped through its range beginning with position X_1. At each step, the preamplifier's attenuator was rotated through its full scale. It was desired to find the most sensitive DC amplifier attenuation at which the stylus did not deflect upon rotating the preamplifier's attenuator. The result was that a DC amplifier attenuation of X50 was possible without any stylus deflection upon rotation of the preamplifier's attenuator through its full range.

The following steps were then taken to determine the procedure to be used before each test for the calibration of this system:

1. The DC amplifier was balanced in accordance with Appendix G and the preamplifier balanced in accordance with Appendix F.
2. The DC amplifier's attenuator was set at position X50.
3. The CENTERING control of the DC amplifier was adjusted to set

the stylus at mid-scale of the read-out paper, while the SENSITIVITY control was at full right.

4. The preamplifier's attenuator, B, was set at X20 and SENSITIVITY control at full right.

5. With the base of the model fixed against movement, the mass was deflected a known amount, U = 0.50 in.

6. It was noted that the stylus deflection, d, was 16 2/3 blocks.

7. The basic sensitivity, therefore, was

$$S = \left(\frac{U}{d}\right) \left(\frac{1}{B}\right) = \frac{0.50}{16.67} \; \frac{1}{20} \; \frac{\text{inches}}{\text{blocks}}$$

The results of the preceding steps was a procedure that was used to calibrate the system before each test. It is as follows:

a. The Sanborn DC amplifier was adjusted in accordance with Appendix G.

b. The preamplifier was adjusted in accordance with Appendix F.

c. The SENSITIVITY controls of both the DC amplifier and preamplifier were set at full right.

d. The attenuator of the DC amplifier was set at X50.

The resulting basic sensitivity was

$$S = 0.0015 \; \frac{\text{inches}}{\text{blocks}}$$

and correspondingly, the resulting relative displacement between the mass and the model's base, i.e. the shaking talbe, was calculated as

$$D_r = (0.0015) \; d \; B \qquad (38)$$

where,

D_r = relative displacement between mass and table, inches.

d = stylus deflection, blocks

B = attenuation of preamplifier

Dynamic Properties of Model

Determination of Model Spring Constant

The model spring constant, k, or the amount of force required to produce a deflection, X_m, of the mass, M_m, was determined experimentally. The procedure followed to measure k was to apply a known force, Q, to the free end of the model and to measure the resulting deflection, X_m, at the free end of the model, i.e. the position of the mass. The spring constant was then calculated as

$$k = \frac{Q}{X_m} \quad \frac{\text{lb.}}{\text{in.}} \tag{39}$$

A schematic diagram of the arrangement used to measure k is shown in Fig. 19. The base of the model was prevented from moving by fixing it to a vertical wall. The mass at the free end of the model was removed and, in its place, was attached a tray. The force, Q, was applied by placing known weights on the tray. The deflection, X_m, was measured by a Starrett dial gage, with a least count of 0.001 inches.

After a sufficient number of measurements of corresponding Q's and X_m's, a statistical distribution of "k" vs. "Number of Occurrences" was plotted. The data, graph, and calculations are included in Appendix H. The spring constant was determined by assuming a Normal distribution of data, calculating the arithmetic mean $\bar{k}$, and calculating

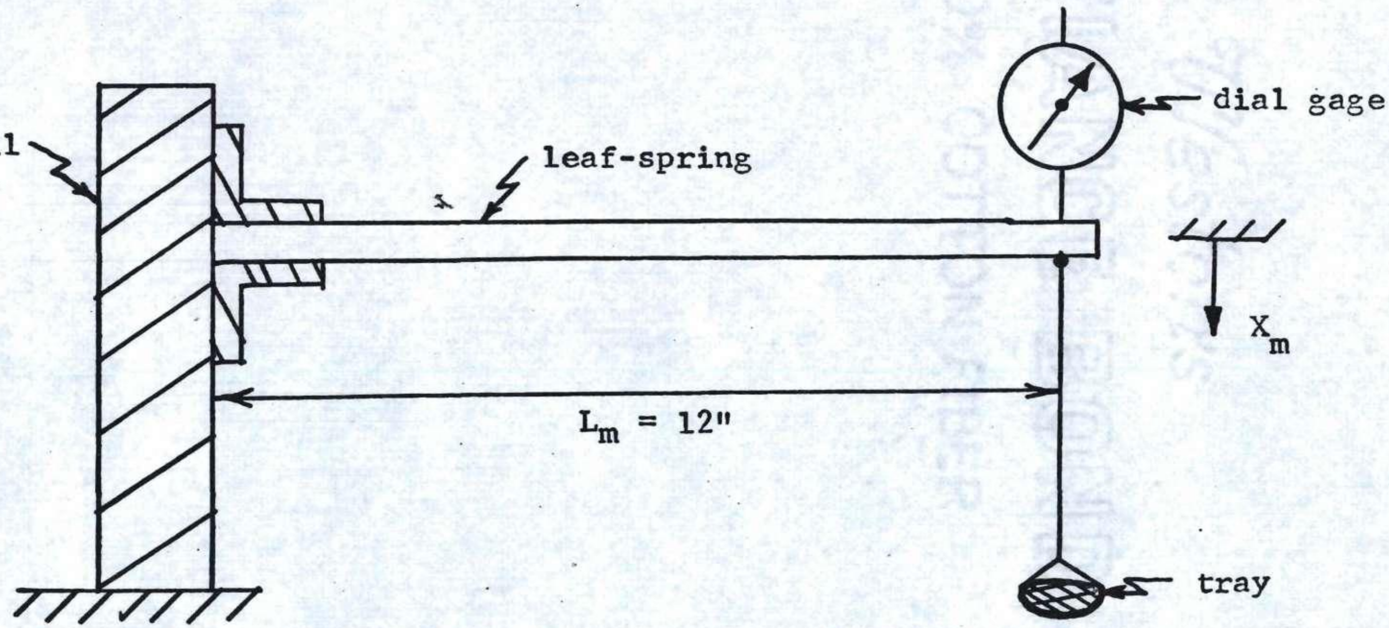

Figure 19. Experimental Determination of the Model Spring Constant, k

the standard deviation, S_d. The results were that

$$\bar{k} = 5.63 \ \frac{\text{lb.}}{\text{in.}}$$

$$S_d = 0.15 \ \frac{\text{lb.}}{\text{in.}}$$

With a 95 per cent probability

$$k = \bar{k} \pm 2S_d \tag{40}$$

Therefore,

$$k = 5.63 \ \frac{\text{lb.}}{\text{in.}} \pm 0.30 \ \frac{\text{lb.}}{\text{in.}} \tag{41}$$

Determination of the Equivalent Mass, Natural Frequency, Weight, Damping Ratio, Critical Damping, and Damping Constant of Model

The other dynamic properties of the model determined experimentally were the equivalent mass, M_m, natural frequency, q_m, or f_m, weight, W_m, damping ratio or per cent of critical damping, Z_m, critical damping, C_{mcr}, and damping constant, C_m.

The theoretical development leading to the formulae necessary to calculate these parameters has been covered in Chapter II and will not be repeated here. Only the results will be used.

With the mass put back in place, the procedure followed to determine these parameters was to apply an arbitrary set of initial conditions, velocity and displacement, to the model. The resulting free vibration was recorded by the Sanborn recorder. The damped natural frequency, f_m, was determined directly from the recording by counting the number of cycles per second. From the same recording, amplitude X_1 and X_i were chosen, and Eq. 21 applied to calculate the damping ration, Z_m. Since the spring constant, k, had previously been determined, the equivalent mass, M_m, and weight, W_m, could then be calculated by Eqs. 22 and 23.

The data and calculations are tabulated in Appendix J. Five tests were run and the arithmetic mean of each of the parameters calculated are as follows:

$$f_m = 5.10 \ \frac{\text{cycles}}{\text{sec.}}$$

$$q_m = 32.04 \ \frac{\text{radians}}{\text{sec.}}$$

$$M_m = 0.00548 \ \frac{\text{lb.-sec.}^2}{\text{in.}}$$

$$W_m = 2.12 \text{ lb.}$$

$$Z_m = 1.78 \text{ per cent}$$

$$C_{mcr} = 0.35 \ \frac{\text{lb.-sec.}}{\text{in.}}$$

$$C_m = 0.0063 \ \frac{\text{lb.-sec.}}{\text{in.}}$$

CHAPTER IV

RESPONSE OF SHAKING TABLE TO BREAKING WIRES

Determination of the Type of Applied Load to the Shaking Table

The shaking table was used as the source of the forcing function exciting the model structures. Since the response of model structures to known forcing functions was to be studied, the problem of determining and controlling the table's motion had to be solved.

Only the first few oscillations of the table were of interest, those which caused the maximum model response. Since the damping ratio was only 6.7 per cent, it had very little effect on the initial response of the table and therefore was neglected.

The method of applying the load to the shaking table was designed so that an impulse load could be derived from breaking the wires. The following development (5) shows the criteria for, and effect of an impulse load on the table.

Consider a typical dynamic load, P(t), as shown in Fig. 20a, where T is defined as the duration of the load to be applied to the equivalent single-degree-of-freedom table system as shown in Fig. 20b. R(x) represents the internal resistance of the system and is a function of mass displacement.

The basic equation of motion is

$$M_t \frac{dx^2}{dt^2} = P(t) - R(x) \tag{42}$$

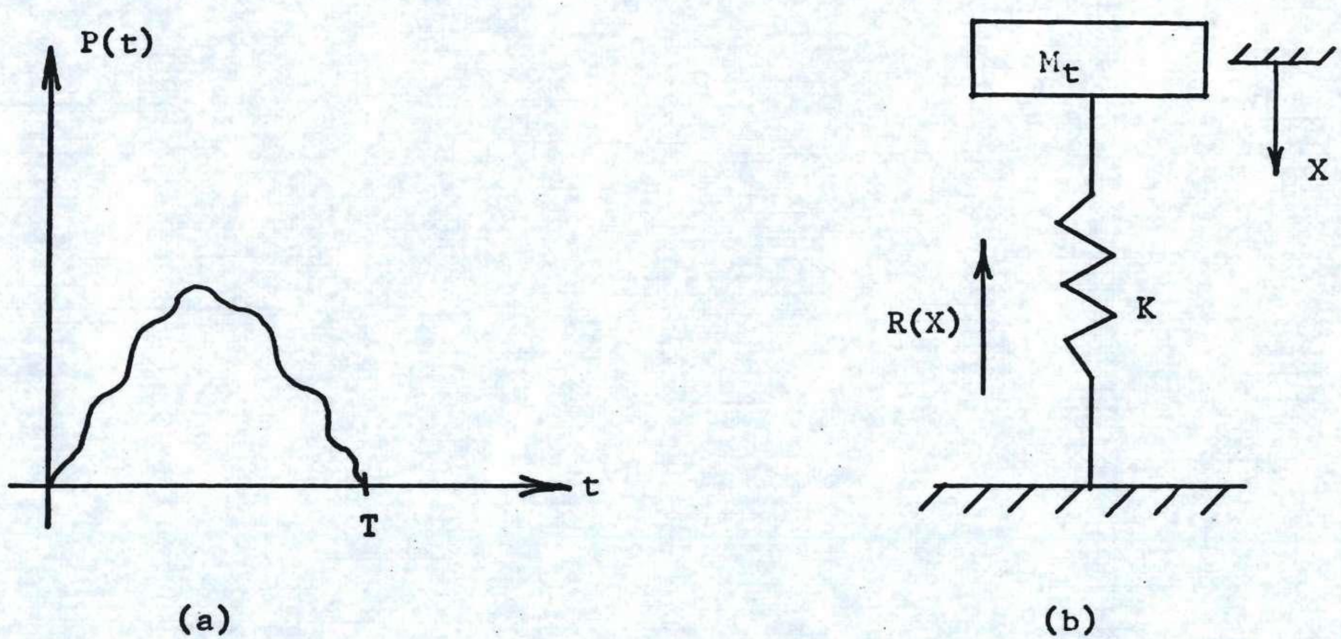

Figure 20. Typical Dynamic Load and Single-Degree-of-Freedom System

The external work done up to any time t is given by

$$W(t) = \int_o^{x(t)} P(t)\, dx' = \int_o^{t} P(t) \frac{dx}{dt}\, dt \tag{43}$$

In order to evaluate the work done, the velocity $\frac{dx}{dt}$ must be determined by integration of Eq. 42.

$$\frac{dx}{dt} = \frac{1}{M_t} \int_o^{t} \left[P(t)-R(x)\right] dt \tag{44}$$

Substituting Eq. 44 into Eq. 43 results in

$$W(t) = \int_o^{t} P(t) \left\{ \frac{1}{M_t} \int_o^{t} \left[P(t)-R(x)\right] dt \right\} dt \tag{45}$$

This expression is integrated between t=o and $t=t_m$, the time of maximum deflection, in order to obtain the work done by the load in this time interval. If the time of maximum deflection, t_m, is greater than the duration of the load T, Eq. 45 need only be integrated up to the latter time. Thereafter, the work done remains constant. If t_m is much grater than T, the resistance R(x) is small during the application of the load and may be neglected. The expression for work then becomes

$$W_r = \int_o^{t} P(t) \left[\frac{1}{M_t} \int_o^{t} P(t) dt \right] dt \tag{46}$$

which when integrated becomes

$$W_r = \frac{H^2}{2M_t} \tag{47}$$

in which

$$H = \int_o^{t} P(t) dt \tag{48}$$

W_r is the work done ignoring the contribution of the resistance. H is the total impulse of the external load and is equal to the area under the load-time curve. The external force in this case may be termed a pure impulsive load, and during its application the resistance and internal strain energy of the system may be assumed to be zero. After the application of the load, the mass has acquired a kinetic energy equal to the work done:

$$\frac{1}{2} M_t V_o^{\,2} = \frac{H^2}{2M_t}$$

The initial velocity of the mass is therefore given by

$$V_o = \frac{H}{M_t} \tag{49}$$

The criteria for a pure impulsive load was based on Figs. 7.5 and 7.6 of reference (5). It is that

$$T \leq 0.1\, T_n \tag{50}$$

where,

T = duration of the load,

$T_n = 2\pi \sqrt{\frac{M_t}{K}}$ = natural period of the system.

In short, if the time of the applied load, i.e. the time of breaking the wires, satisfies the relationship of Eq. 50, then the applied load may be termed a pure impulsive load. The effect of the impulse load is to impart an initial velocity to the table, such that for a given mass, M_t, the velocity is directly proportional to the area under the load-time curve.

Effect of breaking various numbers of wires Connected to the Shaking Table

The natural period of the table was

$$T_n = \frac{1}{f_d} = \frac{1}{5.45}$$

$$T_n = 0.18 \text{ sec.} \tag{51}$$

Therefore, as long as the time of breaking the wires was equal to or less than $0.1\ T_n$ or 0.018 sec., the effect was to impart an initial velocity to the table. It was desired to determine the relationship between number of wires and initial velocity.

The procedure was to break a known number of wires and measure the resulting velocity. Eq. 49 was not used since the area under the load-time curve, H, was not measured. Only the time of breaking the wires was to be measured to assure that the applied load is an impulse. Consider the equation of motion for the free vibration of the equivalent single-degree-of-freedom system, neglecting damping and with initial conditions of velocity, $\dot{X}_o = V_o$, and displacement, $X_o = 0$,

$$M_t \ddot{X}_t + K X_t = 0 \tag{52}$$

Dividing by M_t,

$$\ddot{X}_t + \frac{K}{M_t} X_t = 0 \tag{53}$$

The solution of Eq. 53 satisfying the initial conditions given is well known (2) and is

$$X_t = \frac{V_o}{q_t} \operatorname{Sin} q_t t \tag{54}$$

where,

X_t = displacement of M_t at any time t,

$q_t = \sqrt{\frac{K}{M_t}}$

Upon breaking the known number of wires, the Sanborn recorder plots the deflection-time history of the table. The first maximum amplitude, X_{tmax}, that which is least affected by damping, occurred at a time, t, such that

$$\text{Sin } q_t t = 1$$

or,

$$X_{tmax} = \frac{V_o}{q_t} \tag{55}$$

Since q_t was known and X_{tmax} measured, the initial velocity of the table due to breaking various numbers of wires was calculated as

$$V_o = X_{tmax} \, q_t \tag{56}$$

Wire Testing

Discussion

Various numbers of wires were connected to the posts at one end of the table. The configuration of the wires was controlled by supporting a known length, L_w, between points one and two as shown in Fig. 21 such that

$$L_w = 2 \sqrt{r_w^{\,2} + (6\ 3/4)^2} + 4 \tag{57}$$

The configuration selected consisted of wires of the same length and $r_w = 13\frac{1}{4}$ in. Therefore,

$$L_w = 33\ 3/4 \text{ in.} \tag{58}$$

This position corresponds to the vertical position of the pendulum, i.e. the maximum kinetic energy of the pendulum,

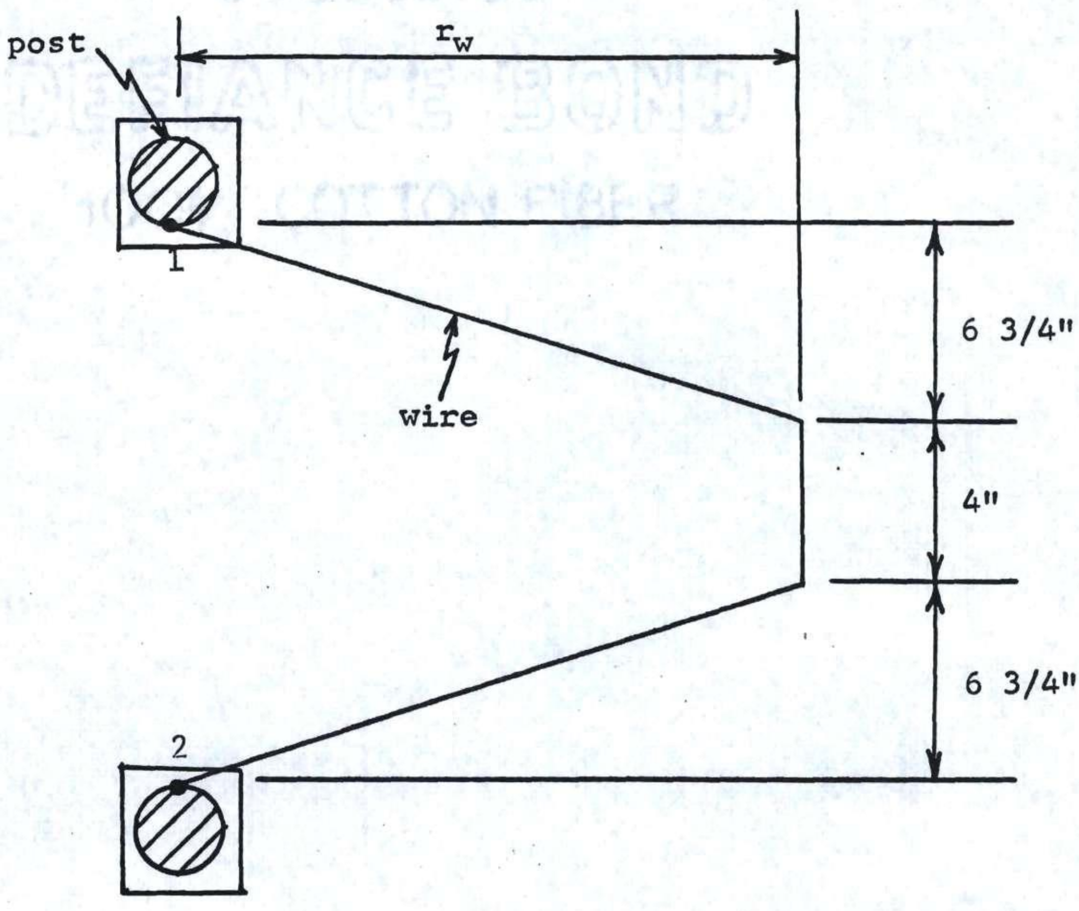

Figure 21. Configuration of Wires at Time of Breaking

and results in the fastest time of breaking the wires.

The pendulum, after being raised to its position of maximum potential energy, is released and swings down breaking the wires thereby imparting an initial velocity to the table. The change in potential energy of the pendulum due to breaking the wires will now be derived.

The maximum potential energy of the pendulum without breaking any wires, J_t is

$$J_t = (W_p + 2W_{PL}) \left(\frac{L_p}{2}\right) (1 - \cos \theta_t) \tag{59}$$

where,

W_p = total weight of pendulum,

W_{PL} = weight of plate at end of pendulum,

L_p = length of pendulum,

θ_t = angle to which the pendulum rises, measured from the vertical, without breaking any wires.

The maximum potential energy of the pendulum after breaking the wires, J_b, is

$$J_b = (W_p + 2W_{PL}) \left(\frac{L_p}{2}\right) (1 - \cos \theta_b) \tag{60}$$

where,

θ_b = angle to which the pendulum rises, measured from the vertical, after breaking wires.

The change in potential energy, ΔJ, therefore, is

$$\Delta J = J_t - J_b \tag{61}$$

Substituting Eqs. 59 and 60 into Eq. 61 results in

$$\Delta J = (W_p + 2W_{PL}) \left(\frac{L_p}{2}\right) (\cos(\theta_t - \Delta\theta) - \cos\theta_t) \tag{62}$$

where,

$$\Delta\theta = \theta_t - \theta_b$$

Procedure

The general procedure used to prepare the wires for a test was as follows:

1. Individual wires, each 80 inches long, were cut from a roll of 0.029 inch diameter music wire.
2. The selected number of wires were then placed together in a group, one end of which was clamped to a rigid fastener. At a distance of approximately 15 inches from this end, all the wires were placed in a common plane. A piece of tape was then wrapped around the wires to hold this configuration. A short piece of soft wire was also wrapped around the group a few inches beyond the tape to hold the group intact. From this point, the wires in the group were intertwined to form a cable and insure that all the wires were of the same length. Another short piece of soft wire was again wrapped tightly around the cable. A few inches further, or a total of 33 3/4 inches from the first tape, a second piece of tape was wrapped around the cable to hold all the wires in a common plane. Each end and the middle of the cable was also wrapped tightly with soft wires. The resulting cable was then ready

to be tested.

3. The tapes marked the place where the cable was tangent to the supporting posts. Each section of cable beyond the tapes was wrapped around and bolted to the supporting posts. The desired length of cable between points (a) and (b) as shown in Fig. 21, or 33 3/4 inches, now existed.
4. Since the cable was unable to hold itself in a horizontal plane, a small wire, one end attached to the ceiling and the other end hooked around the middle of the cable, was used to accomplish this.
5. One edge of the pendulum's flange was rounded so that all the wires would break at the opposite sharp edge. A thick layer of clay was placed around the sharp edge so that no electrical contact between the pendulum and cable would be made until some initial small force existed in the cable.
6. The Sanborn Strain Gage Amplifier and DC Amplifier, measuring table and pendulum motion respectively, were checked for balance in accordance with Appendices B and G.
7. The pendulum was lifted to its position of maximum potential energy and connected to a support at the ceiling.
8. The Cathode Ray Oscilloscope was set to measure the time of breaking the cable.
9. The power supply feeding the potentiometer was checked for six volts.
10. With all systems running, the pendulum was mechanically released to swing down, thereby breaking the cable.

11. The time of breaking the wires was read directly from the oscilloscope.
12. The first maximum table deflection was calculated using Eq. 7
13. The initial velocity imparted to the table was calculated using Eq. 56.

The observed angle θ_t was 76.0°. The total weight of the pendulum, W_p, was 131.4 lb., the length of the pendulum, L_p, was 85.7 inches, and the weight of the plate at the end of the pendulum, W_{PL}, was 26.4 lb. It was also observed that the stylus moved through 36 blocks when no wires were broken by the pendulum. Applying Eq. 11, the change in angle $\Delta\theta$ becomes

$$\Delta\theta = 4.1\ (36\text{-}d) \tag{63}$$

where d represents the stylus deflection after breaking the wires. Eq. 62 was then applied to calculate the change in potential energy, ΔJ, of the pendulum.

Results

The table's response, the change in potential energy of the pendulum, and the time of breaking the wires were recorded and tabulated in Appendix K.

The results can be found in Figs. 22, 23, 24, and 25. Fig. 22 shows the variation of the first maximum table displacement, X_{tm}, with the number of wires being broken, N. Fig. 23 shows the variation of initial table velocity, V_o, with N. This plot was obtained by applying Eq. 38 to each of the X_{tm}'s of Fig. 22. Fig. 24 shows the variation of wire breaking time, T, with N. Fig. 25 shows the variation of loss in potential energy of pendulum J, with N. The heavy solid lines in each plot represents the range of X_{tm}, $\dot{V}_o$, T or J measured for each set of wires tested, while the dotted line represents the corresponding expected values.

Sufficient tests were not run such that a statistical analysis could be made to determine the best value of V_o for any N. However, Fig. 23 was used successfully to predict the motion of the shaking table and model as will be shown in Chapter V.

Fig. 24 shows conclusively that for ten wires or less the time of the applied load, i.e. the time of breaking the wires, is less than 0.1 T_n or 0.018 sec. Therefore, the applied load due to breaking up to ten wires may be considered as a pure impulse load. Also, by extending the expected value line, it is indicated that up to 30 wires could be used while still satisfying the criteria for a pure impulse load. Correspondingly, a table deflection of 0.66 in. is indicated by extending the expected value line of Fig. 22 to 30 wires.

A load-strain curve for the wire was determined up to its ultimate load and can be found in Appendix N. The area under this curve represents the energy per unit length required to break the wire. The resulting area was approximately 2 $\frac{\text{in.-lb.}}{\text{in.}}$. However, since the wires were broken at an extremely fast rate, an increase in strength of approximately 50 per cent was assumed. Therefore, 3 $\frac{\text{in.-lb.}}{\text{in.}}$, or a total of approximately 100 in.-lb. was required to break the 33 3/4 in. long wires. This result is plotted as line (1) in Fig. 25. Line (1) is on the conservative side of the measured values of J. This indicates that

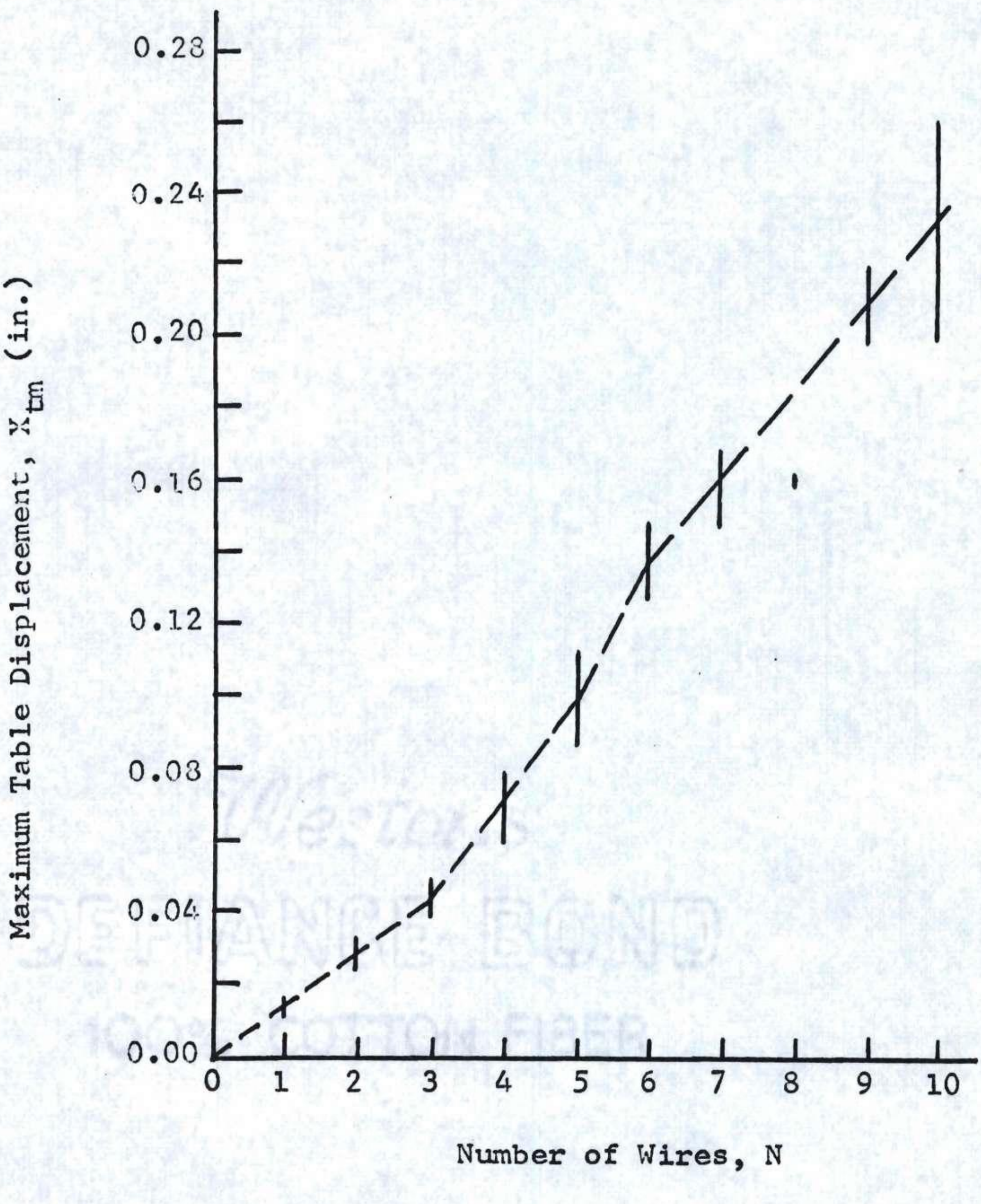

Figure 22. Variation of Maximum Table Displacement with Number of Wires Broken

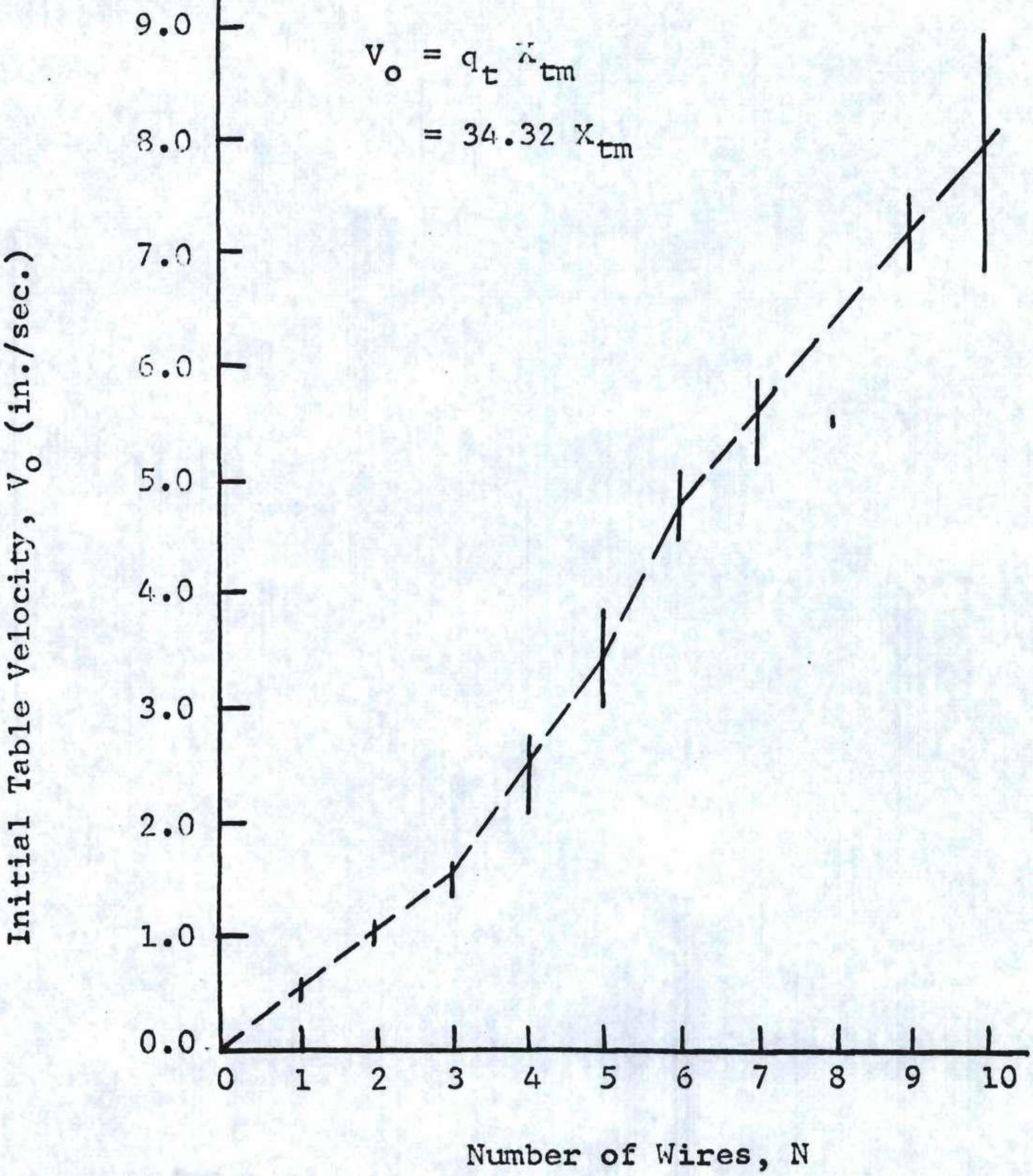

Figure 23. Variation of Initial Table Velocity with Number of Wires Broken

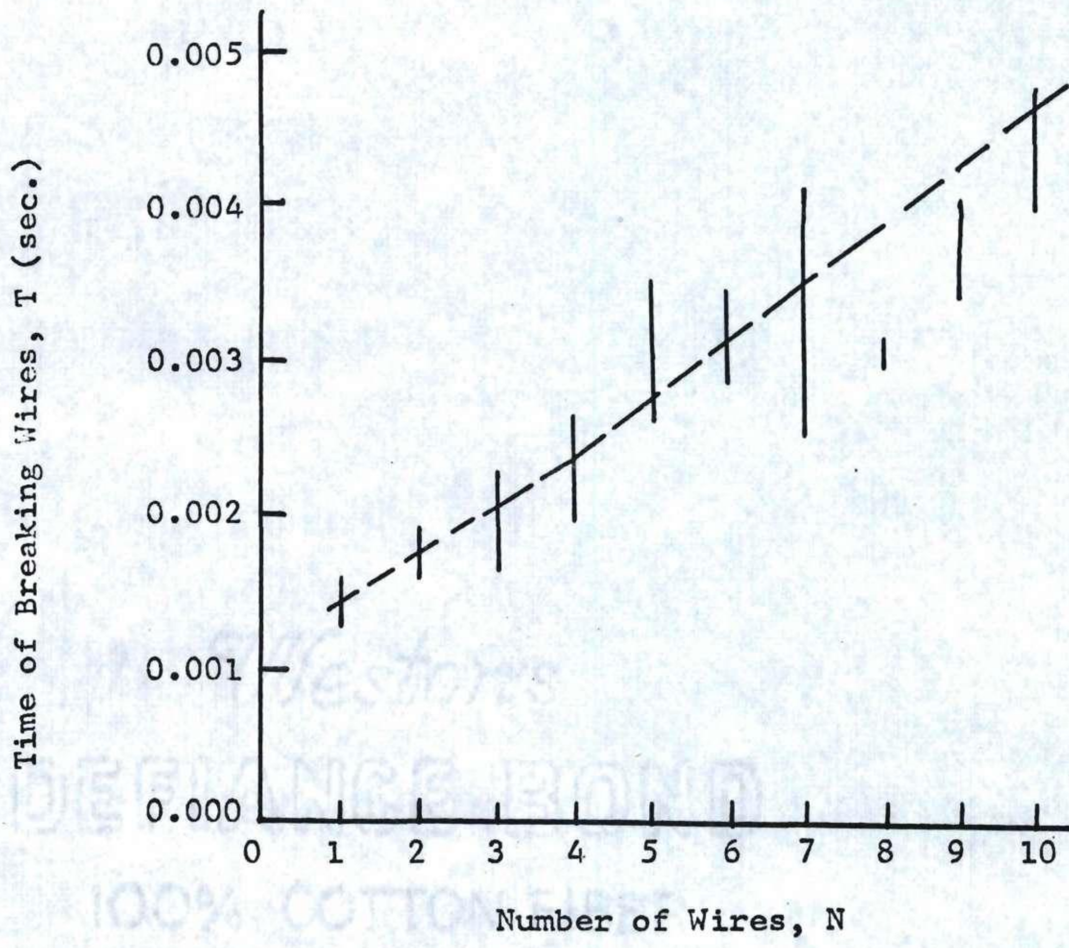

Figure 24. Variation of Time of Breaking Wires with Number of Wires Broken

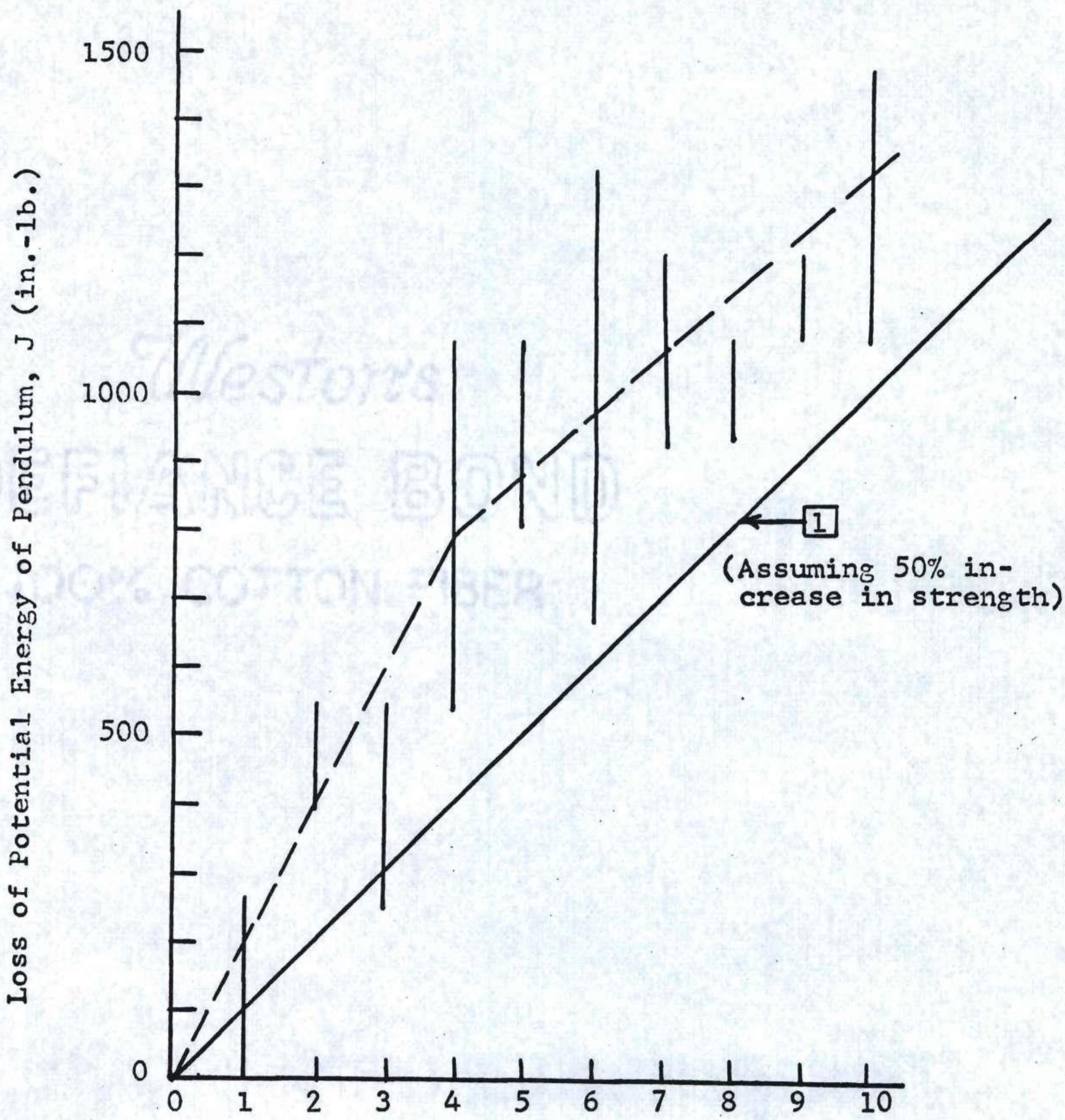

Figure 25. Variation of Loss of Potential Energy of the Pendulum with Number of Wires Broken

there probably was more than a 50 per cent increase in strength due to dynamic breaking.

However, even though the range of measured values of J is headed in the proper direction as determined from the load-strain curve, it is too large to allow Fig. 25 to be used with any degree of reliance. As a result, a more sophisticated measuring system should be devised so that more accurate measurements of J can be made.

CHAPTER V

INSTRUMENTATION CHECK-OUT

To determine whether or not the instrumentation was operating in a predictable manner, the response of the shaking table and model, due to breaking wires connected to the table, was theoretically calculated and compared to the measured response.

The model had been designed on the basis that the table would supply a base excitation while the model, in turn, did not appreciably affect the table's motion. However, preliminary tests involving the application of arbitrary initial conditions to the table showed that the model and table acted as a two-degree-of-freedom system. As a result, the model could not be considered as a single-degree-of-freedom system being excited by an initial velocity imparted to the table. Referring to Fig. 26, M_m represents the mass of the model, M_t represents the mass of the table, k represents the stiffness of the model, and K represents the stiffness of the table. Damping was neglected in the theoretical analysis of this system, since it was small and, therefore, would not appreciably affect the amplitude of the table's or model's motion during the first few seconds of response. The equations of motion of the system are:

$$M_t \ddot{X}_t + KX_t + k (X_t - X_m) = 0 \tag{64}$$

and,

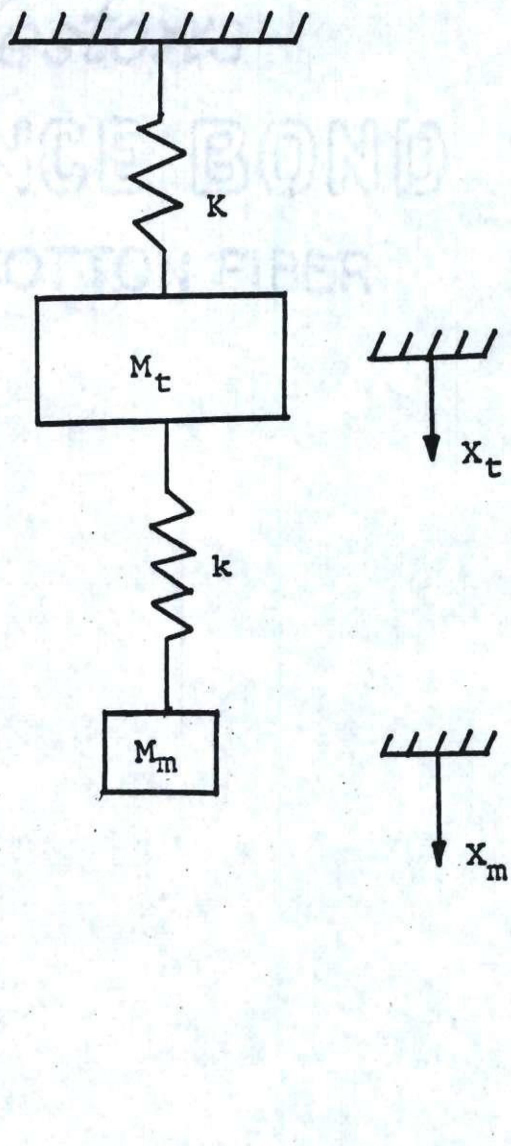

Figure 26. Equivalent Two-Degree-of-Freedom System of Model and Table

$$M_m \ddot{X}_m - k\,(X_t - X_m) = 0 \tag{65}$$

The general solution of Eqs. 64 and 65 is well known (2) and is

$$X_t(t) = \left(\frac{Y_2\,X_{10} - X_{20}}{Y_2 - Y_1}\right) \text{Cos}\,(q_1 t) \tag{66}$$

$$+ \left(\frac{Y_2\,V_{10} - V_{20}}{q_1\,(Y_2 - Y_1)}\right) \text{Sin}\,(q_1 t)$$

$$+ \left(\frac{X_{20} - Y_1 X_{10}}{Y_2 - Y_1}\right) \text{Cos}\,(q_2 t)$$

$$+ \left(\frac{V_{20} - Y_1\,V_{10}}{q_2\,(Y_2 - Y_1)}\right) \text{Sin}\,(q_2 t)$$

$$X_m(t) = Y_1 \left(\frac{Y_2\,X_{10} - X_{20}}{Y_2 - Y_1}\right) \text{Cos}\,(q_1 t) \tag{67}$$

$$+ Y_1 \left(\frac{Y_2\,V_{10} - V_{20}}{q_1\,(Y_2 - Y_1)}\right) \text{Sin}\,(q_1 t)$$

$$+ Y_2 \left(\frac{X_{20} - Y_1\,X_{10}}{Y_2 - Y_1}\right) \text{Cos}\,(q_2 t)$$

$$+ Y_2 \left(\frac{V_{20} - Y_1\,V_{10}}{q_2\,(Y_2 - Y_1)}\right) \text{Sin}\,(q_2 t)$$

where,

$X_t\,(t)$ = displacement of table at any time, t

$X_m\,(t)$ = displacement of model at any time, t

V_{10} = initial velocity of table

V_{20} = initial velocity of model

X_{10} = initial displacement of table

X_{20} = initial displacement of model

$$Y_1 = \frac{K+k - M_t\, q_1^{\;2}}{k}$$

$$Y_2 = \frac{K+k - M_t\, q_2^{\;2}}{k}$$

The first and second natural frequencies of the system, q_1 and q_2, are

$$q^2{}_{1,2} = \frac{1}{2} \left(\frac{K+k}{M_t} + \frac{k}{M_m}\right)$$

$$\mp \frac{1}{2} \left(\frac{K+k}{M_t} + \frac{k}{M_m}\right)^2 - 4\, \frac{Kk}{M_t\, M_m}$$

It has been shown that the effect of the applied load, i.e. the breaking of the wires, is to impart an initial velocity, V_o, to the table. So,

$V_{10} = V_o$

$V_{20} = 0$

$X_{10} = 0$

$X_{20} = 0$

The resulting equations of motion, therefore, are

$$X_t\ (t) = \frac{Y_2\, V_o}{q_1\ (Y_2 - Y_1)} \operatorname{Sin}\ (q_1 t) \tag{68}$$

$$- \frac{Y_1\, V_o}{q_2\ (Y_2 - Y_1)} \operatorname{Sin}\ (q_2 t)$$

$$X_m\ (t) = Y_1\ \left(\frac{Y_2\, V_o}{q_1\ (Y_2 - Y_1)}\right) \operatorname{Sin}\ (q_1 t) \tag{69}$$

$$- Y_2 \left(\frac{Y_1 V_o}{q_2 (Y_2 - Y_1)}\right) \text{Sin}\ (q_2 t)$$

Eqs. 68 and 69 were used to check-out the deflection-time history as measured by the Wheatstone Bridge circuits and Sanborn recorder. The acceleration-time history, measured by the accelerometer mounted on the model, was verified by the following equation which is the result of the second differentiation of Eq. 69.

$$\ddot{X}_m\ (t) = - \frac{Y_1\ Y_2 V_o q_1}{Y_2 - Y_1} \text{Sin}\ (q_1 t) + \frac{Y_1\ Y_2 V_o q_2}{Y_2 - Y_1} \text{Sin}\ (q_2 t) \tag{70}$$

where,

$\ddot{X}_m$ (t) = acceleration of model at any time, t.

A computer program was used to solve Eqs. 68 and 70 for the first two seconds of motion at 0.025 second intervals. The program also solved for the difference between Eqs. 68 and 69, D_r, since the Wheatstone bridge circuit on the model actually measured D_r where

$$D_r = X_t - X_m \tag{71}$$

To check the deflection measuring instrumentation, a known number of wires was attached to the table and broken. The resulting motions, X_t and D_r, were plotted by the Sanborn recorder. The theoretical motions were based on an initial table velocity, V_o, taken from Fig. 23. Tests were run using five, seven, and ten wires. A comparison of the measured and calculated peak values of X_t and D_r for the tests run is shown in Appendix L. Fig. 27 shows the total response, X_t, and Fig. 28 shows the total response, D_r, as measured and calculated for a seven wire test during the first two seconds of motion.

A phenomenon observed but not shown in Fig. 28, was that the D_r record as measured showed a high frequency response superimposed on the expected response during the first second or two of motion. This secondary response, attributed to a higher mode being excited in the model, had very little effect on the measured response that was to be compared to the calculated response since the amplitudes associated with it were very small and also it was damped out very quickly.

The results showed that the measured and calculated response checked within ten per cent in every test. Therefore, it can be concluded that the vibration characteristics determined for the table and model are correct and also that the deflection-measuring systems are adequate.

A similar procedure was followed to check-out the acceleration measuring system for the model. The accelerometer was first mounted directly on the model's leaf-spring at the same level as the mass. Upon breaking various numbers of wires, the accelerations measured were two or more times greater than expected. The high accelerations measured were attributed to high frequency vibrations induced in the model's leaf-spring by the shock wave, caused by breaking the wires, and traveling back and forth through the shaking table.

The accelerometer was then mounted on an aluminum plate which was attached directly to the mass at the free end of the leaf-spring. It was hoped that this would mechanically filter out the high frequency vibrations induced in the leaf-spring by the shock wave. However, upon further acceleration measurements, even though the frequency of the ac-

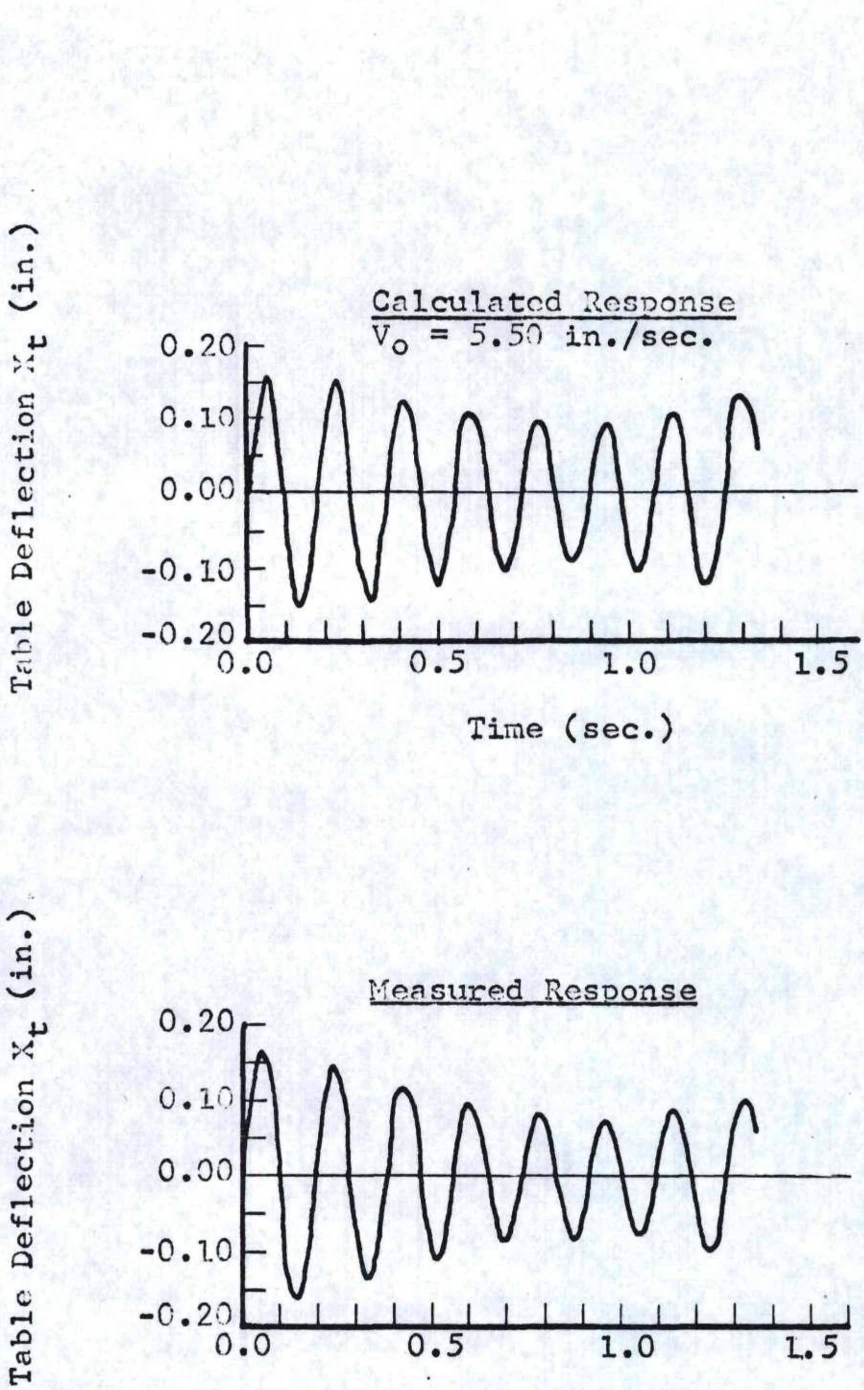

Figure 27. Comparison of Calculated and Measured Table Deflections for a Seven-Wire Test

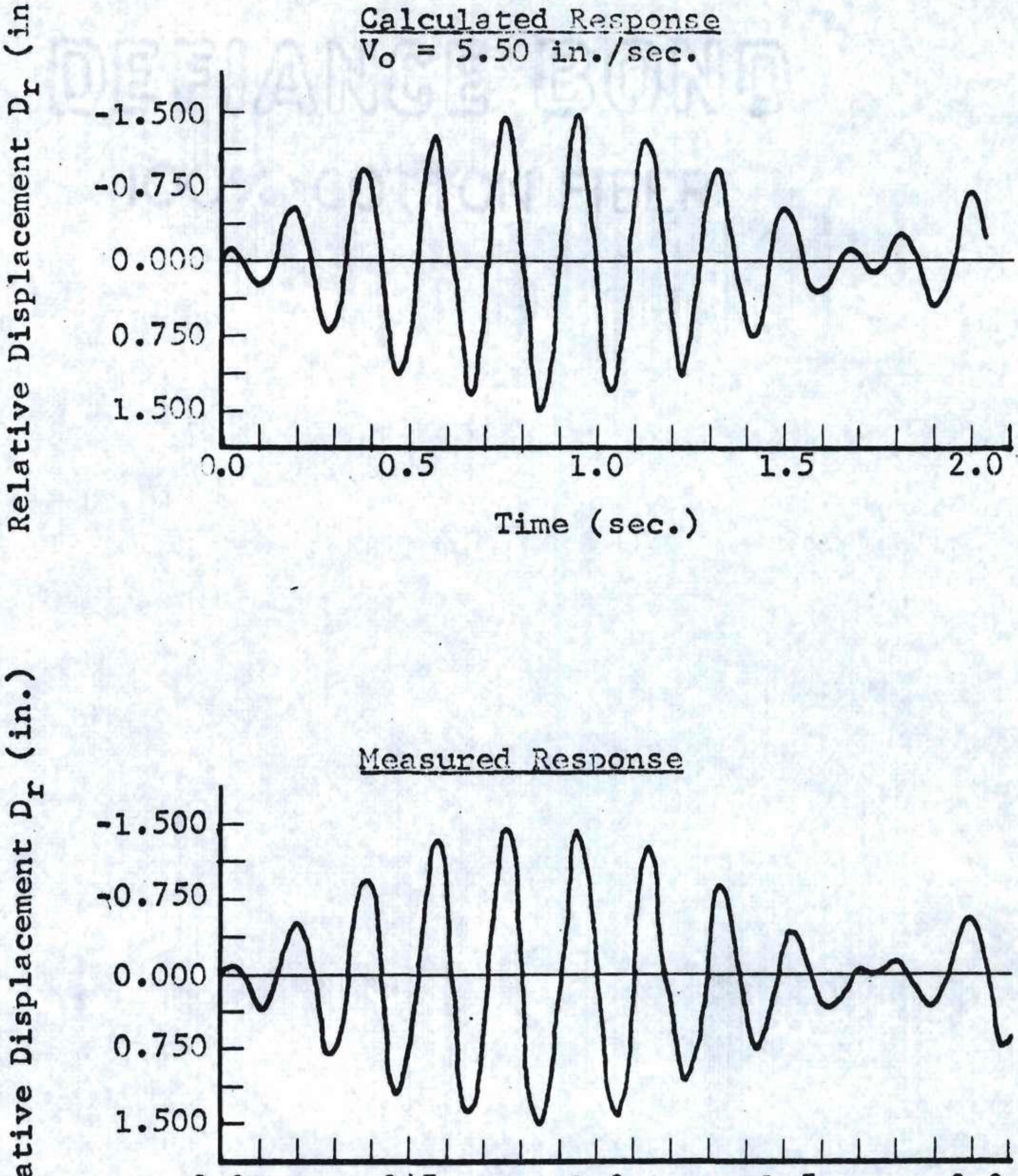

Figure 28. Comparison of Calculated and Measured Values of D_r for a Seven-Wire Test

celeration-time record measured was as expected, the amplitude was 50 to 60 per cent greater than expected. This was still attributed to the shock waves. Finally, the aluminum plate that the accelerometer was then mounted on was separated from the mass by rubber washers. This would act as an even better mechanical filter. The resulting acceleration-time record measured was in close correspondence with the expected values.

With the accelerometer mounted as last described, tests were run using one, three and five wires. A comparison of a few measured and calculated peak values of $\ddot{X}_m$, for the tests run is shown in Appendix M. Fig. 29 shows the total response, $\ddot{X}_m$, as measured and calculated for the three wire test during the first two seconds of motion. The first 0.4 seconds of the measured response is not shown. The reason for this is that the shock wave's high frequency, large amplitude accelerations blocked out the model's measured response. Apparently, the rubber washers could not fully filter out these accelerations until 0.4 seconds.

The results of the one and three wire tests showed that the measured and calculated accelerations check within five per cent. However, the five wire test showed the measured values to be approximately 35 per cent lower than the calculated values of acceleration. Assuming all elements of the measuring system to be operating properly and at their stated calibration, the discrepancy could be explained by the following:

(1) The filtering properties of the rubber washers are unknown. Therefore, the washers could be filtering out more than just the high frequencies induced by the shock waves in the

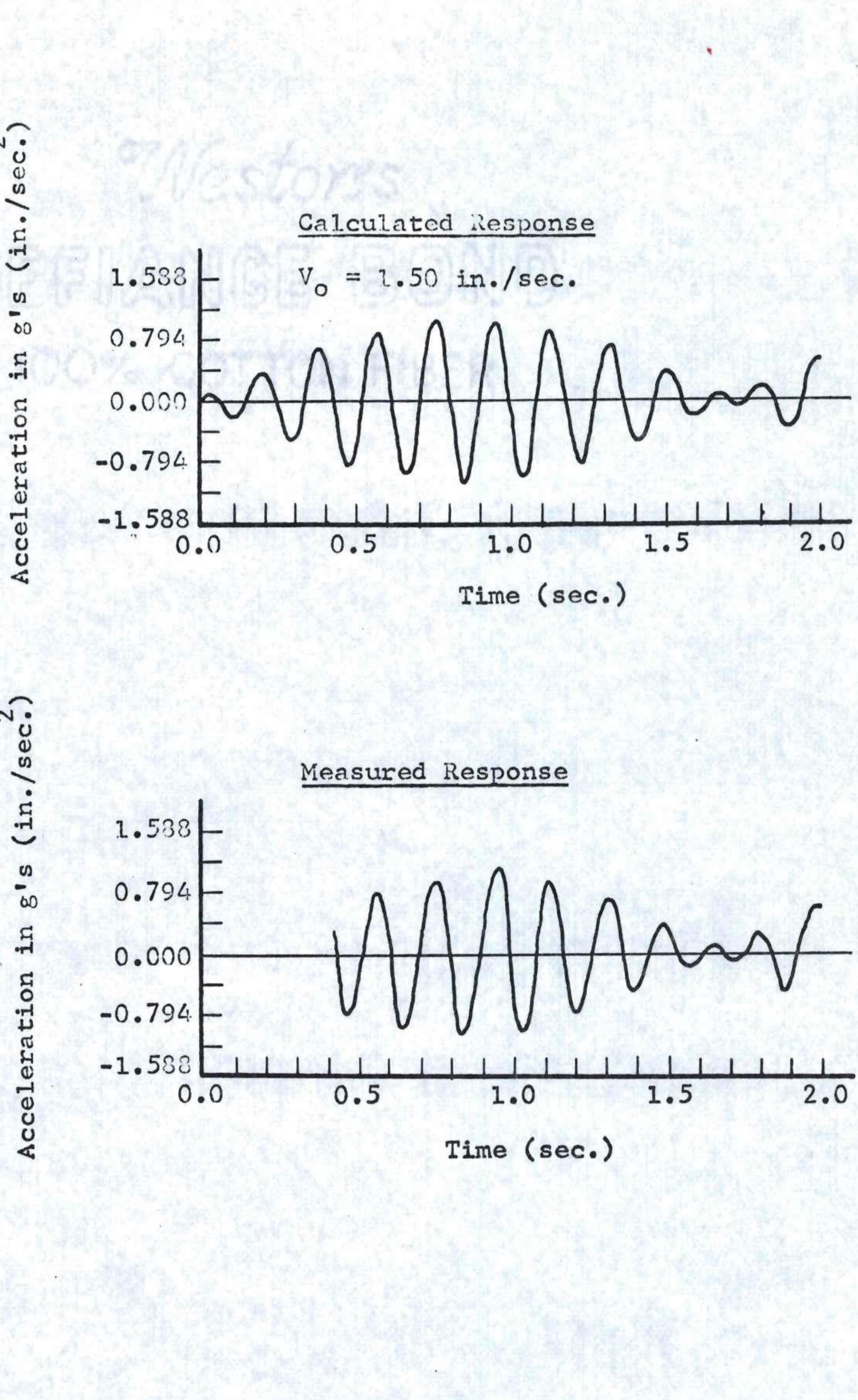

Figure 29. Comparison of Calculated and Measured Model Accelerations for a Three-Wire Test

table.

(2) The large model deflections could be causing cable whip which, in turn, could be causing an apparent decrease in model accelerations.

(3) The model could be vibrating in more modes than just the fundamental mode such that the net effect is seen as lower accelerations.

As a result, futher refinements of the acceleration measuring system for the model are necessary.

CHAPTER VI

CONCLUSIONS

The following conclusions are drawn from this study:

1. The deflection measuring system for the shaking table is behaving in a predictable manner.
2. The deflection measuring system for the model is behaving in a predictable manner.
3. Further refinements of the acceleration measuring system for the model are necessary.
4. The methods outlined to determine the dynamic properties of the shaking table and model are adequate and may be used with other dynamic systems.
5. The applied load, derived from breaking one to ten wires, may be considered as an impulse load.
6. The table could not be used as a source of base excitation for the model structure studied since the model and table acted as a two-degree-of-freedom system.

CHAPTER VII

RECOMMENDATIONS

Before testing more complicated structural models, the following recommendations are proposed:

1. Further testing should be carried out to verify the correspondence between maximum table displacement, X_{tm}, and number of wires broken, N.
2. Further testing should be carried out to determine the maximum number of wires that can be broken while still satisfying the criterion for an impulse load as stated by Eq. 50.
3. Aluminum leaf-springs should be used as the spring restoring force of the shaking table. This will allow a wider range of table spring constants while still permitting large table deflections.
4. The correspondence between table spring constant and number of wires broken vs. initial table velocity or maximum table deflection should be determined.
5. It is recommended that a device such as a mechanical catch be used to stop the table at any desired deflection. This could be used to study the effect of sudden base displacements on model structures.
6. A variable electrical filter with known properties should be used to filter out all undesirable accelerations while

allowing only model accelerations to be measured. Upon obtaining reliable acceleration-time measurements, deflection measurements of more complicated structural models may then be accomplished by twice integrating the acceleration-time record.

7. An investigation should be made to determine the limitations of model stiffness and mass so that the shaking table could be used as a source of base excitation while the model in turn, has little or no effect on the table's motion.

APPENDIX

APPENDIX A

DESIGN OF TABLE LEAF-SPRINGS

Thin steel leaf-springs were used as the spring restoring force of the shaking table. They were designed to allow at least $\frac{1}{2}$ inch horizontal table deflection when a horizontal force of 300 lb. was applied to the table. This force, assumed to be the static equivalent of the dynamic load, was an arbitrary choice since the dynamic load exciting the table was then not known.

A minimum of four leaf-springs supporting the table was considered. The modulus of elasticity of the plywood, E_w, was taken as 1.8×10^6 psi. Referring to Fig. 30, the moment of inertia of the table, I_w, was

$$I_w = \frac{(48)(2.25)^3}{12}$$

$$= 45.5 \text{ in.}^4$$

The stiffness of the table, $E_w I_w$, was

$$E_w I_w = 82.0 \times 10^6 \text{ lb.-in.}^2$$

The modulus of elasticity of steel, E_s, was taken as 29×10^6 psi. The stiffness of the leaf-springs was assumed to be small enough so that the effect of considering the table as having an infinite stiffness will not appreciably change the results from that obtained by considering the actual stiffness of the table. This will be verified after the dimensions of the leaf-springs are chosen.

Referring to Fig. 5, the moment induced in the leaf-springs, M,

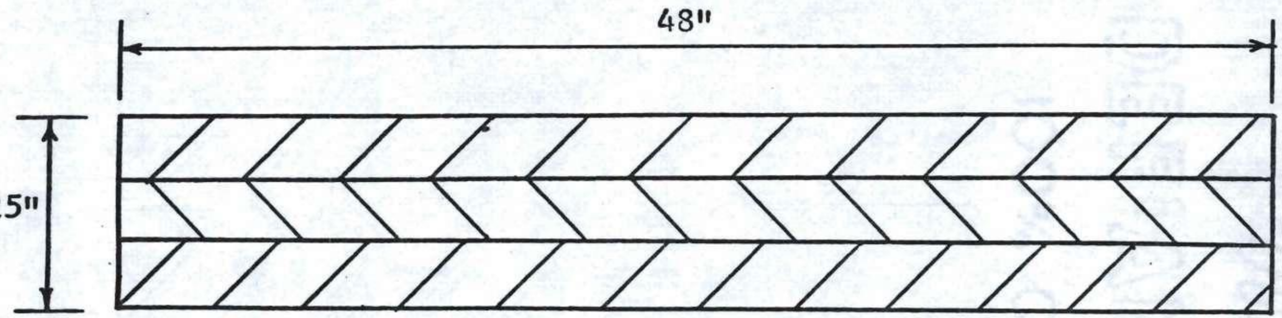

$$I_w = \frac{(48)(2.25)^3}{12}$$

$$= 45.5 \text{ in.}^4$$

Figure 30. Cross-Section of the Shaking Table

due to a deflection, d_r, is

$$M = \frac{6E_s I_t d_r}{L_t^2}$$

The horizontal force, P, must be equal to the induced shears in the leaf-springs to satisfy statics. Therefore,

$$P = 2\frac{M}{L_t} \tag{72}$$

$$= \frac{12\,E_s I_t d_r}{L_t^3}$$

The moment of inertia of two leaf-springs at one end of the table is

$$I_t = \frac{(2b_t)(h_t)^3}{12} \tag{73}$$

Substituting Eq. 73 into Eq. 72 results in

$$P = \frac{2E_s b_t h_t^{\ 3} d_r}{L_t^3}$$

Solving for the required ratio of $\frac{h_t}{L_t}$,

$$\frac{h_t}{L_t} = \sqrt[3]{\left(\frac{P}{2E_s}\right)\left(\frac{1}{b_t d_r}\right)}$$

Since steel plates were available in three inch widths and 1/8 inch thickness,

$$\frac{1/8}{L_t} = \sqrt[3]{\left(\frac{300}{2x29x10^6}\right)\left(\frac{1}{3x\frac{1}{2}}\right)}$$

or,

$$L_t = 8.7 \text{ in.}$$

The final dimensions selected were

$$b_t = 3 \text{ in.}$$

$$h_t = 1/8 \text{ in.}$$

$$L_t = 10 \text{ in.}$$

The moment of inertia, I_t, becomes

$$I_t = \frac{2(3) \quad (1/8)^3}{12}$$

$$= 0.000975 \text{ in.}^4$$

and the stiffness $E_t I_t$ becomes

$$E_t I_t = (29 \times 10^6) \quad (0.000975)$$

$$= 0.0283 \times 10^6 \text{ lb.-in.}^2$$

The ratio $\frac{E_w I_w}{E_t I_t}$ becomes

$$\frac{E_w I_w}{E_t I_t} = \frac{82.0 \times 10^6}{0.0283 \times 10^6}$$

$$= 2{,}900$$

Therefore, the effect of assuming the table to have infinite stiffness will change the results only by a negligible amount.

APPENDIX B

BALANCING PROCEDURE FOR THE SANBORN STRAIN GAGE AMPLIFIER

The following procedure should be carried out to initially balance the Sanborn Strain Gage Amplifier:

1. After connecting and 30 minutes warm-up, set the panel controls:

   R/T .... T

   ATTENUATOR .... OFF

   GAIN .... full right

2. Set the FINE/COARSE switch to FINE. Center the stylus with the ZERO control. Now set the FINE/COARSE switch to COARSE.
3. Remove all strain from the full bridge. Turn the ATTENUATOR to the right for a stylus deflection. Bring the stylus to its null position with the RES BAL and CAP BAL controls. Continue advancing the ATTENUATOR and bringing the stylus back to its null position until the ATTENUATOR is at X_1.
4. Set the FINE/COARSE switch to FINE. Now make a final adjustment of the RES BAL control, so the stylus does not move when turning the ATTENUATOR between X_1 and OFF. Then return the ATTENUATOR to OFF.

The full Wheatstone bridge and Sanborn strain gage amplifier are now in a balanced condition. However, after initial balancing but before each test, step 4 should be repeated to assure that the system is balanced.

APPENDIX C

CALIBRATION DATA AND CALCULATIONS FOR THE PENDULUM'S DEFLECTION MEASURING DEVICE

Table 1 contains the data recorded in the calibration of the deflection measuring device for the postentiometer. Fig. 31 shows the statistical variation of the calibration constant C_{pi} as measured. The calibration procedure has been covered in Chapter II. Referring to Fig. 9, a represents the horizontal distance between the transit and pendulum, r represents the distance from the pendulum's axis to point (1a), G represents the horizontal angle from point (1a) to point (1b), and θ represents the angular rotation of the pendulum. Pertinent measurements are as follows:

$$a = 111.75 \text{ inches}$$

$$r = 47.47 \text{ inches}$$

$$\frac{a}{r} = 2.354$$

$$\theta = \text{Sin}^{-1} (2.354 \text{ Tan } G)$$

Table 1. Data for Determination of Calibration Constant for Pendulum Rotations

Position (i)	Number of Blocks, N	G	Tan G	2,354 Tan G	θ in Degrees	$C_{pi} = \frac{\theta}{N} \frac{\text{Degrees}}{\text{Block}}$
0	0.00	0°00'	0.0000	0.0000	0.00	--
1	4.00	6°53'	0.1207	0.2842	16.52	4.1
2	6.25	10°47'	0.1905	0.4484	26.63	4.3
3	8.00	13°13'	0.2349	0.5529	33.57	4.2
4	9.75	15°23'	0.2751	0.6477	40.37	4.1
5	11.75	17°45'	0.3201	0.7536	48.90	4.2
6	13.50	19°24'	0.3522	0.8291	56.00	4.1
7	15.00	20°50'	0.3805	0.8950	63.62	4.2
8	16.50	21°47'	0.3996	0.9408	70.18	4.3
9	18.00	22°24'	0.4122	0.9703	76.00	4.2
10	4.50	8°23'	0.1474	0.3469	20.30	4.5
11	7.00	11°07'	0.1965	0.4624	27.55	3.9
12	8.50	13°33'	0.2410	0.5674	34.57	4.1
13	10.50	15°36'	0.2792	0.6573	41.10	3.9
14	11.50	17°20'	0.3121	0.7347	47.28	4.1
15	13.50	19°16'	0.3495	0.8229	55.38	4.1
16	15.25	20°30'	0.3739	0.8802	61.67	4.0
17	19.00	22°24'	0.4122	0.9703	76.00	4.0
18	4.75	7°53'	0.1385	0.3260	19.03	4.0
19	9.00	14°14'	0.2537	0.5972	36.67	4.1
20	11.00	16°34'	0.2975	0.7003	44.45	4.0
21	12.75	18°05'	0.3265	0.7687	50.23	3.9
22	15.00	19°30'	0.3541	0.8337	56.48	3.8
23	15.75	20°35'	0.3755	0.8841	62.13	3.9
24	17.00	21°41'	0.3976	0.9361	69.40	4.1
25	19.00	22°24'	0.4122	0.9703	76.00	4.0

Table 1. (Continued)

Position (i)	Number of Blocks, N	G	Tan G	2,354 Tan G	θ in Degrees	$C_{pi} = \frac{\theta}{N} \frac{\text{Degrees}}{\text{Block}}$
26	8.50	12°57'	0.2300	0.5413	32.77	3.9
27	12.00	17°08'	0.3083	0.7258	46.53	3.9
28	16.00	20°50'	0.3805	0.8958	63.62	4.0
29	18.75	22°24'	0.4122	0.9703	76.00	4.1
30	7.50	12°00'	0.2126	0.5004	30.03	4.0
31	11.00	16°53'	0.3035	0.7145	15.60	4.1
32	15.00	20°27'	0.3729	0.8779	61.38	4.1
33	18.25	22°24'	0.4122	0.9703	76.00	4.2

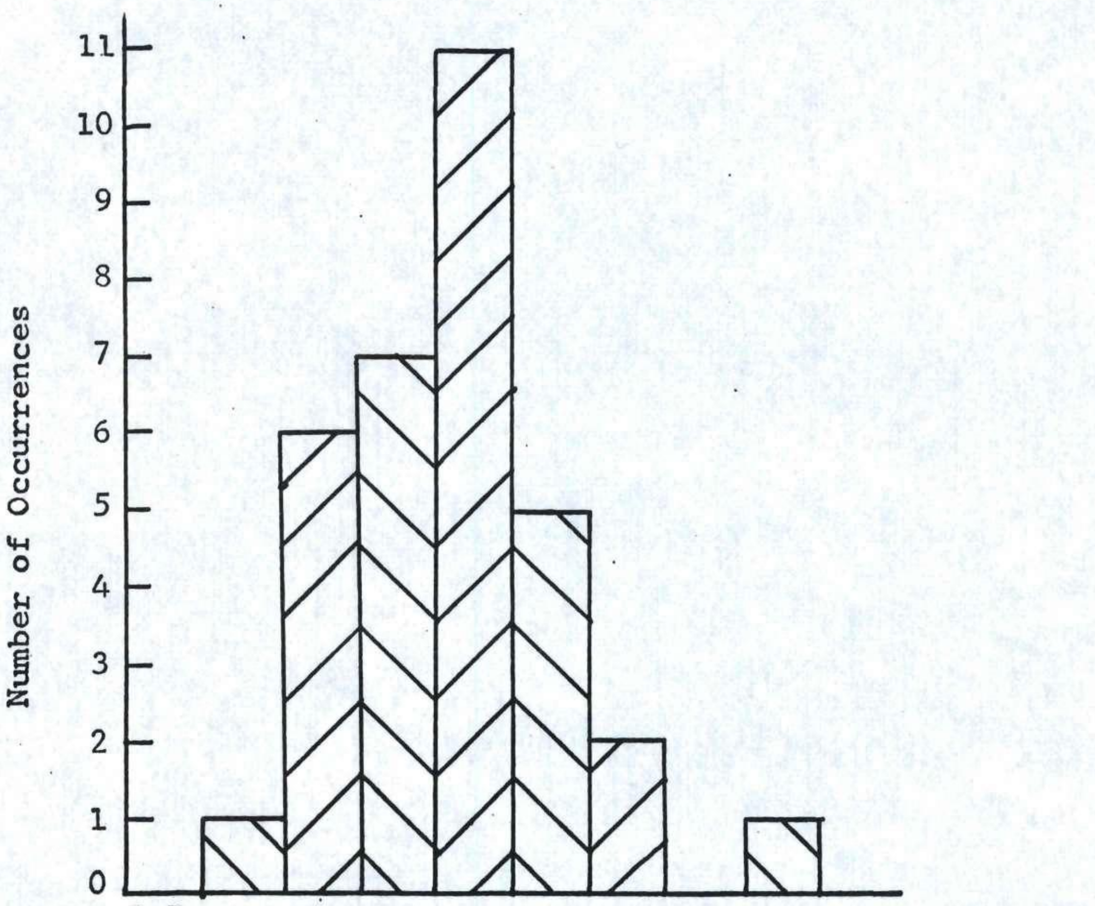

Figure 31. Statistical Variation of C_p

The arithmetic mean, $\bar{C}_{pi}$, of n=33 measured values is

$$\bar{C}_{pi} = \sum_{i=1}^{n} \frac{C_{pi}}{n}$$

$$= 4.1 \ \frac{\text{degrees}}{\text{block}}$$

The standard deviation, S_d, assuming a Normal distribution of the data as graphed in Fig. 31 is

$$S_d = \sqrt{\frac{\sum_{i=1}^{n} (\bar{C}_{pi} - C_{pi})^2}{n-1}}$$

$$= 0.144°$$

So, with a 95 per cent probability

$$C_p = M \pm 2S_d$$

or,

$$C_p = 4.1 \ \frac{\text{degrees}}{\text{block}} \pm 0.288 \ \frac{\text{degrees}}{\text{block}}$$

APPENDIX D

DATA AND CALCULATIONS TO DETERMINE SHAKING TABLE SPRING CONSTANT

The table spring constant, K, was determined by applying a known force, Q, and measuring the resulting deflection, U. The table on the following pages shows the measured values of table spring constant. Fig. 32 shows the statistical variation of the measured spring constant, K_i. C_s represents the calibration constant of the dynamometer. The procedure followed has been outlined in Chapter II. Calculations of the values of K to be used follows Fig. 32.

Table 2. Data for Table Spring Constant Determination

Run (i)	Strain Reading	Total Strain S	Total Load in pounds $Q = S/C_s$	Dial Gage	Total Table Deflection in Inches U	Spring Constant in $\frac{\text{pounds}}{\text{inch}}$ $K_i = Q/U$
--	11780	0	0.00	0.242	0.000	--
1	11850	70	73.22	0.333	0.091	802.0
2	11880	100	104.60	0.372	0.130	807.7
3	11920	140	146.44	0.424	0.182	804.6
4	11970	190	198.74	0.490	0.248	802.7
5	12028	248	259.41	0.561	0.319	814.5
6	12085	305	319.03	0.643	0.401	795.4
7	12115	335	350.41	0.687	0.445	787.4
--	11788	0	0.00	0.265	0.000	--
8	11850	62	64.85	0.346	0.081	800.6
9	11875	87	91.00	0.379	0.114	801.8
10	11907	119	124.47	0.419	0.154	807.7
11	11941	153	160.04	0.468	0.203	790.3
12	11980	192	200.83	0.520	0.255	788.2
13	12020	232	242.67	0.568	0.303	801.1
14	12060	272	284.51	0.623	0.358	794.7
15	12100	312	326.35	0.677	0.412	792.1
--	11789	0	0.00	0.266	0.000	--
16	11853	64	66.94	0.349	0.083	805.5
17	11882	93	97.28	0.389	0.123	790.9
18	11930	141	147.49	0.453	0.187	787.9
19	11970	181	189.33	0.504	0.238	796.5

Table 2. (Continued)

Run (i)	Strain Reading	Total Strain S	Total Load in pounds $Q = S/C_s$	Dial Gage	Total Table Deflection in inches U	Spring Constant in $\frac{\text{pounds}}{\text{inch}}$ $K_i = Q/U$
20	12020	231	241.63	0.570	0.304	795.4
21	12063	274	286.60	0.629	0.363	789.7
--	11789	0	0.00	0.266	0.000	--
22	11860	71	74.27	0.357	0.912	814.4
23	11890	101	105.65	0.402	0.136	778.6
24	11923	134	140.16	0.445	0.179	782.1
25	11967	178	186.19	0.501	0.235	792.3
26	12020	231	241.63	0.572	0.306	790.9

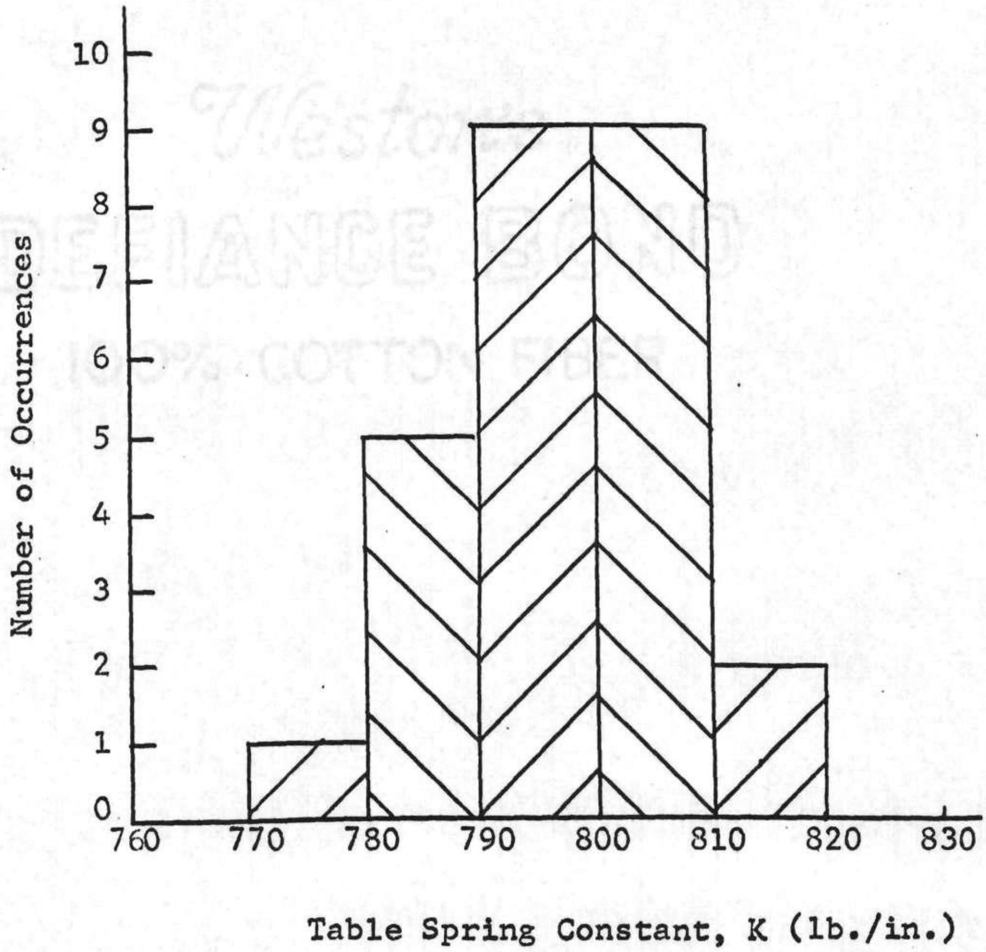

Figure 32. Statistical Variation of K

The arithmetic mean, $\bar{K}$, of n = 26 measured values was

$$\bar{K} = \sum_{i=1}^{n} \frac{K_i}{n}$$

$$= 796.7 \ \frac{\text{lb.}}{\text{in.}}$$

The standard deviation, S_d, assuming a Normal distribution of data as plotted in Fig. 32 was

$$S_d = \sqrt{\frac{\sum_{i=1}^{n} (\bar{K} - K_i)^2}{n - 1}}$$

$$= 9.19 \ \frac{\text{lb.}}{\text{in.}}$$

So, with a 95 per cent probability

$$K = \bar{K} \pm 2S_d$$

or,

$$K = 796.7 \ \frac{\text{lb.}}{\text{in.}} \pm 18.4 \ \frac{\text{lb.}}{\text{in.}}$$

APPENDIX E

DATA AND CALCULATIONS TO DETERMINE THE NATURAL FREQUENCY, DAMPING RATIO, CRITICAL DAMPING, DAMPING CONSTANT, EQUIVALENT MASS, AND WEIGHT OF SHAKING TABLE

To measure the natural frequency, f_t or q_t, damping ratio, Z_t, critical damping, C_{tcr}, damping constant, C_t $\frac{\text{lb.-sec.}}{\text{in.}}$, equivalent mass, M_t, and weight, W_t, an arbitrary set of initial conditions was applied to the table and the resulting motion measured as described in Chapter I.

The attenuation of the strain gage amplifier, A, was set at X100. The spring constant, K, had been determined and was 796.7 $\frac{\text{lb.}}{\text{in.}}$. The resulting table deflection, X_t, was then calculated as

$$X_t = 0.0002\, d\, A$$

$$= 0.02\, d$$

where,

d = stylus deflection.

Five runs were made. The data and calculations follow.

Run 1

$$f_t = \frac{30 \text{ cycles}}{5.48 \text{ seconds}}$$

$$= 5.47 \ \frac{\text{cycles}}{\text{seconds}}$$

$$@ X_{t1}, \quad d = 18.0 \text{ blocks}$$

$$X_{t1} = 0.02\ (18.0)$$

$$= 0.360 \text{ inches}$$

$$@ X_{t31}, \quad d = 2.25 \text{ blocks}$$

$$i=31 \quad X_{t31} = 0.02\ (2.25)$$

$$= 0.045 \text{ inches}$$

$$Z_t = \frac{1}{i-1} \operatorname{Ln} \left(\frac{X_{t1}}{X_{ti}}\right)$$

$$= \frac{1}{31-1} \operatorname{Ln} \left(\frac{.360}{.045}\right)$$

$$= 0.0694 = 6.94 \text{ per cent}$$

$$M_t = \frac{(1-Z_t{}^2)\ K}{(2\pi\ f_t)^2}$$

$$= \frac{(1-(.0694)^2)\ (796.7)}{(2\ \pi\ (5.47))^2}$$

$$= \frac{0.671 \ \text{lb.-sec.}^2}{\text{in.}}$$

Run 1 (Continued)

$$q_t = \sqrt{\frac{K}{M_t}}$$

$$= \sqrt{\frac{796.7}{0.671}}$$

$$= 34.45 \ \frac{\text{radians}}{\text{sec.}}$$

Run 2

$$f_t = \frac{40 \text{ cycles}}{7.32 \text{ sec.}}$$

$$= 5.46 \ \frac{\text{cycles}}{\text{sec.}}$$

@ X_{t1}, $\quad d = 22.75$ blocks

$$X_{t1} = 0.02\ (22.75)$$

$$= 0.455 \text{ inches}$$

@ X_{t41}, $\quad d = 2.0$ blocks

$i=41 \quad X_{t41} = 0.02\ (2.0)$

$$= 0.455 \text{ inches}$$

$$Z_t = \frac{1}{i-1} \text{ Ln } \left(\frac{X_{t1}}{X_{ti}}\right)$$

$$= \frac{1}{41-1} \text{ Ln } \left(\frac{.455}{104}\right)$$

$$= 0.0606 = 6.06 \text{ per cent}$$

$$M_t = \frac{(1-Z_t^{\ 2})\ K}{(2\ \pi\ f_t)^2}$$

$$= \frac{(1-(.0606)^2)\ (796.7)}{(2\ \pi\ (5.46))^2}$$

$$= 0.674 \ \frac{\text{lb.-sec.}^2}{\text{in.}}$$

$$q_t = \sqrt{\frac{K}{M_t}}$$

$$= \sqrt{\frac{796.7}{0.674}}$$

$$= 34.37 \ \frac{\text{radians}}{\text{sec.}}$$

Run 3

$$f_t = \frac{45 \text{ cycles}}{8.24 \text{ seconds}}$$

$$= 5.46 \ \frac{\text{cycles}}{\text{sec.}}$$

$$@\ X_{t1}, \qquad d = 21.0 \text{ blocks}$$

$$X_{t1} = 0.02\ (21.0)$$

$$= 0.420 \text{ inches}$$

$$@\ X_{t46}, \qquad d = 1.0 \text{ blocks}$$

$$i{=}46 \qquad X_{t46} = 0.02\ (1.1)$$

$$= 0.02 \text{ inches}$$

$$Z_t = \frac{1}{i-1} \operatorname{Ln} \left(\frac{X_{t1}}{X_{ti}}\right)$$

$$= \frac{1}{46-1} \quad \left(\frac{.420}{.02}\right)$$

$$= 0.0677 = 6.77 \text{ per cent}$$

$$M_t = \frac{(1-{Z_t}^2)K}{(2\,\pi\, f_t)^2}$$

$$= \frac{(1-(.0677)^2)(796.7)}{(2\,\pi\ (5.46))^2}$$

$$= 0.674 \ \frac{\text{lb.-sec.}^2}{\text{in.}}$$

$$q_t = \sqrt{\frac{K}{M_t}}$$

$$= \sqrt{\frac{796.7}{0.674}}$$

$$= 34.37 \ \frac{\text{radians}}{\text{sec.}}$$

Run 5

$$f_t = \frac{30 \text{ cycles}}{5.52 \text{ sec.}}$$

$$= 5.43 \ \frac{\text{cycles}}{\text{sec.}}$$

@ X_{t1} $\quad d = 21.0$ blocks

$$X_{t1} = 0.02\ (21.0)$$

$$= 0.420 \text{ inches}$$

@ X_{t31} $\quad d = 2.75$ blocks

$i=31$ $\quad X_{t31} = 0.02\ (2.75)$

$$= 0.055 \text{ inches}$$

$$Z_t = \frac{1}{i-1} \operatorname{Ln} \left(\frac{X_{t1}}{X_{ti}}\right)$$

$$= \frac{1}{31-1} \operatorname{Ln} \left(\frac{.420}{.055}\right)$$

$$= 0.0679 = 679 \text{ per cent}$$

$$M_t = \frac{(1-Z_t^{\ 2})\ K}{(2\ \pi\ f_t)^2}$$

$$= \frac{(1-(.0679)^2)(796.7)}{(2\ \pi\ (5.43))^2}$$

$$= 0.681 \ \frac{\text{lb.-sec.}^2}{\text{in.}}$$

$$q_t = \sqrt{\frac{K}{M_t}}$$

Run 5 (Continued)

$$= \sqrt{\frac{796.7}{0.681}}$$

$$= 34.20 \ \frac{\text{radians}}{\text{sec.}}$$

Table 3. Summary of Measured Dynamic Properties of Shaking Table

Run	f_t	Z_t	M_t	q_t
1	5.47	6.94	0.671	34.45
2	5.46	6.06	0.674	34.37
3	5.46	6.77	0.674	34.37
4	5.43	6.97	0.681	34.20
5	5.43	6.79	0.681	34.20
Σ =	27.25	33.53	3.381	171.59

The values of f_t, Z_t, M_t, and q_t was taken as the arithmetic mean of the measured values. Therefore,

$$f_t = \frac{\Sigma f_t}{5}$$

$$= \frac{25.25}{5}$$

$$= 5.45 \frac{\text{cycles}}{\text{second}}$$

$$Z_t = \frac{\Sigma Z_t}{5}$$

$$= \frac{33.53}{5}$$

$$= 6.71 \text{ per cent}$$

$$M_t = \frac{\Sigma M_t}{5}$$

$$= \frac{3.381}{5}$$

$$= 0.676 \ \frac{\text{lb.-sec.}^2}{\text{in.}}$$

$$q_t = \frac{\Sigma \, q_t}{5}$$

$$= \frac{171.59}{5}$$

$$= 34.32 \ \frac{\text{radians}}{\text{sec.}}$$

The other dynamic properties of the table were then calculated as,

$$W_t = M_t \, g$$

$$= (0.676) \, (386)$$

$$= 261.2 \text{ lb.}$$

$$C_{tcr} = 2M_t \, q_t$$

$$= (2) \, (0.676) \, (34.32)$$

$$= 46.40 \ \frac{\text{lb.-sec.}}{\text{in.}}$$

$$C_t = C_{tcr} \, Z_t$$

$$= (46.40) \, (0.0671)$$

$$= 3.11 \ \frac{\text{lb.-sec.}}{\text{in.}}$$

$$T_n = \frac{1}{f_t} = \text{natural period of shaking table}$$

$$= \frac{1}{5.45}$$

$$= 0.18 \text{ seconds}$$

APPENDIX F

BALANCING PROCEDURE FOR THE SANBORN

TRANSDUCER AMPLIFIER

The following steps were followed to balance the Sanborn Transducer Amplifier. One or two hours of warm-up time is recommended before final balancing.

1. Set the ATTENUATOR to OFF, the ZERO SUPPRESSION switches to OUT, and turn the SENSITIVITY control fully clockwise.
2. Set the USE-BAL switch to USE. Adjust the pointer of the meter to center scale with the POSITION control, then set the USE-BAL switch to BAL.
3. Check that there is no strain on the Bridge. Turn the ATTENUATOR clockwise until the meter pointer deflects near the edge of the scale. Bring the pointer to a null position toward center scale with the R BAL and C BAL controls. Continue advancing the ATTENUATOR and returning the meter pointer toward center scale with the R BAL and C BAL controls until the ATTENUATOR is at X1. If the null point becomes off scale, turn down the SENSITIVITY control to return the null on scale.
4. Set the USE-BAL switch to USE. Turn SENSITIVITY control back to its fully clockwise position. Make a final adjustment to the R BAL control so that the meter pointer

does not move when the ATTENUATOR is turned from X1 to X200. Return the ATTENUATOR to OFF.

5. The instrument is now balanced and ready for use.

APPENDIX G

BALANCING PROCEDURE FOR THE SANBORN DC GENERAL PURPOSE AMPLIFIER

The following procedure should be carried out to balance the Sanborn DC General Purpose Amplifier:

1. After warm-up, set the ATTENUATOR to OFF and the SENSITIVITY control fully counterclockwise. Set the stylus to mid-scale with the CENTERING control.
2. Set the SENSITIVITY control fully clockwise. Remove the protective button and return the stylus to mid-scale with the BALANCE control.
3. Turn the SENSITIVITY control back and forth between its limits. There should be no stylus motion. If a small amount of stylus motion is still present, repeat steps 1, 2, and 3.
4. The Amplifier is now balanced. Replace the protective button.

APPENDIX H

DATA AND CALCULATIONS TO DETERMINE MODEL SPRING CONSTANT

The model spring constant, k, was determined by applying a known force, Q, to the end of the leaf spring and measuring the resulting deflection, U. The table on the following pages shows the measured values of model spring constant. Fig. 33 shows the statistical variation of k. Calculations of the value of k to be used follows Fig. 33.

Table 4. Data For Model Spring Constant Determination

Run (i)	Applied Load in Pounds (Q)	Dial Gage Reading	Total Deflection of Mass in Inches (U)	Spring Constant in Pounds/Inches $k_i = Q/U$
0	0.00	0.090	0.000	--
1	0.86	0.239	0.149	5.77
2	2.04	0.449	0.359	5.68
3	2.85	0.590	0.500	5.71
4	4.27	0.833	0.743	5.75
5	4.71	0.908	0.818	5.76
	--	0.033*	0.818	--
6	6.25	0.291	1.077	5.81
7	7.84	0.563	1.349	5.81
8	9.17	0.781	1.567	5.85
9	7.58	0.527	1.313	5.77
10	6.75	0.389	1.175	5.75
11	5.57	0.193	0.979	5.69
12	4.73	0.051	0.836	5.66
	--	0.974*	0.836	--
13	3.40	0.752	0.614	5.54
14	1.98	0.508	0.370	5.35
	0.00	0.012*	0.000	--
15	1.18	0.224	0.212	5.57
16	2.77	0.505	0.493	5.62
17	4.10	0.734	0.722	5.68
18	5.52	0.967	0.955	5.78
	--	0.055*	0.955	--
19	7.06	0.312	1.212	5.82
20	8.74	0.593	1.493	5.86
21	9.17	0.666	1.566	5.86
22	7.75	0.431	1.331	5.82
23	6.21	0.173	1.073	5.79
24	5.78	0.099	0.999	5.78
	--	0.942*	0.999	--
25	4.10	0.660	0.717	5.72
26	2.51	0.389	0.446	5.62
27	1.18	0.157	0.214	5.52
	0.00	0.060	0.000	--
28	1.42	0.320	0.260	5.46

*Dial Gage Reset

Table 4. (Continued)

Run (i)	Applied Load in Pounds (Q)	Dial Gage Reading	Total Deflection of Mass in Inches (U)	Spring Constant in $\frac{\text{Pounds}}{\text{Inches}}$ $k_i = Q/U$
29	3.01	0.608	0.548	5.49
30	4.34	0.847	0.787	5.52
31	4.77	0.928	0.868	5.49
	--	0.058*	0.868	--
32	6.45	0.349	1.159	5.56
33	7.99	0.616	1.426	5.60
34	9.17	0.820	1.630	5.63
35	7.49	0.540	1.350	5.55
36	5.95	0.278	1.088	5.47
37	4.77	0.070	0.880	5.42
	--	0.939	0.880	--
38	3.35	0.688	0.629	5.33
39	1.76	0.400	0.341	5.16
	0.00	0.039	0.000	--
40	1.18	0.251	0.212	5.57
41	2.72	0.529	0.489	5.56
42	4.40	0.827	0.788	5.59
43	4.83	0.905	0.866	5.53
	--	0.057*	0.866	--
44	6.16	0.288	1.098	5.61
45	7.75	0.561	1.371	5.65
46	9.17	0.805	1.615	5.68
47	7.58	0.541	1.351	5.61
48	6.25	0.310	1.120	5.58
49	4.83	0.061	0.871	5.55
	--	0.948*	0.871	--
50	3.65	0.739	0.662	5.52
51	1.97	0.439	0.362	5.45
52	0.43	0.161	0.084	5.14
	0.00	0.061	0.000	--
53	1.33	0.299	0.238	5.58
54	2.75	0.551	0.490	5.62
55	4.43	0.838	0.777	5.70
	--	0.089*	0.777	--
56	5.61	0.283	0.981	5.72

*Dial Gage Reset

Table 4. (Continued)

Run (i)	Applied Load in Pounds (Q)	Dial Gage Reading	Total Deflection of Mass in Inches (U)	Spring Constant in Pounds/Inches $k_i = Q/U$
57	7.20	0.555	1.252	5.75
58	8.74	0.813	1.510	5.79
	--	0.191*	1.510	--
59	9.17	0.265	1.583	5.79
60	9.56	0.328	1.647	5.81
61	10.00	0.400	1.719	5.82
62	10.42	0.468	1.786	5.83
	0.00	0.045	0.000	--
63	1.54	0.321	0.276	5.59
64	2.96	0.576	0.531	5.57
65	4.29	0.814	0.769	5.58
	--	0.050*	0.769	--
66	5.97	0.348	1.067	5.59
67	7.56	0.629	1.348	5.61
68	8.74	0.839	1.558	5.61
	--	0.268	1.558	--
69	10.19	0.517	1.807	5.64
70	8.60	0.243	1.533	5.61
	--	0.888*	1.533	--
71	4.64	0.194	0.839	5.53

*Dial Gage Reset

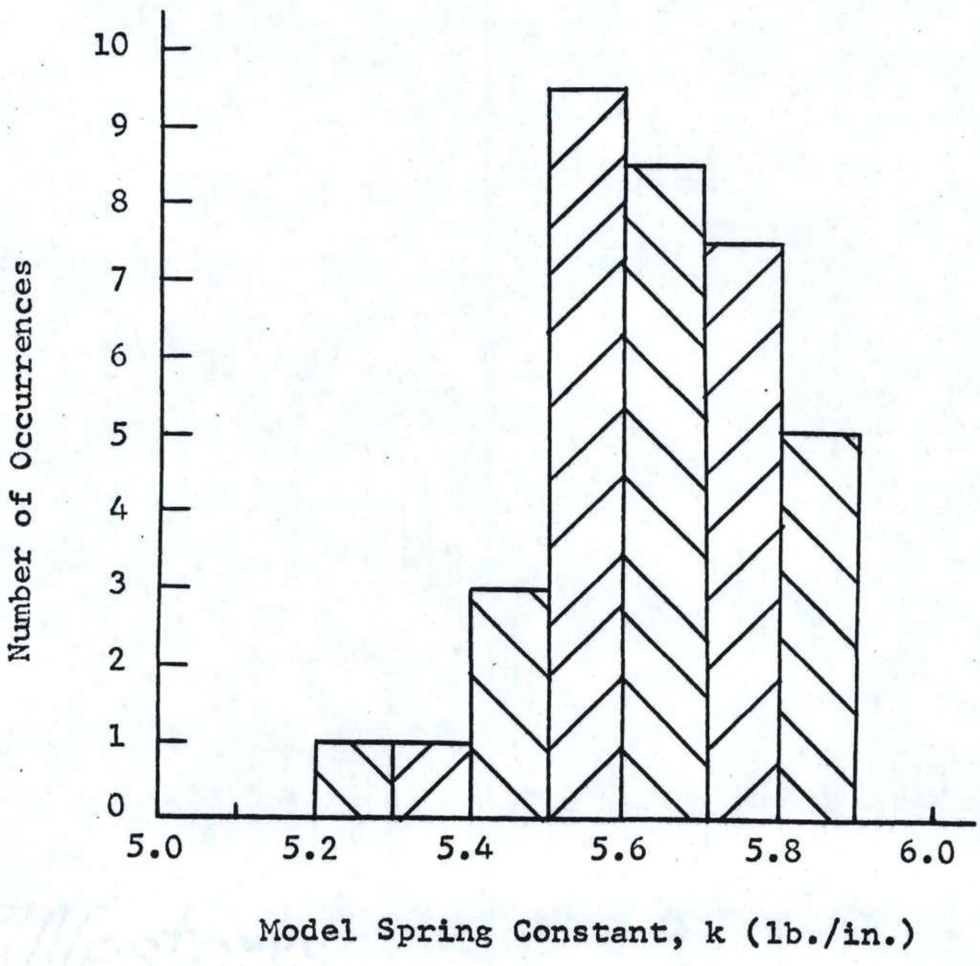

Figure 33. Statistical Variation of k

The arithmetic mean, $\bar{k}$, of n = 71 measured values is

$$\bar{k} = \sum_{i=1}^{n} \frac{k_i}{n}$$

$$= 5.63 \frac{\text{pounds}}{\text{inch}}$$

The standard deviation, S_d, assuming a normal distribution of data as plotted in Fig. 33 is

$$S_d = \sqrt{\frac{\sum_{i=1}^{n} (\bar{k} - k_i)^2}{n - 1}}$$

$$= 0.15 \frac{\text{pounds}}{\text{inch}}$$

So, with a 95 per cent probability

$$k = \bar{k} \pm 2S_d$$

or,

$$k = 5.63 \frac{\text{pounds}}{\text{inch}} \pm 0.30 \frac{\text{pounds}}{\text{inch}}$$

APPENDIX J

DATA AND CALCULATIONS TO DETERMINE THE NATURAL FREQUENCY, DAMPING RATIO, CRITICAL DAMPING, DAMPING CONSTANT, EQUIVALENT MASS, AND WEIGHT OF MODEL

To measure the natural frequency, f_m or q_m, damping ratio, Z_m, critical damping, C_{mcr}, damping constant, C_m, equivalent mass, M_m, and equivalent weight, W_m, an arbitrary set of initial conditions were applied to the table and the resulting motion measured.

The attenuation of the preamplifier, B, was set at X50. The spring constant, k, had been determined and was $5.63 \frac{\text{lb.}}{\text{in.}}$. The resulting table deflection, X_m, was then calculated as

$$X_m = 0.0015 \, d \, B$$

$$= 0.075 \, d$$

where,

$$d = \text{stylus deflection.}$$

Five runs were made. The data and calculations follow.

Run 1

$$f_m = \frac{30 \text{ cycles}}{5.92 \text{ sec.}}$$

$$= 5.07 \ \frac{\text{cycles}}{\text{sec.}}$$

$$@\ X_{m1}:\ d = 7 \text{ blocks}$$

$$X_{m1} = (0.075)\ (11.25)$$

$$= 0.844 \text{ in.}$$

$$@\ X_{m31}:\ d = 7 \text{ blocks}$$

$$i{=}31 \quad X_{m31} = (0.075)\ (7)$$

$$= 0.525 \text{ in.}$$

$$Z_m = \frac{1}{i-1}\ \text{Ln}\left(\frac{X_{m1}}{X_{mi}}\right)$$

$$= \frac{1}{31-1}\ \text{Ln}\left(\frac{.544}{.525}\right)$$

$$= 0.0158 = 1.58 \text{ per cent}$$

$$M_m = \frac{(1-(.0158)^2)(5.63)}{(2\pi\ (5.07))^2}$$

$$= 0.00555 \ \frac{\text{lb. - sec.}^2}{\text{in.}}$$

$$q_m = \sqrt{\frac{k}{M_m}}$$

$$= \sqrt{\frac{5.63}{.00555}}$$

$$= 31.85 \ \frac{\text{radians}}{\text{sec.}}$$

Run 2

$$f_m = \frac{25 \text{ cycles}}{4.9 \text{ sec.}}$$

$$= 5.10 \frac{\text{cycles}}{\text{sec.}}$$

@ X_{m1}: $\quad d = 10\ 3/4$ blocks

$$X_{m1} = (0.075)(10.75)$$

$$= 0.806 \text{ in.}$$

@ X_{m26} $\quad d = 7$ blocks

$$i=26 \quad X_{m26} = (0.075)(7.0)$$

$$= 0.525 \text{ in.}$$

$$Z_m = \frac{1}{i-1} \text{ Ln } \frac{X_{m1}}{X_{mi}}$$

$$= \frac{1}{26-1} \text{ Ln } \left(\frac{.806}{.525}\right)$$

$$= 0.0172 = 172 \text{ per cent}$$

$$M_m = \frac{(1-Z_m^{\ 2})\ k}{(2\pi\ f_m)^2}$$

$$= 0.00548 \ \frac{\text{lb.-sec.}^2}{\text{in.}}$$

$$q_m = \sqrt{\frac{k}{M_m}}$$

$$= \sqrt{\frac{5.63}{.00548}}$$

$$= 32.05 \ \frac{\text{radians}}{\text{sec.}}$$

Run 3

$$f_m = \frac{20 \text{ cycles}}{3.91 \text{ sec.}}$$

$$= 5.12 \ \frac{\text{cycles}}{\text{sec.}}$$

$@\ X_{m1}$: $\quad d = 14$ blocks

$$X_{m1} = (.075)\ (14.0)$$

$$= 1.05 \text{ in.}$$

$@\ X_{m21}$: $\quad d = 9\frac{1}{2}$ blocks

$i=21 \quad X_{m21} = (.075)\ (9.5)$

$$Z_m = \frac{1}{i-1} \operatorname{Ln} \left(\frac{X_{m1}}{X_{mi}}\right)$$

$$= \frac{1}{21-1} \operatorname{Ln} \left(\frac{1.05}{.713}\right)$$

$$= 0.0194 = 1.94 \text{ per cent}$$

$$M_m = \frac{(1-Z_m^2)\ k}{(2\pi\ f_m)^2}$$

$$= \frac{(1-(.0194))^2)\ (5.63)}{(2\pi \quad (5.12))^2}$$

$$= 0.00544 \ \frac{\text{lb.-sec.}^2}{\text{in.}}$$

$$q_m = \sqrt{\frac{k}{M_m}}$$

$$= \sqrt{\frac{5.63}{.00544}}$$

$$= 32.16 \frac{\text{radians}}{\text{sec.}}$$

Run 4

$$f_m = \frac{25 \text{ cycles}}{4.90 \text{ sec.}}$$

$$= 5.10 \ \frac{\text{cycles}}{\text{sec.}}$$

$$@\ X_{m1}: \qquad d = 13 \text{ blocks}$$

$$X_{m1} = (.075)\ (13.0)$$

$$= 0.975 \text{ in.}$$

$$@\ X_{m26}: \qquad d = 8 \text{ blocks}$$

$$i\text{-}26 \qquad X_{m26} = (0.75)\ (8.0)$$

$$= 0.600 \text{ in.}$$

$$Z_m = \frac{1}{i-1} \operatorname{Ln} \left(\frac{X_{m1}}{X_{mi}}\right)$$

$$= \frac{1}{26-1} \operatorname{Ln} \left(\frac{.975}{.600}\right)$$

$$= 0.0194 = 1.94 \text{ per cent}$$

$$M_m = \frac{(1-Z_m{}^2)\ k}{(2\pi\ f_m)^2}$$

$$= \frac{(1-(.0194)^2)\ (5.63)}{(2\pi\ (5.10))^2}$$

$$= 0.00548 \ \frac{\text{lb.-sec.}^2}{\text{in.}}$$

$$q_m = \sqrt{\frac{k}{M_m}}$$

$$= \sqrt{\frac{5.63}{.00548}}$$

$$= 32.05 \ \frac{\text{radians}}{\text{sec.}}$$

Run 5

$$f_m = \frac{35 \text{ cycles}}{6.85 \text{ sec.}}$$

$$= 5.11 \frac{\text{cycles}}{\text{sec.}}$$

$@\ X_{m1}$: $\quad d = 11$ blocks

$$X_{m1} = (.075)\ (11.0)$$

$$= 0.825 \text{ in.}$$

$@\ X_{m36}$: $\quad d = 6$ blocks

$$i=36 \quad X_{m36} = (.075)\ (6.0)$$

$$= 0.450 \text{ in.}$$

$$Z_m = \frac{1}{i-1} \text{ Ln } \left(\frac{X_{m1}}{X_{m36}}\right)$$

$$= \frac{1}{36-1} \text{ Ln } \left(\frac{.825}{.450}\right)$$

$$= 0.0173 = 1.73 \text{ per cent}$$

$$M_m = \frac{(1-Z_m^{\ 2})\ k}{(2\ \pi\ f_m)^2}$$

$$= \frac{(1-(.0173)^2)\ (5.63)}{(2\ \pi\ (5.11))^2}$$

$$= 0.00546 \ \frac{\text{lb. - sec.}^2}{\text{in.}}$$

$$q_m = \sqrt{\frac{k}{M_m}}$$

$$= \sqrt{\frac{5.63}{.00546}}$$

$$= 32.11 \, \frac{\text{radians}}{\text{sec.}}$$

Table 5. Summary of Measured Dynamic Properties of Model

Run	f_m	Z_m	M_m	q_m
1	5.07	1.58	0.00555	31.85
2	5.10	1.72	0.00548	32.05
3	5.12	1.94	0.00544	32.16
4	5.10	1.94	0.00548	32.05
5	5.11	1.73	0.00546	32.11
Σ =	25.50	8.91	0.02741	160.22

The values of f_m, Z_m, M_m, and q_m was taken as the arithmetic mean of the measured values. Therefore,

$$f_m = \frac{\Sigma f_m}{5}$$

$$= \frac{25.50}{5}$$

$$= 5.10 \frac{\text{cycles}}{\text{sec.}}$$

$$Z_m = \frac{\Sigma Z_m}{5}$$

$$= \frac{8.91}{5}$$

$$= 1.78 \text{ per cent}$$

$$M_m = \frac{\Sigma M_m}{5}$$

$$= \frac{0.02741}{5}$$

$$= 0.00548 \ \frac{\text{lb.-sec.}^2}{\text{in.}}$$

$$q_m = \frac{\Sigma \ q_m}{5}$$

$$= \frac{160.22}{5}$$

$$= 32.04 \ \frac{\text{radians}}{\text{sec.}}$$

The other dynamic proerties of the model were then calculated as,

$$W_m = M_m g$$

$$= (0.00548)\ (386)$$

$$= 2.12 \text{ lb.}$$

$$C_{mcr} = 2M_m \ q_m$$

$$= 2\ (.00548)\ (32.04)$$

$$= 0.35 \ \frac{\text{lb.-sec.}}{\text{in.}}$$

$$C_m = C_{mcr} \ Z_m$$

$$= (0.35)\ (0.0178)$$

$$= 0.0063 \ \frac{\text{lb.-sec.}}{\text{in.}}$$

$$T_n = \frac{1}{f_m} = \text{natural period of model}$$

$$= \frac{1}{5.10}$$

$$= 0.196 \text{ sec.}$$

APPENDIX K

DATA SHOWING THE EFFECT OF BREAKING WIRES CONNECTED TO THE SHAKING TABLE

Upon breaking various numbers of wires connected to the shaking table, the table's response, the change in potential energy of the pendulum, and the time of braking the wires were measured.

The results of the tests are tabulated in Table 6 on the following pages.

The notation used in Table 6 is as follows:

N = number of wires broken

A = attenuation of Sanborn strain gage amplifier

d_1 = stylus deflection of Sanborn strain gage amplifier

X_{max} = $(0.0002)\ (d_1)\ (A)$ or first maximum deflection of table, inches

V_o = $34.32\ X_{max}$ or initial velocity of table, in./sec.

T = time of breaking wires, sec.

d_2 = stylus deflection of Sanborn DC amplifier

$\Delta\theta$ = $4.1\ (36 - d_2)$ degrees

J = loss of potential energy of pendulum, in. - lb.

Table 6. Results of Wire Testing

N	A	d_1	X_{max}	V_o	$T \times 10^{-3}$	d_2	$\Delta\theta$	J
1	10	7.0	0.014	0.48	1.5	36.0	0.0	0
1	10	7.0	0.014	0.48	1.4	36.0	0.0	0
1	10	7.0	0.014	0.48	1.5	35.5	2.0	268
1	10	6.0	0.012	0.41	1.5	35.5	2.0	268
1	10	6.5	0.013	0.45	1.5	35.75	1.0	134
2	10	15.5	0.031	1.06	1.9	35.0	4.1	545
2	10	14.0	0.028	0.96	1.7	35.25	3.1	410
2	10	15.25	0.031	1.06	1.8	35.0	4.1	545
3	20	11.0	0.044	1.51	1.7	35.25	3.1	410
3	20	10.0	0.040	1.37	1.9	35.5	2.0	268
3	20	11.0	0.044	1.51	2.3	35.0	4.1	545
3	20	12.0	0.048	1.64	2.1	35.0	4.1	545
3	20	12.0	0.048	1.64	2.2	35.25	3.1	410
4	20	20.0	0.080	2.74	2.6	34.0	8.2	1073
4	20	15.25	0.061	2.09	2.0	35.0	4.1	545
4	20	16.0	0.064	2.19	2.4	35.0	4.1	545
5	50	11.25	0.113	3.87	3.5	34.0	8.2	1073
5	50	9.75	0.098	3.36	3.2	34.5	6.1	805
5	50	8.75	0.088	3.01	2.7	34.25	7.2	947
5	50	8.75	0.088	3.01	2.6	34.25	7.2	947
5	50	9.75	0.098	3.36	3.4	34.5	6.1	805
6	50	13.0	0.130	4.46	3.0	34.0	8.2	1073
6	50	13.5	0.135	4.63	3.2	33.5	10.2	1326
6	50	14.0	0.140	4.81	3.5	34.0	8.2	1073
6	50	14.75	0.148	5.08	3.5	34.75	5.1	671

Table 6. (Continued)

N	A	d_1	X_{max}	V_o	$T \times 10^{-3}$	d_2	$\Delta\theta$	J
7	100	7.5	0.150	5.15	2.6	34.25	7.2	947
7	100	5.5	0.150	5.15	2.9	34.25	7.2	947
7	100	7.75	0.155	5.32	3.6	33.75	9.2	1200
7	100	8.5	0.170	5.84	4.2	not measured		
8	100	8.0	0.160	5.50	3.2	34.25	7.2	947
8	100	8.0	0.160	5.50	3.0	34.0	8.2	1073
9	100	11.0	0.220	7.55	4.0	34.0	8.2	1073
9	100	10.0	0.100	6.86	3.6	33.75	9.2	1200
10	100	10.0	0.200	6.86	4.1	34.0	8.2	1073
10	100	13.0	0.260	8.92	4.8	33.25	11.3	1460

APPENDIX L

COMPARISON OF MEASURED AND CALCULATED PEAK VALUES OF X_t AND D_r

The following table shows the measured and calculated peak values of table displacement, X_t, and relative displacement between model and table for the first five peaks. Also shown is the ratio of calculated to measured values which is an indication of the reliance of the measuring systems.

Table 7. Comparison of Measured and Calculated Peak Values of X_t and D_r for Five, Seven and Ten Wire Tests

No. of Wires	Measured Peak X_t in inches	Calculated Peak X_t in inches	Ratio of Calculated to Measured X_t	Measured Peak D_r in inches	Calculated Peak D_r in inches	Ratio of Claculated to Measured D_r
5	0.110	0.098	0.89	-0.067	-0.067	1.00
5	-0.100	-0.090	0.90	0.200	0.177	0.90
5	0.089	0.094	1.05	-0.300	-0.331	1.10
5	-0.088	-0.088	1.00	0.502	0.441	0.90
5	0.075	0.080	1.06	0.600	-0.586	0.78
7	0.169	0.158	0.93	-0.100	-0.107	1.07
7	-0.165	-0.150	0.91	0.320	0.284	1.89
7	0.148	0.151	1.01	-0.525	-0.530	1.01
7	-0.140	-0.141	1.01	0.805	0.708	0.89
7	0.118	0.128	1.09	-0.975	-0.939	0.96
10	0.240	0.227	0.95	-0.150	-0.154	1.03
10	-0.210	-0.207	0.99	0.450	0.407	0.91
10	0.200	0.217	1.08	-0.750	-0.761	1.02
10	-0.190	-0.202	1.06	1.050	1.015	0.97
10	0.165	0.184	1.10	-1.350	-1.347	1.00

APPENDIX M

COMPARISON OF MEASURED AND CALCULATED PEAK VALUES OF $\ddot{X}_m$

The following table shows measured and calculated values of model accelerations for five arbitrarily chosen peaks. Also shown is the ratio of calculated to measured values of $\ddot{X}_m$.

Table 8. Comparison of Measured and Calculated Peak Values of $\ddot{X}_m$ for One, Three and Five Wire Tests

Number of Wires	Measured Peak $\ddot{X}_m$ in g's	Calculated Peak $\ddot{X}_m$ in g's	Ratio of Calculated to Measured $\ddot{X}_m$
1	0.28	0.28	1.0
1	-0.29	-0.29	1.0
1	0.32	0.32	1.0
1	-0.33	-0.33	1.0
1	0.32	0.32	1.0
3	-0.94	-0.94	1.0
3	0.97	1.03	1.05
3	-1.03	-1.08	1.05
3	1.10	1.06	0.96
3	-0.95	-0.96	1.01
5	-1.60	-2.15	1.34
5	1.80	2.37	1.32
5	-1.90	-2.48	1.31
5	1.80	2.41	1.32
5	1.70	2.18	1.28

APPENDIX N

LOAD-STRAIN CURVE OF THE WIRE

Table 9 on the following page contains the data obtained in the load-strain test of the wire. Figure 34 shows the load-strain curve.

Table 9. Data for the Determination of the Load-Strain Curve of the Wire

Load in Pounds	Strain in $\frac{\text{inches}}{\text{inch}}$
0.0	0.0000
10.5	0.0006
30.5	0.0016
49.5	0.0026
68.5	0.0036
88.5	0.0046
109.3	0.0056
129.5	0.0066
149.5	0.0076
168.8	0.0086
185.5	0.0096
198.5	0.0106
207.0	0.0116
213.0	0.0122
221.0	0.0133
227.0	0.0142
230.0	0.0152
231.0	0.0156

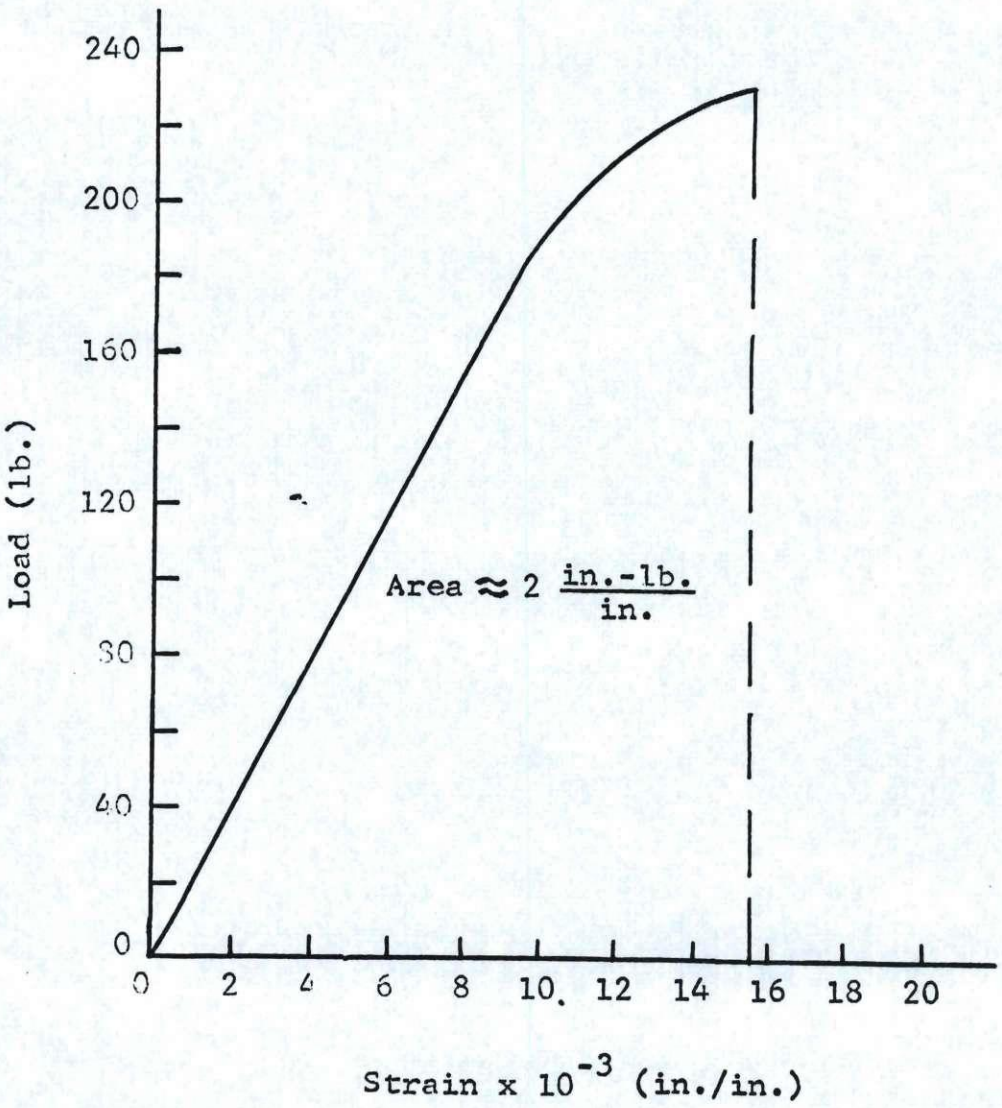

Figure 34. Load-Strain Curve of the Wire

LITERATURE CITED

(1) R. C. Dove and P. H. Adams, Experimental Stress Analysis and Motion Measurement, Charles E. Merrill Brooks, Inc., Columbus, Ohio, 1964.

(2) W. T. Thomson, Vibration Theory and Applications, Prentice-Hall, Inc., Englewood Cliffs, N. J., 1948.

(3) C. H. Norris and J. B. Wilbur, Elementary Structural Analysis, McGraw-Hill, New York, 1948.

(4) L. S. Jacobsen and R. S. Ayre, Engineering Vibrations, McGraw-Hill, New York, 1958.

(5) C. H. Norris, R. J. Hansen, M. J. Holley, J. M. Biggs, S. Namyet, and J. K. Minami, Structural Design For Dynamic Loads, McGraw-Hill, New York, 1959.